OPTIMAL SPATIAL MODULATION FOR RECIPROCAL CHANNELS

JEFFREY H. SHAPIRO

TECHNICAL REPORT 476

APRIL 30, 1970

MASSACHUSETTS INSTITUTE OF TECHNOLOGY
RESEARCH LABORATORY OF ELECTRONICS
CAMBRIDGE, MASSACHUSETTS 02139

The Research Laboratory of Electronics is an interdepartmental laboratory in which faculty members and graduate students from numerous academic departments conduct research.

The research reported in this document was made possible in part by support extended the Massachusetts Institute of Technology, Research Laboratory of Electronics, by the JOINT SERVICES ELECTRONICS PROGRAMS (U.S. Army, U.S. Navy, and U.S. Air Force) under Contract No. DA 28-043-AMC-02536(E), and by the National Aeronautics and Space Administration (Grant NGL 22-009-013).

MASSACHUSETTS INSTITUTE OF TECHNOLOGY
RESEARCH LABORATORY OF ELECTRONICS

Technical Report 476 April 30, 1970

OPTIMAL SPATIAL MODULATION FOR RECIPROCAL CHANNELS

Jeffrey H. Shapiro

This report is based on a thesis submitted to the Department of Electrical Engineering, M.I.T., January 1970, in partial fulfillment of the requirements for the degree of Doctor of Philosophy.

(Manuscript received January 6, 1970)

Abstract

The purpose of this research is to find ways of improving optical communication through atmospheric turbulence by using spatial modulation. The performance of a class of adaptive spatially modulated communication systems, in which the antenna pattern at the transmitter is modified in accordance with the knowledge of the channel state obtained from a beacon signal transmitted from the receiving terminal to the transmitter, is examined.

For time-invariant channels satisfying a certain reciprocity condition, there exists an adaptive system that achieves the maximum energy transfer possible from transmitter to receiver. This result is applied to the turbulent atmospheric channel by regarding the atmosphere as undergoing a succession of fixed states, and proving that instantaneously the atmosphere is reciprocal. The performance of adaptive spatially modulated systems for the turbulent channel is derived for both point-to-point and deep-space applications. In the deep-space case we find that the turbulence does not increase the average far-field beamwidth attainable with a given diameter aperture, but fluctuations about this average beamwidth do occur as the state of the atmosphere changes.

The effects of noise and approximate transmitter implementations on the performance of the adaptive systems under discussion are considered. A hypothetical deep-space system is specified and its performance is evaluated.

TABLE OF CONTENTS

CONTENTS

I. INTRODUCTION

Optical communication systems in which the clear turbulent atmosphere comprises part of the transmission medium are characterized by reduced system performance when compared with free-space systems. From a communications viewpoint, the loss of spatial coherence caused by the turbulence limits the performance of optical systems in two ways: (i) a receiving aperture diameter (for a heterodyne receiver) beyond which the signal-to-noise ratio is not enhanced by increased aperture size; and (ii) a maximum transmitting aperture diameter (for a plane-wave transmitter) beyond which the far-field beamwidth is turbulence-limited and independent of aperture size. Each of these effects may be taken to define a coherence length for the turbulence, so that performance saturates when the related aperture diameter is made larger than this length.

In point-to-point applications on the Earth with the receiving aperture in the near field of the transmitter, the first of these limitations is the significant one. For Earth-to-Deep Space applications the receiving aperture at the spacecraft contains only a single coherence area, and thus the second of these limitations is the significant one.

Much work has been devoted to finding receiver structures for the point-to-point problem that are capable of using more receiver aperture than a coherence area.[1-3] These approaches, which assume a fixed (usually a plane-wave) antenna pattern at the transmitter, are fruitful because in point-to-point applications the turbulence does not greatly affect the total carrier energy incident upon the receiving aperture. This energy is no longer in a single plane-wave component, and thus spatial diversity or wavefront tracking techniques must be employed, but the energy is there at the receiving aperture. This is not the case in Earth-to-Deep Space applications. The energy received at the spacecraft is proportional to the energy in the proper plane-wave component of the field leaving the top of the atmosphere. Any energy that is scattered out of this component during propagation from the ground to the top of the atmosphere is lost, as far as the spacecraft is concerned. Our primary aim will be to find a system for which the carrier energy received at the spacecraft does not saturate, that is, become turbulence-limited rather than diffraction-limited, as the transmitting aperture diameter is increased.

We shall study a class of adaptive spatially modulated transmitters in which the antenna pattern of the transmitter is modified in accordance with the knowledge of the atmospheric "state" obtained from a beacon signal sent from the receiving terminal to the transmitter. The principal conclusion that we reach is that there exists a transmitter of the type described whose average far-field beamwidth (over the turbulence ensemble) is the same as the diffraction-limited beamwidth of a lens of the same aperture diameter.

This report is organized as follows. In Sections II and III an abstract model is developed for communication through a time-invariant inhomogeneous spatially modulated channel. We show that for a class of channels (reciprocal channels) it is possible to greatly improve system performance (measured in terms of received carrier energy)

by use of spatial modulation and feedback, even if the exact state of the channel were unknown a priori at both the transmitter and receiver. The results are extended to the time-variant turbulent atmosphere in Sections IV, V, VI, and VII with primary emphasis on deep-space applications.

In Sections II-VII a noiseless environment is assumed. This restriction is removed in Section VIII, and the effects of noise are considered. Section IX concludes with a calculation of the performance of a hypothetical adaptive system.

II. APODIZATION IN THE ABSENCE OF NOISE

2.1 CHANNEL MODEL

We begin our study of spatial modulation by developing some abstract results for a time-invariant inhomogeneous spatially modulated channel. The model that we shall postulate approximates the state of the turbulent atmospheric channel at a single instant of time.

Consider the system geometry shown in Fig. 1. We wish to transmit information using electromagnetic radiation. We shall assume narrow-band signals and

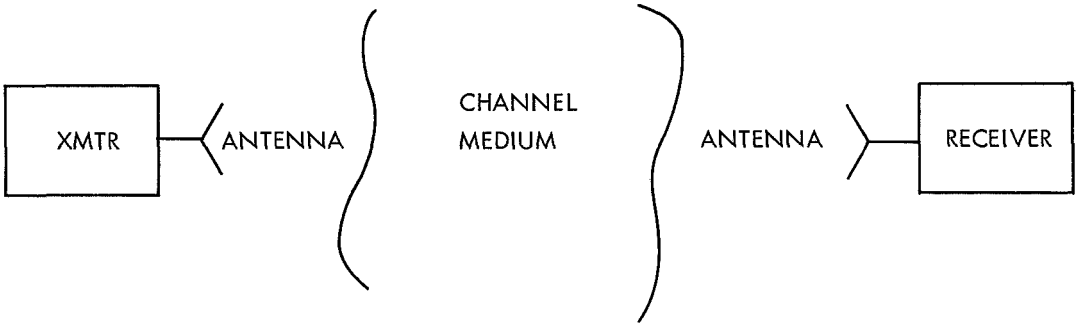

Fig. 1. System configuration.

describe the electric field at any point in space as

$$\vec{E}(\vec{r}, t) = \mathrm{Re}\left[\underline{\vec{E}}(\vec{r}, t)\, e^{j\omega_c t}\right] \tag{1}$$

where $\vec{E}(\vec{r}, t)$ is the field at a point $\vec{r}$ and time t, $\underline{\vec{E}}(\vec{r}, t)$ is the complex field amplitude, and ω_c is the carrier radian frequency. Note that the time dependence of the complex-field amplitude, $\underline{\vec{E}}(\vec{r}, t)$, is due solely to temporal modulation at the transmitter. Since our work is concerned only with improving the received carrier energy, we shall neglect any temporal modulation at the transmitter and suppress the time dependence of $\underline{\vec{E}}(\vec{r}, t)$. Thus the electric field is

$$\vec{E}(\vec{r}, t) = \mathrm{Re}\left[\underline{\vec{E}}(\vec{r})\, e^{j\omega_c t}\right]. \tag{2}$$

We would like to eliminate the vector nature of the channel. We do this by assuming that the channel has no depolarizing effect on the field sent through it, and by communicating with a single transverse component of the electric field. For that component we now have

$$E(\vec{r}, t) = \mathrm{Re}\left[\underline{E}(\vec{r})\, e^{j\omega_c t}\right]. \tag{3}$$

From the linearity of Maxwell's equations (either in time or frequency domain) we conclude that the system shown in Fig. 1 is linear. To describe this linear system we introduce an impulse response (Green's function), and for convenience we choose to define it in terms of the complex-field amplitude. Let the transmitting antenna be a

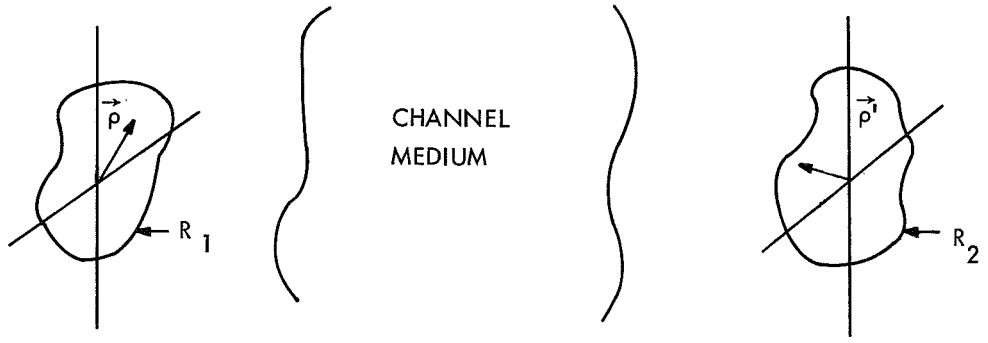

Fig. 2. Antenna geometry.

planar aperture R_1, and the receiving antenna be a planar aperture R_2, whose plane is parallel to that of R_1 (see Fig. 2). The impulse response, $\underset{\rightarrow}{h}(\vec{\rho}', \vec{\rho})$, of the system is the complex-field amplitude at a point $\vec{\rho}'$ in R_2 in response to a complex-field amplitude point source located at point $\vec{\rho}$ in R_1. If there is some arbitrary source distribution $u(\vec{\rho})$ in R_1, then the resulting output-field amplitude, $v(\vec{\rho}')$, in R_2 is

$$v(\vec{\rho}') = \int_{R_1} u(\vec{\rho})\, \underset{\rightarrow}{h}(\vec{\rho}', \vec{\rho})\, d\vec{\rho}. \tag{4}$$

Eventually we shall need to study the field at R_1 that results when a field is transmitted from R_2, so we define another impulse response, $\underset{\leftarrow}{h}(\vec{\rho}, \vec{\rho}')$, to be the complex-field amplitude at a point $\vec{\rho}$ in R_1 in response to a point source located at point $\vec{\rho}'$ in R_2. Once again, if there is an arbitrary complex-field source distribution $v(\vec{\rho}')$ in R_2, then the resulting output field, $u(\vec{\rho})$, is given by the convolution of the input with the impulse response. That is,

$$u(\vec{\rho}) = \int_{R_2} v(\vec{\rho}')\, \underset{\leftarrow}{h}(\vec{\rho}, \vec{\rho}')\, d\vec{\rho}'. \tag{5}$$

Within the framework just described there are some interesting questions that can be posed.

1. What unit energy source distribution $u(\vec{\rho})$ on R_1 maximizes the total carrier energy received over the aperture R_2, given that the channel state (that is, the impulse responses $\underset{\rightarrow}{h}$ and $\underset{\leftarrow}{h}$) is known to both the transmitter and the receiver? (By energy

we mean $\int_{R_1} |u(\vec{\rho})|^2 \, d\vec{\rho}$, which really corresponds to the power in the original field – not field amplitude. Since we consistently suppress the time behavior of the spatial waveforms, it is convenient to call the expression the "energy." This convention will be maintained throughout the report.)

2. What unit energy source distribution $u(\vec{\rho})$ on R_1 maximizes the total carrier energy received over R_2 if the state is unknown a priori at both ends of the system, but a channel beacon (from R_2 to R_1) is available?

3. What are the resulting output energies of these optimal known-channel and unknown-channel systems?

The extent to which an unknown-channel communication system can perform as well as the optimum known-channel system, for the spatially modulated channel under discussion, is the crux of this report.

2.2 APODIZATION FOR KNOWN CHANNELS

We shall consider the first problem. Apodization problems (that is, maximizing the received energy for a given transmitted energy) when the channel state is known at both terminals are easily solved, in principle, by solving for the natural "spatial modes" of the system. In order to formulate the problem in these terms, we must introduce some added definitions. These known-channel results are not new[4-6] and no proofs will be given.

We define two kernels

$$\underset{\rightarrow}{K}(\vec{\rho}, \vec{r}) = \int_{R_2} \underset{\rightarrow}{h}(\vec{\rho}', \vec{r}) \, \underset{\rightarrow}{h}^*(\vec{\rho}', \vec{\rho}) \, d\vec{\rho}' \tag{6}$$

$$\underset{\leftarrow}{K}(\vec{\rho}', \vec{r}') = \int_{R_1} \underset{\leftarrow}{h}(\vec{\rho}, \vec{r}') \, \underset{\leftarrow}{h}^*(\vec{\rho}, \vec{\rho}') \, d\vec{\rho}. \tag{7}$$

These kernels are both Hermitian and non-negative definite.

Let the $\underset{\rightarrow}{K}$ kernel have orthonormal eigenfunctions $\Psi_i(\vec{\rho})$, and associated eigenvalues η_i, and let the $\underset{\leftarrow}{K}$ kernel have orthonormal eigenfunctions $\phi_i(\vec{\rho}')$, and associated eigenvalues λ_i; that is, $\{\Psi_i\}$ is a set of orthonormal functions defined on R_1 such that

$$\int_{R_1} \underset{\rightarrow}{K}(\vec{\rho}, \vec{r}) \, \Psi_i(\vec{r}) \, d\vec{r} = \eta_i \Psi_i(\vec{\rho}), \tag{8}$$

and similarly $\{\phi_i\}$ satisfies the corresponding Fredholm integral equation in terms of the kernel $\underset{\leftarrow}{K}$. These sets of eigenfunctions may be assumed to be complete on their respective domains if we augment them to include eigenfunctions with zero eigenvalues. (The Fredholm integrals must be over finite regions, otherwise the eigenfunctions will not be countable. When we make use of eigenfunction expansions, we shall be careful to

Table 1. Kernels $\underset{\rightarrow}{K}$, $\underset{\leftarrow}{K}$, and Q.

DEFINITIONS	MODEL
$\underset{\rightarrow}{K}(\vec{\rho}, \vec{r}) = \int_{R_2} \underset{\rightarrow}{h}^*(\vec{\rho}', \vec{\rho})\, \underset{\rightarrow}{h}(\vec{\rho}', \vec{r})\, d\vec{\rho}'$	R_1 R_2
$\int_{R_1} \underset{\rightarrow}{K}(\vec{\rho}, \vec{r})\, \Psi_i(\vec{r})\, d\vec{r} = \eta_i \Psi_i(\vec{\rho})$	$\Psi_i(\vec{\rho}) \rightarrow \boxed{\underset{\rightarrow}{h}(\vec{\rho}', \vec{\rho})} \rightarrow \sqrt{\eta_i}\, \psi_i(\vec{\rho}')$
$\sqrt{\eta_i}\, \psi_i(\vec{\rho}') = \int_{R_1} \Psi_i(\vec{\rho})\, \underset{\rightarrow}{h}(\vec{\rho}', \vec{\rho})\, d\vec{\rho}$	IF $\eta_1 \geq \eta_2 \geq \ldots$ THEN $\Psi_1(\vec{\rho})$ IS THE UNIT ENERGY WAVEFORM THAT DELIVERS MAXIMUM ENERGY TO R_2
$\underset{\leftarrow}{K}(\vec{\rho}', \vec{r}') = \int_{R_1} \underset{\leftarrow}{h}^*(\vec{\rho}, \vec{\rho}')\, \underset{\leftarrow}{h}(\vec{\rho}, \vec{r}')\, d\vec{\rho}$	R_1 R_2
$\int_{R_2} \underset{\leftarrow}{K}(\vec{\rho}', \vec{r}')\, \phi_i(\vec{r}')\, d\vec{r}' = \lambda_i \phi_i(\vec{\rho}')$	$\sqrt{\lambda_i}\, \Phi_i(\vec{\rho}) \leftarrow \boxed{\underset{\leftarrow}{h}(\vec{\rho}, \vec{\rho}')} \leftarrow \phi_i(\vec{\rho}')$
$\sqrt{\lambda_i}\, \Phi_i(\vec{\rho}) = \int_{R_2} \phi_i(\vec{\rho}')\, \underset{\leftarrow}{h}(\vec{\rho}, \vec{\rho}')\, d\vec{\rho}'$	IF $\lambda_1 \geq \lambda_2 \geq \ldots$ THEN $\phi_1(\vec{\rho}')$ IS THE UNIT ENERGY WAVEFORM THAT DELIVERS MAXIMUM ENERGY TO R_1
$Q(\vec{\rho}', \vec{r}') = \int_{R_1} \underset{\leftarrow}{h}^*(\vec{\rho}, \vec{\rho}')\, \underset{\rightarrow}{h}(\vec{r}', \vec{\rho})\, d\vec{\rho}$	R_1 R_2
$\int_{R_2} Q(\vec{\rho}', \vec{r}')\, \zeta_i^*(\vec{\rho}')\, d\vec{\rho}' = a_i \zeta_i^*(\vec{r}')$	$\boxed{\underset{\leftarrow}{h}(\vec{\rho}, \vec{\rho}')} \leftarrow \zeta_i(\vec{\rho}')$ CONJUGATION TRANSMITTER $\boxed{\underset{\rightarrow}{h}(\vec{r}', \vec{\rho})} \rightarrow a_i \zeta_i^*(\vec{r}')$

use finite domains for the kernels $\underset{\rightarrow}{K}$ and $\underset{\leftarrow}{K}$. On occasion we shall use these kernels over infinite domains, but in these instances we shall not refer to the eigenfunctions or eigenvalues.) Since both kernels are Hermitian and non-negative definite, we have

$$\eta_i \geq 0, \qquad \lambda_i \geq 0.$$

We now define the function $\sqrt{\eta_i}\ \psi_i(\vec{\rho}')$ to be the response at R_2 to a source field $\Psi_i(\vec{\rho})$ at R_1; in other words,

$$\sqrt{\eta_i}\ \psi_i(\vec{\rho}') = \int_{R_1} \Psi_i(\vec{\rho})\ \underset{\rightarrow}{h}(\vec{\rho}', \vec{\rho})\ d\vec{\rho}. \tag{9}$$

We also define the function $\sqrt{\lambda_i}\ \Phi_i(\vec{\rho})$ to be the response at R_1 to a source field $\phi_i(\vec{\rho}')$ at R_2; that is,

$$\sqrt{\lambda_i}\ \Phi_i(\vec{\rho}) = \int_{R_2} \phi_i(\vec{\rho}')\ \underset{\leftarrow}{h}(\vec{\rho}, \vec{\rho}')\ d\vec{\rho}'. \tag{10}$$

It may be shown that $\{\psi_i\}$ and $\{\Phi_i\}$ are orthonormal sets of functions on their respective domains. Furthermore, by properly augmenting $\{\psi_i\}$ and $\{\Phi_i\}$ to include functions whose associated eigenvalues are zero, we may regard these sets as being complete on their respective domains. These properties of the input and output eigenfunctions of the kernels $\underset{\rightarrow}{K}$ and $\underset{\leftarrow}{K}$ will be used frequently, and so they have been summarized in Table 1 for future reference. They lead to parallel channel decompositions of the original channels[5, 6] (see Fig. 3).

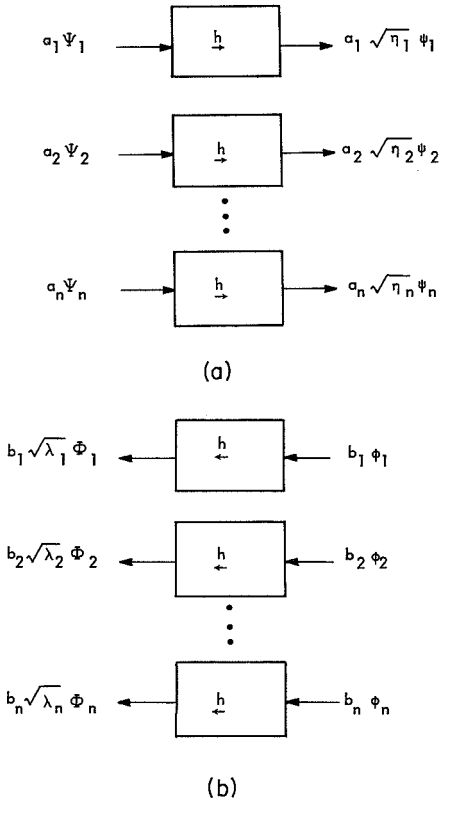

Fig. 3. Parallel channel models.
(a) $\underset{\rightarrow}{h}$ channel. (b) $\underset{\leftarrow}{h}$ channel.

Slepian[7, 8] has shown that the eigenfunctions associated with propagation through free-space are the prolate spheroidal wave functions, and Greenspan[4] has used this result to obtain bounds on probability of error for the spatially modulated free-space channel. The impulse response of the medium that we are modeling (the turbulent atmosphere) is unknown, however, and were it known it would still be difficult, if not impossible, to solve the resulting Fredholm equations for the eigenfunctions and eigenvalues. Nevertheless, we shall suppose that not only are the impulse responses $\underset{\rightarrow}{h}$ and $\underset{\leftarrow}{h}$

known at each terminal but also the eigenfunctions and eigenvalues of their associated kernels $\underset{\rightarrow}{K}$ and $\underset{\leftarrow}{K}$ are known.

Consider the apodization problem from R_1 to R_2. Suppose that we have an available energy E_t to be used at R_1, and wish to adjust the transmitter to maximize the energy received at R_2. Assuming that the eigenfunctions $\{\Psi_i\}$ are ordered in such a way that

$$\eta_1 \geq \eta_2 \geq \eta_3 \geq \ldots,$$

we find that the optimum waveform to use is[7, 9]

$$\sqrt{E_t}\ \Psi_1(\vec{\rho})$$

and the received waveform is

$$\sqrt{E_t \eta_1}\ \psi_1(\vec{\rho'})$$

which has energy $E_t \eta_1$. Note that by conservation of energy $\eta_1 \leq 1$. Similarly, we can show that

$$\eta_i \leq 1, \quad \lambda_i \leq 1.$$

It is easy to see that if we had energy E_t available at R_2 and wished to maximize the energy received at R_1, then with $\{\phi_i\}$ ordered such that

$$\lambda_1 \geq \lambda_2 \geq \lambda_3 \geq \ldots$$

the optimum waveform is

$$\sqrt{E_t}\ \phi_1(\rho')$$

and the resulting received waveform is

$$\sqrt{E_t \lambda_1}\ \Phi_1(\vec{\rho})$$

which has energy $E_t \lambda_1$.

Thus the solution to the apodization problem when the channel state is known reduces to the problem of finding the solutions to a Fredholm integral equation. The solution of the resulting integral equation is nontrivial; for the free-space channel answers are known only for certain simple antenna geometries.[4, 7, 9, 10] Nevertheless, some interesting comments can be made.

In transmitting from R_1 to R_2 the maximum received energy, when an energy E_t was transmitted, is $E_t \eta_1$, and $\eta_1 \leq 1$. When will η_1 be close to unity? This question may be answered in terms of the so-called degrees of freedom of the channel, a number that tells how many of the eigenvalues are "close" to unity. We shall discuss degrees of freedom in more detail after we study apodization for unknown channels.

2.3 APODIZATION FOR UNKNOWN CHANNELS

There are many ways of trying to find the optimum waveform for apodization through a time-invariant unknown spatial channel. Since we wish to apply our work to the (time-variant) turbulent atmosphere, without justification, we shall specify a method of communication and examine its performance. In Section III we show that for reciprocal channels the performance of the system proposed here approaches the optimal energy transfer if the channel is known at each terminal, and eventually we shall show that the atmosphere is a reciprocal channel.

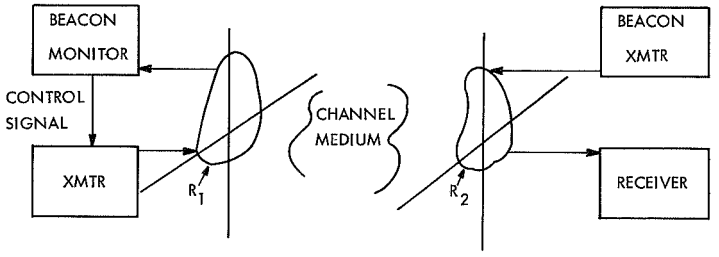

Fig. 4. Two-way apodization, unknown channel.

Suppose we are trying to maximize the energy received at R_2 using the system shown in Fig. 4, subject to the following constraints.

1. We transmit a unit energy beacon from R_2 to R_1.
2. Using the received beacon waveform (in a yet unspecified way), we adjust the transmitter at R_1.
3. We transmit energy E_t from R_1, regardless of the amount of energy received from the beacon.

We denote the beacon waveform (at R_2) as $v(\vec{\rho}')$; thus the received signal at R_1, $u_o(\vec{\rho})$, is

$$u_o(\vec{\rho}) = \int_{R_2} v(\vec{\rho}')\, \underleftarrow{h}(\vec{\rho}, \vec{\rho}')\, d\vec{\rho}'. \tag{11}$$

Let us now assume the following transmitter implementation at R_1: We receive the waveform $u_o(\vec{\rho})$ and transmit a replica of the $u_o(\vec{\rho})$ waveform, scaled to have energy E_t, and propagating in the opposite direction. Mathematically, the transmitted waveform, $\tilde{u}^*(\vec{\rho})$, may be written (see Appendix A)

$$\tilde{u}^*(\vec{\rho}) = \left[\frac{E_t}{\iint_{R_2} v^*(\vec{\rho}')\, \underleftarrow{K}(\vec{\rho}', \vec{r}')\, v(\vec{r}')\, d\vec{\rho}' d\vec{r}'}\right]^{1/2} u_o^*(\vec{\rho})\, e^{-2j\omega_c T_d}, \tag{12}$$

where T_d is the lumped delay time of the propagation of the beacon from R_2 to R_1 and the transmitter adjustment time. Since T_d is a constant, and just adds a delay to the time-domain fields, we shall delete it from the expression for $\tilde{u}^*(\vec{\rho})$. This makes the transmitter at R_1 nonrealizable, but at any later point in the analysis we may add the delay in our results. When we transmit $\tilde{u}^*(\vec{\rho})$ the signal received at R_2 is

$$\hat{v}^*(\vec{r}') = \int_{R_1} \tilde{u}^*(\vec{\rho})\, \underset{\rightarrow}{h}(\vec{r}', \vec{\rho})\, d\vec{\rho}$$

$$= \left[\frac{E_t}{\iint_{R_2} v^*(\vec{\rho}')\, \underset{\leftarrow}{K}(\vec{\rho}', \vec{r}')\, v(\vec{r}')\, d\vec{\rho}' d\vec{r}'} \right]^{1/2} \int_{R_1} d\vec{\rho} \int_{R_2} d\vec{\rho}'\, v^*(\vec{\rho}')\, \underset{\rightarrow}{h}(\vec{r}', \vec{\rho})\, \underset{\leftarrow}{h}^*(\vec{\rho}, \vec{\rho}'). \tag{13}$$

Now we assume that the receiver at R_2 cannot use all the energy in $\hat{v}^*(\vec{\rho}')$, but rather it heterodynes (see Appendix A) $\hat{v}^*(\vec{\rho}')$ with the beacon waveform $v(\vec{\rho}')$. Thus the energy that the (heterodyne) receiver measures is

$$\left| \int_{R_2} \hat{v}^*(\vec{r}')\, v(\vec{r}')\, d\vec{r}' \right|^2 = \frac{E_t \left| \iint_{R_2} v^*(\vec{\rho}') \left(\int_{R_1} \underset{\rightarrow}{h}(\vec{r}', \vec{\rho})\, \underset{\leftarrow}{h}^*(\vec{\rho}, \vec{\rho}')\, d\vec{\rho} \right) v(\vec{r}')\, d\vec{\rho}' d\vec{r}' \right|^2}{\iint_{R_2} v^*(\vec{\rho}')\, \underset{\leftarrow}{K}(\vec{\rho}', \vec{r}')\, v(\vec{r}')\, d\vec{\rho}' d\vec{r}'}, \tag{14}$$

where we have used the fact that $v(\vec{\rho}')$ has unit energy, and substituted from Eq. 13 for $\hat{v}^*(\vec{r}')$. We define a kernel

$$Q(\vec{\rho}', \vec{r}') = \int_{R_1} \underset{\rightarrow}{h}(\vec{r}', \vec{\rho})\, \underset{\leftarrow}{h}^*(\vec{\rho}, \vec{\rho}')\, d\vec{\rho} \tag{15}$$

in terms of which Eq. 14 may be written

$$\left| \int_{R_2} \hat{v}^*(\vec{r}')\, v(\vec{r}')\, d\vec{r}' \right|^2 = \frac{E_t \left| \iint_{R_2} v^*(\vec{\rho}')\, Q(\vec{\rho}', \vec{r}')\, v(\vec{r}')\, d\vec{\rho}' d\vec{r}' \right|^2}{\iint_{R_2} v^*(\vec{\rho}')\, \underset{\leftarrow}{K}(\vec{\rho}', \vec{r}')\, v(\vec{r}')\, d\vec{\rho}' d\vec{r}'}. \tag{16}$$

The Q-kernel defined in Eq. 15 is more than a notational convenience; it has the following interpretation. Let $\{\zeta_i\}$ be the orthonormal eigenfunctions of the Q-kernel, with eigenvalues $\{a_i\}$. That is

$$\int_{R_2} Q(\vec{\rho}', \vec{r}')\, \zeta_i^*(\vec{\rho}')\, d\vec{\rho}' = a_i \zeta_i^*(\vec{r}'). \tag{17}$$

(As with the eigenfunctions of the $\underset{\rightarrow}{K}$ and $\underset{\leftarrow}{K}$ kernels the eigenfunctions of the Q-kernel are countable only if R_2 is finite.)

Note that the integration is performed on the first variable of Q, which is why the eigenfunctions are conjugated in (17). If Q is Hermitian symmetric, then (17) is equivalent to the usual Fredholm equation. Without further information about $\underset{\rightarrow}{h}$ and $\underset{\leftarrow}{h}$ we cannot tell whether or not Q is Hermitian or non-negative definite. Substituting for Q from (15) and interchanging the orders of integration, we may write (17)

$$\int_{R_1} \left(\int_{R_2} \zeta_i(\vec{\rho}') \, \underset{\leftarrow}{h}(\vec{\rho}, \vec{\rho}') \, d\vec{\rho}' \right)^* \underset{\rightarrow}{h}(\vec{r}', \vec{\rho}) \, d\vec{\rho} = \alpha_i \zeta_i^*(\vec{r}'). \tag{18}$$

In other words, if one transmits $\zeta_i(\vec{\rho}')$ from R_2 and uses the "turn around" (conjugation operation) transmitter at R_1, then the signal received at R_2 is $\alpha_i \zeta_i^*(\vec{r}')$, where the conjugation arises from the difference in propagation direction (R_1 to R_2 instead of R_2 to R_1). The energy in the signal received at R_2 is $|\alpha_i|^2$, since ζ_i has unit energy. This property of the Q-kernel will be used often later in this report, and so it is included in Table 1 (with the properties of the $\underset{\rightarrow}{K}$ and $\underset{\leftarrow}{K}$ kernels) for future reference.

Up to this point, we have arbitrarily assigned a great deal of structure to the apodization problem that we are solving. To be able to compare our two-way (Q-kernel) system with the one-way ($\underset{\rightarrow}{K}$-kernel) system of section 2.2 we must make some further assumptions. Throughout we shall refer to the optimum known-channel (one-way) apodization system described in section 2.2 as the $\underset{\rightarrow}{K}$-kernel system. Similarly, we shall refer to the unknown-channel (two-way) system described here as the Q-kernel system. Basically we are denoting each system by the kernel describing the system's energy performance. We shall now discuss the performance of one-way systems in terms of degrees of freedom. We shall return to two-way apodization systems in the context of reciprocal channels in Section III.

2.4 DEGREES OF FREEDOM

The discussion here will be restricted to one-way apodization problems. We use the $\underset{\rightarrow}{h}$ channel as an example, but all comments apply equally well to the $\underset{\leftarrow}{h}$ channel.

The degrees of freedom, D_f, of the channel has the following properties.[4, 8, 11]

1. D_f is a function of the antenna areas (R_1 and R_2) and the impulse response of the intervening medium, and D_f increases monotonically as either or both of the antenna areas are increased.

2. Under the assumption that the eigenfunctions $\{\Psi_i\}$ are arranged in order of decreasing eigenvalues, then if

$$i \leq D_f \qquad \eta_i \sim 1$$

$$i > D_f \qquad \eta_i \sim 0.$$

3. For the free-space channel with concentric apertures

$$D_f = \frac{A_1 A_2}{(\lambda z)^2},$$

where A_1 is the area of region R_1, A_2 is the area of region R_2, λ is the wavelength of the radiation, and z is the perpendicular distance between R_1 and R_2.

Thus D_f determines how many of the spatial modes can propagate through the channel without excessive loss. It is analogous to the 2TW limitation on the number of time-limited, "essentially" bandlimited orthonormal signals in the time domain.[12] Also, since the higher numbered eigenfunctions will resemble sinusoids of increasing spatial frequencies,[13] it is apparent that the channel severely attenuates the high spatial frequencies. Spatial bandwidth considerations will be treated in detail in Section VIII, and extensive use will be made of the degrees-of-freedom concept.

III. RECIPROCAL CHANNELS AND STATE KNOWLEDGE

3.1 RECIPROCITY CONDITIONS

We have made few assumptions concerning the impulse responses, $\underset{\rightarrow}{h}$ and $\underset{\leftarrow}{h}$, and their associated kernels $\underset{\rightarrow}{K}$, $\underset{\leftarrow}{K}$, and Q. We might expect that if there is some strong "correlation" between the functions $\underset{\rightarrow}{h}$ and $\underset{\leftarrow}{h}$, then the unknown-channel communication system could perform as well as the optimum known-channel communication system. We shall now investigate possible "correlations" between the two impulse responses, called "reciprocity conditions," and the communication-oriented consequences of reciprocity.

For our purposes, the most important reciprocity condition is point reciprocity. We shall say that the channel under consideration is point-reciprocal if and only if

$$\underset{\rightarrow}{h}(\vec{\rho}', \vec{\rho}) = \underset{\leftarrow}{h}(\vec{\rho}, \vec{\rho}') \qquad \forall\ \vec{\rho} \in R_1,\ \vec{\rho}' \in R_2. \tag{19}$$

This condition implies that if we had a unit-energy point source located at a point $\vec{\rho}$ in R_1, then the field received at a point $\vec{\rho}'$ in R_2 would be the same as the field received at $\vec{\rho}$ from a unit-energy point source located at $\vec{\rho}'$, hence the "point" nature of the property.

It should be noted that without further assumptions we cannot simply apply the superposition principle to (19) and conclude that transmitting a field from R_1 to R_2 has the same effect as transmitting the same input field from R_2 to R_1. The superposition principle does allow one to draw some interesting conclusions from (19), but they are somewhat different from the (false) conclusion just mentioned. Let $u(\vec{\rho})$ be an input field on R_1. Multiplying (19) by $u(\vec{\rho})$ and integrating (on R_1), we obtain

$$\int_{R_1} u(\vec{\rho})\, \underset{\rightarrow}{h}(\vec{\rho}', \vec{\rho})\, d\vec{\rho} = \int_{R_1} u(\vec{\rho})\, \underset{\leftarrow}{h}(\vec{\rho}, \vec{\rho}')\, d\vec{\rho} \qquad \forall\ \vec{\rho}' \in R_2. \tag{20}$$

The left-hand side is the output field that results when $u(\vec{\rho})$ is the input field. The right-hand side is the output of a receiver that heterodynes $\underset{\leftarrow}{h}(\vec{\rho}, \vec{\rho}')$ with $u(\vec{\rho})$. Equation 20 shows, therefore, that for a point-reciprocal channel the following are equivalent: transmitting $u(\vec{\rho})$ from R_1 and measuring the field at the point $\vec{\rho}'$ in R_2, and placing a point source at $\vec{\rho}'$ in R_2 and heterodyning the field received at R_1 with $u(\vec{\rho})$.

If $u(\vec{\rho}) = 1$ (zero-phase normally incident uniform plane wave), then (20) reduces to

$$\int_{R_1} \underset{\rightarrow}{h}(\vec{\rho}', \vec{\rho})\, d\vec{\rho} = \int_{R_1} \underset{\leftarrow}{h}(\vec{\rho}, \vec{\rho}')\, d\vec{\rho} \qquad \forall\ \vec{\rho}' \in R_2. \tag{21}$$

If a medium satisifes (21), then we say that the medium satisfies a singly integrated reciprocity condition. A similar singly integrated reciprocity condition results from

integrating (19) over R_2. These singly integrated conditions are always satisfied by point-reciprocal channels, but since some arguments will only require singly integrated reciprocity, this weaker condition is defined explicitly.

A doubly integrated reciprocity condition may be obtained by integrating (21) over R_2,

$$\int_{R_2}\int_{R_1} \underset{\rightarrow}{h}(\vec{\rho}', \vec{\rho})\, d\vec{\rho}\, d\vec{\rho}' = \int_{R_2}\int_{R_1} \underset{\leftarrow}{h}(\vec{\rho}, \vec{\rho}')\, d\vec{\rho}\, d\vec{\rho}'. \tag{22}$$

This equation may be interpreted as follows: Each term is the output of a heterodyne receiver when the transmitting and local-oscillator fields are both zero-phase normally incident uniform plane waves, with the transmitter at R_1 on the left side and the transmitter at R_2 on the right side.

We now investigate some conditions stronger than Eq. 19. Let us assume that the channel is point-reciprocal, and also that the impulse responses, $\underset{\rightarrow}{h}$ and $\underset{\leftarrow}{h}$, are spatially invariant. That is,

$$\underset{\rightarrow}{h}(\vec{\rho}', \vec{\rho}) = F(\vec{\rho}'-\vec{\rho}) = \underset{\leftarrow}{h}(\vec{\rho}, \vec{\rho}') \qquad \forall\, \vec{\rho} \in R_1,\ \vec{\rho}' \in R_2. \tag{23}$$

Point reciprocity implies that the two impulse responses are equal, spatial invariance means that the impulse responses only depend on the single vector quantity $\vec{\rho}' - \vec{\rho}$. Spatial invariance allows us to rewrite our usual convolution integral (4) in the form

$$v(\vec{\rho}') = \int_{R_1} u(\vec{\rho})\, F(\vec{\rho}'-\vec{\rho})\, d\vec{\rho}. \tag{24a}$$

It is readily seen that the output field is invariant with respect to a spatial translation in the input field. That is,

$$v(\vec{\xi}+\vec{\rho}') = \int_{R_1} u(\vec{\xi}+\vec{\rho})\, F(\vec{\rho}'-\vec{\rho})\, d\vec{\rho} \qquad \forall\, \vec{\xi}, \tag{24b}$$

which is the spatial analog of the usual time-invariance property of linear systems in the time domain.

The spatial invariance of the impulse responses, in addition to point reciprocity, allows us to prove the following relation. For a spatially invariant, point-reciprocal channel if an input field $u(\vec{\rho})$ at R_1 causes an output field $v(\vec{\rho}')$ at R_2, then an input $u(-\vec{\rho}')$ at R_2 causes an output $v(-\vec{\rho})$ at R_1. In other words, if

$$v(\vec{\rho}') = \int_{R_1} u(\vec{\rho})\, \underset{\rightarrow}{h}(\vec{\rho}', \vec{\rho})\, d\vec{\rho},$$

then

$$v(-\vec{\rho}) = \int_{R_2} u(-\vec{\rho}')\, \underset{\leftarrow}{h}(\vec{\rho}, \vec{\rho}')\, d\vec{\rho}'. \tag{25}$$

The proof of this property is presented in Appendix A, but the essential nature of (25) can be illustrated by the following example. For this example we use a ray optics interpretation of the impulse responses $\underset{\rightarrow}{h}$ and $\underset{\leftarrow}{h}$. The function $\underset{\rightarrow}{h}(\vec{\rho}', \vec{\rho})$ is assumed to be the complex amplitude of the ray leaving the point $\vec{\rho}$ in R_1 that arrives at the point $\vec{\rho}'$ in R_2. Thus for point-reciprocal channels the complex amplitude of the ray from $\vec{\rho}$ to $\vec{\rho}'$ is the same as the complex amplitude of the ray from $\vec{\rho}'$ to $\vec{\rho}$. From Fermat's principle it is apparent that the two rays in question ($\vec{\rho}$ to $\vec{\rho}'$ and $\vec{\rho}'$ to $\vec{\rho}$) travel along the same path through the channel medium but in opposite directions. Point reciprocity therefore tells us that rays going in opposite directions on the same path are equivalent (same complex amplitudes). For spatially invariant channels we have $\underset{\rightarrow}{h}(\vec{\rho}', \vec{\rho}) = F(\vec{\rho}' - \vec{\rho})$ and in our ray optics terminology this means that the complex amplitude of a ray from $\vec{\xi}$ in R_1 to $\vec{\zeta}$ in R_2 depends only on the difference $\vec{\zeta} - \vec{\xi}$. This implies that two rays are equivalent if the vectors from their source points to their output points are parallel; hence, such rays will be called parallel rays. With this ray optics interpretation in mind consider the following example. Let

$$u(\vec{\rho}) = \delta(\vec{\rho} - \vec{a}) + \delta(\vec{\rho} - \vec{b}),$$

where $\delta(\cdot)$ denotes a unit-amplitude point source. Consider a point $\vec{c}$ in R_2; since the medium is point-reciprocal, we have

$$\underset{\rightarrow}{h}(\vec{c}, \vec{a}) + \underset{\rightarrow}{h}(\vec{c}, \vec{b}) = \underset{\leftarrow}{h}(\vec{a}, \vec{c}) + \underset{\leftarrow}{h}(\vec{b}, \vec{c}). \tag{26}$$

The medium is also spatially invariant, so

$$\begin{aligned} \underset{\leftarrow}{h}(\vec{a}, \vec{c}) + \underset{\leftarrow}{h}(\vec{b}, \vec{c}) &= F(\vec{c} - \vec{a}) + F(\vec{c} - \vec{b}) \\ &= \underset{\leftarrow}{h}(-\vec{c}, -\vec{a}) + \underset{\leftarrow}{h}(-\vec{c}, -\vec{b}). \end{aligned} \tag{27}$$

As shown in Fig. 5, the vectors from the points $\vec{a}$ and $\vec{b}$ in R_1 to the point $\vec{c}$ in R_2 are antiparallel to the vectors from $-\vec{a}$ and $-\vec{b}$ in R_2 to $-\vec{c}$ in R_1. Equation 25 (or Eq. 27) shows that these antiparallel rays are equivalent. This is what we would expect, since as we have seen point reciprocity implies the equivalence of rays going in opposite directions on the same line, and spatial invariance implies that any two parallel rays are equivalent; together they imply (27). In fact, spatial invariance (see Eq. 24b) allows us to generalize (25) to

$$v(\vec{\zeta} - \vec{\rho}) = \int_{R_2} u(\vec{\zeta} - \vec{\rho}')\, \underset{\leftarrow}{h}(\vec{\rho}, \vec{\rho}')\, d\vec{\rho}' \qquad \forall\ \vec{\zeta}. \tag{28}$$

The necessity of using $u(-\vec{\rho}')$ in (25) may be removed by imposing an additional

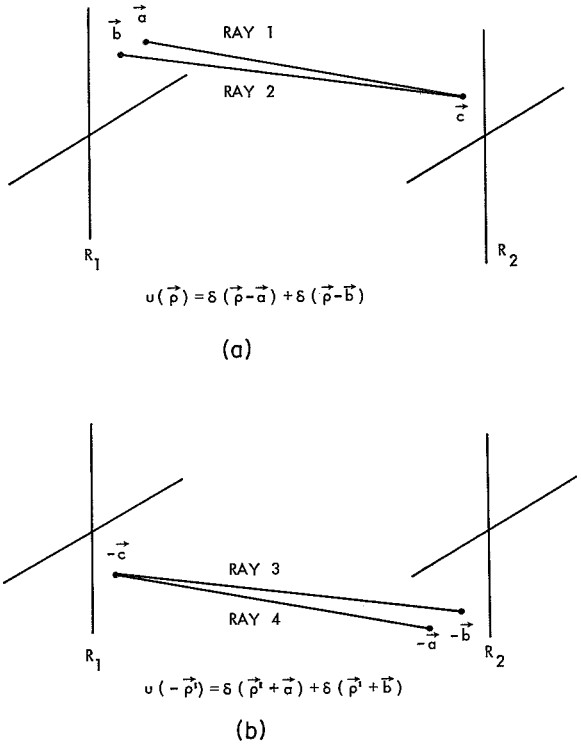

Fig. 5. Reciprocity for spatially invariant channels. Rays 1 and 4 are antiparallel, rays 2 and 3 are antiparallel.

constraint on the channel medium. Let the channel be point-reciprocal, and spatially invariant, and in addition let it be isotropic. Thus we now have

$$\underset{\rightarrow}{h}(\vec{\rho}', \vec{\rho}) = F(|\vec{\rho}'-\vec{\rho}|) = \underset{\leftarrow}{h}(\vec{\rho}, \vec{\rho}') \qquad \forall\ \vec{\rho} \in R_1,\ \vec{\rho}' \in R_2. \tag{29}$$

Using (29), we can show (see Appendix A) that if

$$v(\vec{\rho}') = \int_{R_1} u(\vec{\rho})\ \underset{\rightarrow}{h}(\vec{\rho}', \vec{\rho})\ d\vec{\rho},$$

then

$$v(\vec{\rho}) = \int_{R_2} u(\vec{\rho}')\ \underset{\leftarrow}{h}(\vec{\rho}, \vec{\rho}')\ d\vec{\rho}'. \tag{30}$$

The hierarchy of reciprocity conditions, and some of their immediate consequences, are summarized in Table 2. Before turning to the communication-oriented consequences of reciprocity, it is worth while to note that the free-space channel studied by Greenspan[4] satisfies all of the conditions in Table 2. This is easy to verify because we have explicit formulas for the impulse responses $\underset{\rightarrow}{h}$ and $\underset{\leftarrow}{h}$. The inhomogeneous medium of our

Table 2. Summary of reciprocity conditions.

NAME	CONDITION	CONSEQUENCES
DOUBLY INTEGRATED POINT RECIPROCITY	$\int_{R_2}\int_{R_1} \underline{\underline{h}}(\vec{\rho}', \vec{\rho})\, d\vec{\rho}\, d\vec{\rho}' = \int_{R_2}\int_{R_1} \underline{\underline{h}}(\vec{\rho}, \vec{\rho}')\, d\vec{\rho}\, d\vec{\rho}'$	EQUIVALENCE OF PLANE WAVE XMTR-HETERODYNE RECEIVER SYSTEMS: $R_1 \rightarrow R_2$ AND $R_2 \rightarrow R_1$
SINGLY INTEGRATED POINT RECIPROCITY	(a) $\int_{R_1} \underline{\underline{h}}(\vec{\rho}', \vec{\rho})\, d\vec{\rho} = \int_{R_1} \underline{\underline{h}}(\vec{\rho}, \vec{\rho}')\, d\vec{\rho} \quad \forall\, \vec{\rho}' \in R_2$ (b) $\int_{R_2} \underline{\underline{h}}(\vec{\rho}', \vec{\rho})\, d\vec{\rho}' = \int_{R_2} \underline{\underline{h}}(\vec{\rho}, \vec{\rho}')\, d\vec{\rho}' \quad \forall\, \vec{\rho} \in R_1$	EQUIVALENCE OF POINT-SOURCE XMTR-HETERODYNE RECEIVER TO PLANE-WAVE XMTR-POINT RECEIVER (a) point XMTR at R_2; plane-wave XMTR at R_1 (b) point XMTR at R_1; plane-wave XMTR at R_2
POINT RECIPROCITY	$\underline{\underline{h}}(\vec{\rho}', \vec{\rho}) = \underline{\underline{h}}(\vec{\rho}, \vec{\rho}') \quad \forall\, \vec{\rho} \in R_1, \vec{\rho}' \in R_2$	EQUIVALENCE OF POINT-SOURCE XMTR-POINT RECEIVER $R_1 \rightarrow R_2$ AND $R_2 \rightarrow R_1$
POINT RECIPROCITY + SPATIAL INVARIANCE	$\underline{\underline{h}}(\vec{\rho}', \vec{\rho}) = F(\vec{\rho}' - \vec{\rho}) = \underline{\underline{h}}(\vec{\rho}, \vec{\rho}')$ $\forall\, \vec{\rho} \in R_1, \vec{\rho}' \in R_2$	IF $v(\vec{\rho}') = \int_{R_1} u(\vec{\rho})\, \underline{\underline{h}}(\vec{\rho}', \vec{\rho})\, d\vec{\rho}$ THEN $v(-\vec{\rho}) = \int_{R_2} u(-\vec{\rho}')\, \underline{\underline{h}}(\vec{\rho}, \vec{\rho}')\, d\vec{\rho}'$
POINT RECIPROCITY + SPATIAL INVARIANCE + ISOTROPY	$\underline{\underline{h}}(\vec{\rho}', \vec{\rho}) = F(\lvert \vec{\rho}' - \vec{\rho} \rvert) = \underline{\underline{h}}(\vec{\rho}, \vec{\rho}')$ $\forall\, \vec{\rho} \in R_1, \vec{\rho}' \in R_2$	IF $v(\vec{\rho}') = \int_{R_1} u(\vec{\rho})\, \underline{\underline{h}}(\vec{\rho}', \vec{\rho})\, d\vec{\rho}$ THEN $v(\vec{\rho}) = \int_{R_2} u(\vec{\rho}')\, \underline{\underline{h}}(\vec{\rho}, \vec{\rho}')\, d\vec{\rho}'$
Note: Each Condition Implies All Those above It.		

turbulence model is neither spatially invariant nor isotropic, but it may still satisfy point reciprocity or one of the integrated reciprocity conditions. This is a question of importance for this work, and we shall return to it.

3.2 APODIZATION FOR POINT-RECIPROCAL CHANNELS

We shall compare the performance of the $\underrightarrow{K}$-kernel (known-channel) and Q-kernel (unknown-channel) systems described in Section II. Extensive use will be made of the properties of the $\underrightarrow{K}$, $\underleftarrow{K}$, and Q kernels, hence the reader may find it helpful to review Table 1. We assume throughout that the channel under consideration is point-reciprocal. From the definitions in Section II it is apparent that for any point-reciprocal channel

$$Q(\vec{\rho}', \vec{r}') = \underleftarrow{K}(\vec{\rho}', \vec{r}'), \qquad \forall\ \vec{\rho}', \vec{r}' \in R_2 \tag{31}$$

and

$$\zeta_i(\vec{\rho}') = \phi_i(\vec{\rho}'), \quad \alpha_i = \lambda_i. \tag{32}$$

Therefore, since ϕ_i is now an eigenfunction of Q, if we transmit ϕ_i from R_2 and use the conjugation transmitter at R_1, we receive $\lambda_i \phi_i^*$ at R_2. On the other hand, ϕ_i is an eigenfunction of $\underleftarrow{K}$, so when we transmit ϕ_i from R_2 we receive $\sqrt{\lambda_i}\ \Phi_i$ at R_1. Therefore we have shown that $\{\Phi_i^*\}$ has the following interesting property. It is a set of orthonormal functions on R_1 that maps into a set of orthonormal functions on R_2 through the linear filter $\underrightarrow{h}(\vec{\rho}', \vec{\rho})$. This is the same property that the input eigenfunctions of the $\underrightarrow{K}$ kernel, $\{\Psi_i\}$, have. In fact, it may be verified that Φ_i^* is a solution of the Fredholm integral equation with the $\underrightarrow{K}$ kernel, and that the associated eigenvalue is λ_i. So, for a point-reciprocal channel, we have

$$\Psi_i(\vec{\rho}) = \Phi_i^*(\vec{\rho}), \quad \eta_i = \lambda_i. \tag{33}$$

Recalling that the optimum waveform for apodization in the known-channel case is $\sqrt{E_t}\ \Psi_1(\vec{\rho})$, we see that if we used $\phi_1(\vec{\rho}')$ as a beacon waveform in the unknown-channel case the renormalized waveform used at R_1 would then be $\sqrt{E_t}\ \Phi_1^*(\vec{\rho})$, which is the optimum one-way result. Unfortunately, for an unknown channel there may be no way to determine $\phi_1(\vec{\rho}')$. We shall return to comment about what can be done without knowing $\phi_1(\vec{\rho}')$.

We have just shown that for reciprocal channels, knowing $\phi_1(\vec{\rho}')$ is equivalent to knowing $\Psi_1(\vec{\rho})$. We would like to obtain the weakest condition sufficient to prove this property. In Appendix A it is shown that if $Q = \underleftarrow{K}$, then we may make the identification (33), and the optimality of the Q-kernel system follows in the same manner as presented above. It is also readily apparent that any channel satisfying (33) also must satisfy (32), thereby implying that $Q = \underleftarrow{K}$. Thus $Q = \underleftarrow{K}$ is a necessary and sufficient

condition for Eq. 33.

From the definitions of Q and $\underset{\leftarrow}{K}$ it directly follows that the two kernels are equal if and only if

$$\int_{R_1} \underset{\leftarrow}{h}^*(\vec{\rho}, \vec{\rho}')(\underset{\rightarrow}{h}(\vec{r}', \vec{\rho}) - \underset{\leftarrow}{h}(\vec{\rho}, \vec{r}'))\, d\vec{\rho} = 0 \qquad \forall\, \vec{\rho}', \vec{r}' \in R_2. \tag{34}$$

That is, $\underset{\leftarrow}{h}(\vec{\rho}, \vec{\rho}')$ is orthogonal (in $L^2(R_1)$) to $\underset{\rightarrow}{h}(\vec{r}', \vec{\rho}) - \underset{\leftarrow}{h}(\vec{\rho}, \vec{r}')$ $\forall\, \vec{\rho}', \vec{r}' \in R_2$. This orthogonality condition is somewhat weaker than point reciprocity, as may be seen from applying the Schwarz inequality to (34). We obtain

$$0 = \int_{R_1} \underset{\leftarrow}{h}^*(\vec{\rho}, \vec{\rho}')(\underset{\rightarrow}{h}(\vec{r}', \vec{\rho}) - \underset{\leftarrow}{h}(\vec{\rho}, \vec{r}'))\, d\vec{\rho}$$

$$\leq \left(\int_{R_1} \left| \underset{\leftarrow}{h}(\vec{\rho}, \vec{\rho}') \right|^2 d\vec{\rho} \right)^{1/2} \left(\int_{R_1} \left| \underset{\rightarrow}{h}(\vec{r}', \vec{\rho}) - \underset{\leftarrow}{h}(\vec{\rho}, \vec{r}') \right|^2 d\vec{\rho} \right)^{1/2} \qquad \forall\, \vec{\rho}', \vec{r} \in R_2. \tag{35}$$

Hence a sufficient, but not necessary, condition for $Q = \underset{\leftarrow}{K}$ is

$$\int_{R_1} \left| \underset{\rightarrow}{h}(\vec{r}', \vec{\rho}) - \underset{\leftarrow}{h}(\vec{\rho}, \vec{r}') \right|^2 d\vec{\rho} = 0 \qquad \forall\, \vec{r}' \in R_2. \tag{36}$$

In other words, $\underset{\rightarrow}{h}(\vec{r}', \vec{\rho}) = \underset{\leftarrow}{h}(\vec{\rho}, \vec{r}')$ in $L^2(R_1)$.

We have derived a relation, (33), between the eigenfunctions and eigenvalues of the $\underset{\rightarrow}{K}$ and $\underset{\leftarrow}{K}$ kernels that is valid for point-reciprocal channels. A necessary and sufficient condition for the validity of (33) has also been derived. These results are summarized in Table 3. The most important result is that (33) allows us to prove the existence of an unknown-channel (Q-kernel) system that performs as well as the optimal known-channel system.

3.3 OPTIMAL SPATIAL MODULATION TECHNIQUES

We return now to the problem of selecting a beacon signal for a Q-kernel communication system, when transmitting through a point-reciprocal channel. We have seen that we can achieve the optimal one-way energy transfer from R_1 to R_2 if we can use $\phi_1(\vec{\rho}')$ as the beacon signal. We shall now discuss what can be done to obtain $\phi_1(\vec{\rho}')$ for two different cases of interest, a "deep-space" channel, and a point-to-point channel on the Earth.

First, consider the deep-space channel, shown in Fig. 6. We assume that all of the inhomogeneities (turbulent eddies) are confined to a small region near R_1 (on the Earth), and that the rest of the path to R_2 (the spacecraft) is through free space. We have called this a deep-space channel, to emphasize the fact that the path length from the top of the atmosphere to the spacecraft is quite long. How long it must be for our purposes must

Table 3. Consequence of reciprocity.

I.	IF $\underset{\leftarrow}{h}(\vec{\rho}', \vec{\rho}) = \underset{\leftarrow}{h}(\vec{\rho}, \vec{\rho}')$ $\forall\ \vec{\rho} \in R_1,\ \vec{\rho}' \in R_2$ THEN $Q(\vec{\rho}', \vec{r}') = \underset{\leftarrow}{K}(\vec{\rho}', \vec{r}')$ $\forall\ \vec{\rho}', \vec{r}' \in R_2$
II.	IF AND ONLY IF $Q(\vec{\rho}', \vec{r}') = \underset{\leftarrow}{K}(\vec{\rho}', \vec{r}')$ $\forall\ \vec{\rho}', \vec{r}' \in R_2$ THEN $\zeta_i(\vec{\rho}') = \phi_i(\vec{\rho}'),\quad \alpha_i = \lambda_i$ $\forall\ i$
III.	IF AND ONLY IF $Q(\vec{\rho}', \vec{r}') = \underset{\leftarrow}{K}(\vec{\rho}', \vec{r}')$ $\forall\ \vec{\rho}', \vec{r}' \in R_2$ THEN $\Psi_i(\vec{\rho}) = \Phi_i^*(\vec{\rho}),\quad \eta_i = \lambda_i$ $\forall\ i$ AND WE HAVE THE FOLLOWING CHANNEL MODELS $\sqrt{\lambda_i}\ \Phi_i(\vec{\rho}) \leftarrow \underset{\leftarrow}{h}(\vec{\rho}, \vec{\rho}') \leftarrow \phi_i(\vec{\rho}')$ $\Phi_i^*(\vec{\rho}) \rightarrow \underset{\leftarrow}{h}(\vec{\rho}', \vec{\rho}) \rightarrow \sqrt{\lambda_i}\ \phi_i^*(\vec{\rho}')$

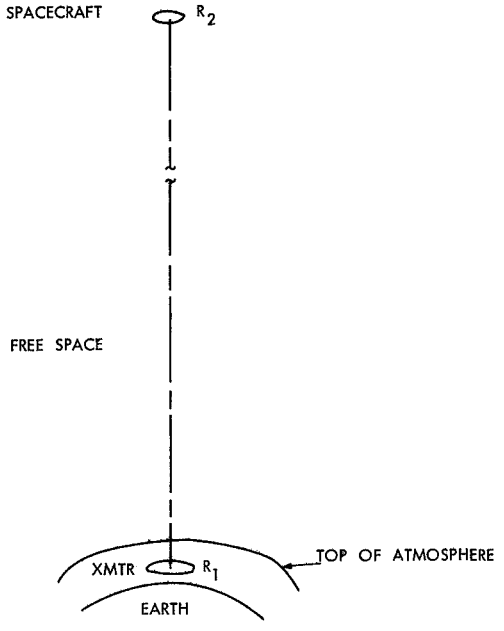

Fig. 6. Deep-space apodization problem.

be considered. Suppose the distance involved is such that when a beacon $v(\vec{\rho}')$ is transmitted from R_2 the field received over a large planar region tangent to the top of the atmosphere and centered on the line from R_2 to R_1 is a normally incident uniform plane wave with amplitude proportional to

$$\int_{R_2} v(\vec{\rho}')\, d\vec{\rho}'. \tag{37}$$

We assume that regardless of the field sent from R_2 the field received at R_1 depends only on the field in that region at the top of the atmosphere where the assumption leading to (37) is valid. We have assumed that there is a large planar region at the top of the atmosphere subtending essentially no solid angle at the spacecraft compared with the far-field beamwidth of the R_2 aperture. (Specifically, we require that the diameter of the region of interest at the top of the atmosphere be much smaller than the minimum of $\sqrt{z\lambda}$ and $z\lambda/d$, where z is the path length from the top of the atmosphere to the spacecraft, λ is the wavelength of the radiation, and d is the diameter of the R_2 aperture.) Furthermore, for any beacon transmitted from R_2, the field received at R_1 only depends on the field in the region at the top of the atmosphere that we have just defined. We shall comment on these assumptions eventually. Let us first consider their consequences for finding ϕ_1, the optimum beacon signal.

Since the field at the top of the turbulence will be a normally incident uniform plane wave (at least as far as R_1 is concerned) regardless of the $v(\vec{\rho}')$ that we choose and $\phi_1(\vec{\rho}')$ is the eigenfunction of $\underset{\leftarrow}{K}$ that maximizes the energy received at R_1, $\phi_1(\vec{\rho}')$ must also maximize the energy received at the top of the atmosphere. The energy received at the top of the atmosphere is proportional to

$$\left| \int_{R_2} v(\vec{\rho}')\, d\vec{\rho}' \right|^2$$

and from the Schwarz inequality we have

$$\left| \int_{R_2} v(\vec{\rho}')\, d\vec{\rho}' \right|^2 \leq \int_{R_2} d\vec{\rho}' \int_{R_2} |v(\vec{\rho}')|^2\, d\vec{\rho}'$$

$$= A_2. \tag{38}$$

Equality holds in (38) if and only if

$$v(\vec{\rho}') = \frac{e^{j\gamma}}{\sqrt{A_2}} \qquad \forall\ \vec{\rho}' \in R_2, \tag{39}$$

where γ is a real constant.

Thus, for the deep-space channel, $\phi_1(\vec{\rho}')$ is a normally incident unit-energy uniform plane wave, regardless of the state of the turbulence, and from section 3.2 we see that the Q-kernel system with this beacon will transfer the maximum energy possible from R_1 to R_2.

Let us return to the assumptions that led to the derivation of Eq. 39. In the absence of any ducting phenomenon in the atmosphere it is quite reasonable to assume that for a finite aperture on the ground there is a large planar region tangent to the top of the atmosphere through which any field energy from the spacecraft that reaches R_1 must pass. By ducting we mean any atmospheric phenomenon that would radically alter the direction of propagation of any incident radiation. Thus in the absence of ducting the distance to the spacecraft need only be long enough that the region of interest at the top of the atmosphere subtends essentially zero solid angle at the spacecraft compared with the far-field beamwidth of the R_2 aperture. For typical apertures on the ground and the spacecraft this condition could be satisfied at synchronous altitude. On the other hand, if there are some atmospheric phenomena that disqualify the previous assumption, the proof of (39) will still be valid if the path length is such that the entire Earth subtends essentially zero solid angle at the spacecraft compared with the far-field beamwidth of R_2. Hereafter, when we refer to a deep-space channel we shall mean that the path length is such that the statements leading to (37) and the proof of (39) are valid. As we have seen, this may be true at synchronous altitude, which ordinarily would not be called a deep-space channel.

Let us now consider what happens when the path length is not extremely long, the

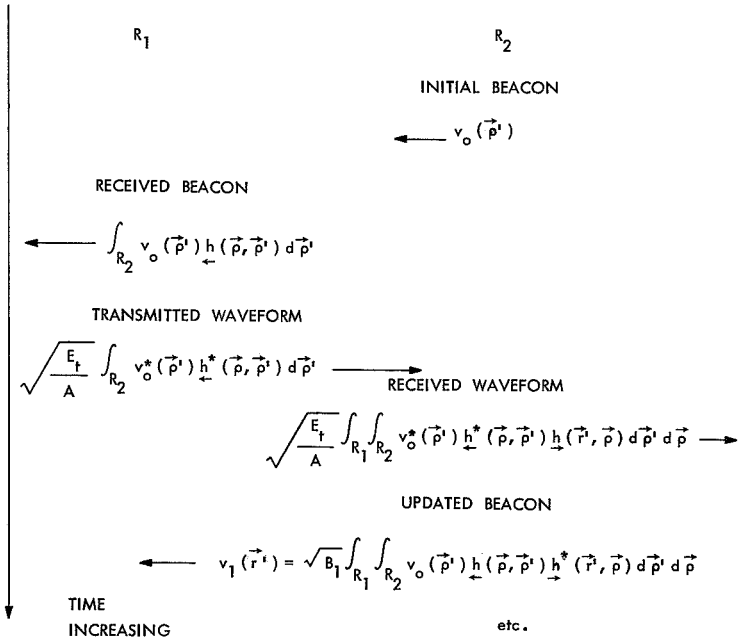

Fig. 7. Adaptive beacon system. (Arrows denote direction of propagation.)

point-to-point channel. For this channel neither $\phi_1(\vec{\rho}')$ nor $\Phi_1^*(\vec{\rho})$ will be uniform plane waves, and since, conceptually, it is as difficult to solve for ϕ_1 as it is to solve for Φ_1^*, we cannot make implementing an optimal system any easier by going to a two-way system. A two-way system can be designed, however, to give near optimal performance (in terms of energy transfer). Suppose an initial beacon signal $v_o(\vec{\rho}')$ is sent from R_2 to R_1 and the conjugation operation transmitter is used at R_1, as described in section 2.3. When the signal returns to R_2, the beacon transmitter "turns around" this received signal, and uses this as an updated beacon, $v_1(\vec{\rho}')$, after proper renormalization. This adaptation process (see Fig. 7) continues until the over-all system is stabilized with a fixed beacon signal $v_F(\vec{\rho}')$. This system will then provide near optimal performance, as can be seen in the following way. Since $\{\phi_i\}$ are complete on R_2, we may express $v_o(\vec{\rho}')$ in the form

$$v_o(\vec{\rho}') = \sum_{i=1}^{\infty} v_{o_i} \phi_i(\vec{\rho}'), \tag{40}$$

where

$$v_{o_i} = \int_{R_2} v_o(\vec{\rho}')\ \phi_i^*(\vec{\rho}')\ d\vec{\rho}'.$$

We shall have occasion to use infinite summations; in all cases this notation should be interpreted as the limit of the partial sums in the L^2 space on which the summands are defined. The beacon signal as received at R_1, therefore, is

$$\sum_{i=1}^{\infty} v_{o_i} \sqrt{\lambda_i}\ \Phi_i(\vec{\rho}), \tag{41}$$

and the signal received at R_2 is

$$\sqrt{\frac{E_t}{A}} \sum_{i=1}^{\infty} v_{o_i}^* \lambda_i \phi_i^*(\rho'), \tag{42}$$

where A is a constant that normalizes the field transmitted from R_1 to have energy E_t. As the process of adaptation continues, the communication system that we have described will tend to use only those components in the expansion of $v_o(\vec{\rho}')$ that propagate through the channel with (essentially) no attenuation. In particular, if $v_k(\vec{\rho}')$ denotes the beacon signal used after k R_2-R_1-R_2 round trips, then we have

$$v_k(\vec{\rho}') = \sqrt{B_k} \sum_{i=1}^{\infty} v_{o_i} \lambda_i^k \phi_i(\vec{\rho}') \qquad k = 1, 2, 3, \ldots, \tag{43}$$

where B_k is a constant that normalizes $v_k(\vec{\rho}')$ to have unit energy. Since we have

$$0 \leq \lambda_i \leq 1,$$

it is apparent that as the adaptation process continues, the beacon signal converges (in $L^2(R_2)$) to a signal that yields the optimum energy transfer from R_1 to R_2. (This statement requires $v_{o_1} \neq 0$. That is,

$$\int_{R_2} v_o(\vec{\rho}')\, \phi_1^*(\vec{\rho}')\, d\vec{\rho}' \neq 0.$$

We assume that $v_o(\vec{\rho}')$ satisfies this condition.) Moreover, this convergence is such that the energy performance increases monotonically as time goes on, and thus an adaptive system could be built that would continue changing the beacon until a certain level of performance, say $0.9E_t$ received at R_2, is achieved and then fix the beacon. Note that the results obtained here apply to a time-invariant channel, in Section VII they will be generalized to the time-variant atmosphere.

Let us consider how long it takes for the convergence that we are talking about to take place. Suppose that the number of degrees of freedom of the channel, D_f, satisfies the following assumptions:

1. $D_f > 1$
2. $\lambda_i \equiv 1 \qquad \forall\ i \leq D_f$
3. $\lambda_i \equiv 0 \qquad \forall\ i > D_f.$

The first of these assumptions means that the two antennas are in the so-called near field, and the second and third assumptions are idealizations of the properties of D_f. If D_f has these properties, then (43) reduces to

$$v_k(\vec{\rho}') = \sqrt{B} \sum_{i=1}^{D_f} v_{o_i} \phi_i(\vec{\rho}') \qquad k = 1, 2, 3, \ldots \tag{44}$$

and the convergence is completed in a single round trip. If any one of these assumptions is not satisfied, then the convergence of the beacon signal will take an infinite number of round trips, although if D_f is greater than one, and assumptions 2 and 3 are approximately true, then the convergence is "essentially" complete in one or two round trips.

Even if the three assumptions are satisfied, and (44) is the beacon signal that we use, there is a difference between the known-channel and the unknown-channel situations. In a known-channel case with D_f degrees of freedom there are D_f orthonormal functions propagating through the channel without loss. The adaptive system that we have just

described allows us to obtain one unit-energy function that propagates through the channel without attenuation, but there seems to be no way of obtaining the other $D_f - 1$ eigenfunctions of unit eigenvalue. This loss of parallel channel capability does not affect our ability to transfer energy from R_1 to R_2, but it does preclude our obtaining D_f useful spatial degrees of freedom for improving the reliability of information transmission. In other words, although our adaptive beacon system can obtain all of the necessary state information from the channel for apodization, it does not tell us all there is to know about the channel. Note that the loss of parallel channel capability is unique to the point-to-point channel because in the deep-space case there is only one branch to the parallel channel model with nonzero gain (see section 6.2).

We have now shown that for communicating through a fixed reciprocal channel a Q-kernel system exists which will achieve optimal energy transfer in the deep-space case, and a system exists that achieves arbitrarily close to optimal energy transfer in point-to-point applications on the Earth. It is interesting to see how our results change if the channel does not satisfy point reciprocity or even the weaker condition (34).

3.4 APPROXIMATELY RECIPROCAL CHANNELS

For some channels that we might wish to study, we may not be able to prove point reciprocity, or even the orthogonality condition (34). We would like to say that if, in some sense, $Q \approx \underset{\leftarrow}{K}$, then our results concerning the optimality of the unknown-channel feedback system would still hold, at least to some degree of approximation. We shall

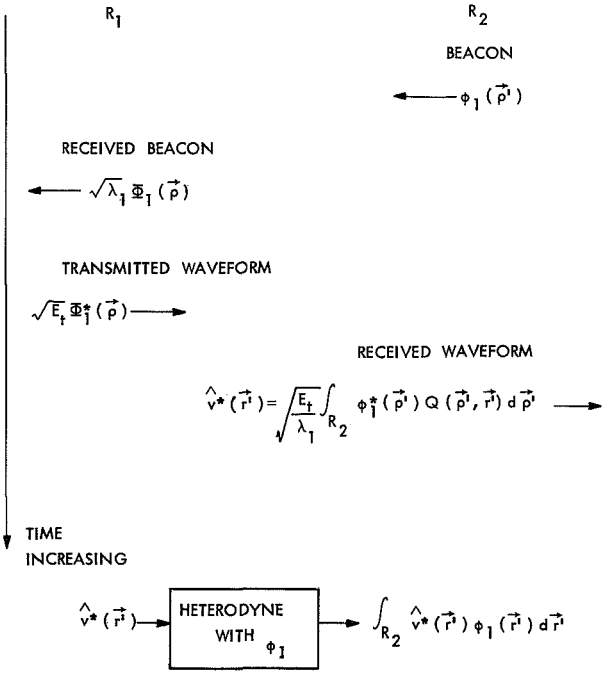

Fig. 8. Performance bound for $Q \neq \underset{\leftarrow}{K}$. (Arrows denote direction of propagation.)

derive a performance bound in terms of the difference kernel

$$R(\vec{\rho}', \vec{r}') = Q(\vec{\rho}', \vec{r}') - \underset{\leftrightarrow}{K}(\vec{\rho}', \vec{r}'). \tag{45}$$

Let the orthonormal eigenfunctions and the eigenvalues of the R kernel be denoted $\xi_i(\vec{\rho}')$ and μ_i. Then we may express the Q kernel in the form[14]

$$Q(\vec{\rho}', \vec{r}') = \sum_{i=1}^{\infty} \left(\mu_i \xi_i(\vec{\rho}')\, \xi_i^*(\vec{r}') + \lambda_i \phi_i(\vec{\rho}')\, \phi_i^*(\vec{r}')\right). \tag{46}$$

We shall lower-bound the energy in the ϕ_1^* component of the field received at R_2 after the round-trip transmission scheme (R_2 to R_1 to R_2) shown in Fig. 8. This result will upper-bound the degradation in the optimality of the Q-kernel system caused by $Q \neq \underset{\leftrightarrow}{K}$. As shown in Fig. 8, the received beacon field at R_1 is "turned around" and renormalized, so that the field received at R_2 is

$$\hat{v}^*(\vec{r}') = \sqrt{E_t \lambda_1}\ \phi_1^*(\vec{r}') + \sqrt{\frac{E_t}{\lambda_1}} \sum_{i=1}^{\infty} \mu_i \left(\int_{R_2} \xi_i(\vec{\rho}')\, \phi_1^*(\vec{\rho}')\, d\vec{\rho}'\right) \xi_i^*(\vec{r}'). \tag{47}$$

The ϕ_1^* component of this field, therefore, is

$$\int_{R_2} \hat{v}^*(\vec{r}')\, \phi_1(\vec{r}')\, d\vec{r}'$$

$$= \sqrt{E_t \lambda_1} + \sqrt{\frac{E_t}{\lambda_1}} \sum_{i=1}^{\infty} \mu_i \left| \int_{R_2} \xi_i(\vec{\rho}')\, \phi_1^*(\vec{\rho}')\, d\vec{\rho}' \right|^2 \tag{48}$$

and the energy in this component is

$$\left| \int_{R_2} \hat{v}^*(\vec{r}')\, \phi_1(\vec{r}')\, d\vec{r}' \right|^2$$

$$= \left| \sqrt{E_t \lambda_1} + \sqrt{\frac{E_t}{\lambda_1}} \sum_{i=1}^{\infty} \mu_i \left| \int_{R_2} \xi_i(\vec{\rho}')\, \phi_1^*(\vec{\rho}')\, d\vec{\rho}' \right|^2 \right|^2$$

$$\geqslant \left(\sqrt{E_t \lambda_1} - \sqrt{\frac{E_t}{\lambda_1}} \sum_{i=1}^{\infty} |\mu_i| \left| \int_{R_2} \xi_i(\vec{\rho}')\, \phi_1^*(\vec{\rho}')\, d\vec{\rho}' \right|^2 \right)^2, \tag{49}$$

where we have used the triangle inequality. Expanding the right-hand side of (49), we obtain

$$\left| \int_{R_2} \hat{v}^*(\vec{r}') \, \phi_1(\vec{r}') \, d\vec{r}' \right|^2$$

$$\geq E_t \left(\lambda_1 - 2 \sum_{i=1}^{\infty} |\mu_i| \left| \int_{R_2} \xi_i(\vec{\rho}') \, \phi_1^*(\vec{\rho}') \, d\vec{\rho}' \right|^2 \right)$$

$$+ \frac{E_t}{\lambda_1} \left(\sum_{i=1}^{\infty} |\mu_i| \left| \int_{R_2} \xi_i(\vec{\rho}') \, \phi_1^*(\vec{\rho}') \, d\vec{\rho}' \right|^2 \right)^2$$

$$\geq E_t \left(\lambda_1 - 2 \sum_{i=1}^{\infty} |\mu_i| \left| \int_{R_2} \xi_i(\vec{\rho}') \, \phi_1^*(\vec{\rho}') \, d\vec{\rho}' \right|^2 \right)$$

$$\geq E_t (\lambda_1 - 2 \max_i |\mu_i|)$$

$$\geq E_t \left(\lambda_1 - 2 \max_i \left| \iint_{R_2} \xi_i^*(\vec{\rho}') \, R(\vec{\rho}', \vec{r}') \, \xi_i(\vec{r}') \, d\vec{\rho}' d\vec{r}' \right| \right). \tag{50}$$

Note that if the channel were reciprocal, then the energy received in the ϕ_1^* component would be $E_t \lambda_1$, so the loss in performance caused by $Q \neq \underset{\leftarrow}{K}$ is bounded by the second term in (50).

The bound that we have derived may not be the strongest possible bound that could be obtained, but it is presented here as one way of measuring how the Q-kernel performance converges to $E_t \lambda_1$ as the channel gets more and more "reciprocal," and the R kernel approaches the null function.

IV. TURBULENT ATMOSPHERIC CHANNEL

4.1 EFFECTS OF TURBULENCE

The central problem of this research is to find ways of improving optical communication through atmospheric turbulence. Atmospheric turbulence causes the major limitation on the performance of optical communication systems transmitting through the clear atmosphere. We shall now summarize those aspects of the turbulent channel that are relevant to our study.

The atmosphere is not in equilibrium, it is constantly subject to turbulent mixing of inhomogeneities of varying sizes. These inhomogeneities cause the index of refraction, $n(\vec{r}, t)$, to be a random function of space and time, and the fluctuations in n, in turn, cause random perturbations in any laser beam propagating through the atmosphere. Qualitatively, the effects of the turbulence on a received beam may be classified as follows.[15]

Beam Steering. The beam may be deviated from the line of sight, thereby possibly placing it entirely outside the receiving aperture.

Image Dancing. Random variations in the angle of arrival of the beam cause images to execute a two-dimensional random walk in the focal plane of a collecting lens.

Beam Spreading. The cross section of the received beam may vary randomly in size.

Image Blurring. A random crumbling of the received wavefront causes images in the focal plane to appear blurred.

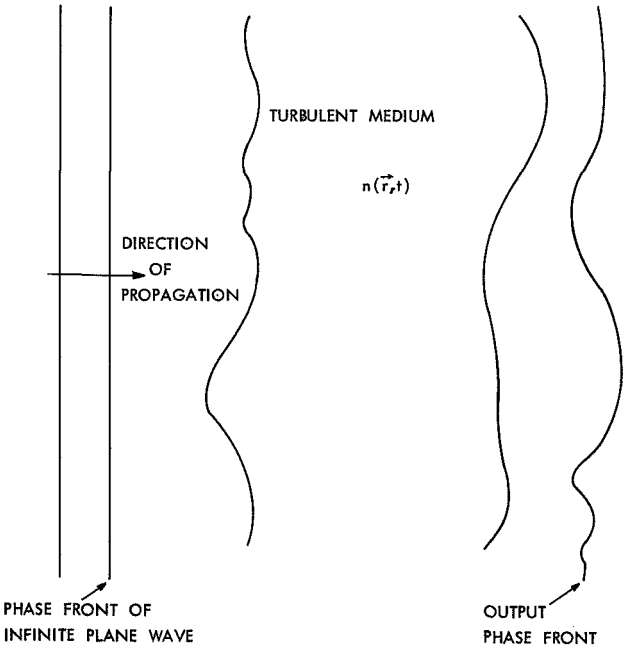

Fig. 9. z-model geometry.

Scintillation. Local variations in received amplitude degrade received signal modulation.

Phase Fluctuations. Temporal fluctuations in the phase of the waveform produce a spurious phase modulation.

Much work has been devoted to obtaining statistical characterizations of the turbulence,[2,16-19] and studying the turbulent atmosphere as a communication channel.[1,3,20] With proper foresight we have collected those results that will be of use in Sections V-VII.

A fairly useful way of studying the effects of turbulence is the $\underline{z}$ model. Assume that an infinite linearly polarized uniform plane wave is normally incident on a slab of turbulence (see Fig. 9). Since it is known that the turbulence has no depolarizing effect on the incident radiation,[21] we need only consider the incident polarization component. For that component the electric field is then

$$E(\vec{r},t) = \mathrm{Re}\left[\underline{E}(\vec{r},t)\, e^{j\omega_c t}\right], \tag{51}$$

with the usual complex field amplitude representation. Let $\underline{E}_o(\vec{r})$ denote the complex field amplitude that would have existed in the absence of turbulence. We define the channel disturbance, $\underline{z}(\vec{r},t)$, as follows

$$\underline{z}(\vec{r},t) = \frac{\underline{E}(\vec{r},t)}{\underline{E}_o(\vec{r})}. \tag{52}$$

It is convenient to write $\underline{z}(\vec{r},t)$ in the form

$$\underline{z}(\vec{r},t) = e^{\underline{\gamma}(\vec{r},t)} = \exp(\chi(\vec{r},t)+j\phi(\vec{r},t)), \tag{53}$$

where $\chi(\vec{r},t)$ and $\phi(\vec{r},t)$ are the real and imaginary parts of the complex process $\underline{\gamma}(\vec{r},t)$. Using the Central limit theorem, we may argue that $\underline{\gamma}(\vec{r},t)$ is a complex Gaussian random process and hence $\underline{z}(\vec{r},t)$ a complex lognormal process,[16] in which case the statistics of $\underline{z}(\vec{r},t)$ are completely characterized by the second order statistics of χ and ϕ.

At this point it is worth showing why the $\underline{z}$ model was not chosen as the point of departure for this work. This research is concerned with the use of spatial modulation to improve the quality of optical communication through the atmosphere. In the definition (52) of $\underline{z}$ it is apparent that $\underline{z}$ depends upon what spatial waveform was used at the transmitter. Thus any statistics for $\underline{z}$ must also be dependent upon the spatial waveform used at the input. This coupling between the channel model and the input field makes analysis of spatially modulated systems difficult. Furthermore, it we examine

analytic expressions for $\underline{z}(\vec{r}, t)$ obtained through the Rytov approximation,[16] we find that the $\underline{z}$ model is not a linear system when spatial modulation is employed. For these reasons, we shall only employ $\underline{z}$-model results for infinite plane-wave sources, where the model seems to adequately predict experimental results.[16]

4.2 INSTANTANEOUS TURBULENCE MODEL

Having qualitatively discussed the turbulent channel, we now show how the model developed in Section II may be applied to the time-variant atmosphere. We have seen that assuming a scalar channel is valid. The only issue that remains is the time variation of the atmosphere.

The temporal behavior of the turbulence may be handled as follows. If the path length of interest (center-to-center distance between R_1 and R_2) is short enough that the atmosphere is essentially "frozen" during one propagation time (the time taken by a signal sent from R_1 to reach R_2), we may model the atmosphere as undergoing a succession of fixed states. Thus if the input spatial waveform (at R_1) is $u(\vec{\rho})$, then the output waveform will be

$$v(\vec{\rho}'; t) = \int_{R_1} u(\vec{\rho})\, \underline{\underline{h}}(\vec{\rho}', \vec{\rho}; t)\, d\vec{\rho}, \tag{54}$$

where $\underline{\underline{h}}(\vec{\rho}', \vec{\rho}; t)$ denotes the state of the atmospheric channel at time t, subject to the condition that the propagation time be small compared with the characteristic time (coherence time) of the turbulence. A corresponding expression exists for the propagation from R_2 to R_1. Since it appears that the turbulence has a power spectrum that is limited to frequencies below 1 kHz, and possibly extending only to a few hundred Hz,[22] most path lengths of interest will satisfy the necessary propagation condition. Specifically, by allowing 0.1 ms of propagation time as a worst case, all path lengths less than 30 km satisfy the propagation condition. Using an exponential atmosphere model with a decay constant of 3 km,[17] we see that the fixed-state model will apply to Earth-to-space channels with near-zenith paths through the atmosphere. For point-to-point channels on the ground there may be situations in which the fixed-state model will not be a good one.

In studying the atmospheric channel we shall place primary emphasis on deep-space applications, since it is here that the narrow beamwidths attainable (in the absence of turbulence) with laser equipment could be used to greatly improve communication.

V. APODIZATION FOR DEEP-SPACE CHANNELS

5.1 Problem Specification

We shall now generalize the results of Section III to time-variant deep-space channels. There we studied a time-invariant point reciprocal channel. We shall now model the atmosphere as undergoing a succession of fixed states, but we shall not assume channel reciprocity at the outset. A great deal of what we have to say will not depend on our ability to prove that the turbulent atmosphere is reciprocal.

We consider an Earth-to-space communication link using a near-zenith path through the atmosphere. The geometry of this system is shown in Fig. 10, and it is somewhat different from the structure previously studied. The aperture R_1 is the transmitting aperture on the ground, as before, but R_2 is now an imaginary "window" at the top of the atmosphere. We assume that R_1 and R_2 are both circular apertures of diameters D and d, respectively. Also, we assume that the plane of R_1 is perpendicular to the line connecting the center of R_1 to the spacecraft, and furthermore that the center of R_2 lies along this line, and the R_2 plane is parallel to the R_1 plane.

The impulse responses $\underset{\rightarrow}{h}(\vec{\rho}', \vec{\rho}; t)$ and $\underset{\leftarrow}{h}(\vec{\rho}, \vec{\rho}'; t)$ determine propagation from R_1 to R_2 and R_2 to R_1 as before, although R_2 is no longer the receiving terminal. For notational convenience we suppress the time dependence of the impulse responses and the output fields whenever it is clear that we are talking about a single fixed state of the atmosphere. Referring to Fig. 10, we see why R_2 was placed at the top of the atmosphere instead of on the spacecraft. Ultimately we want to apply the results for two-way (Q-kernel) systems to the time-variant atmosphere. This will require that the

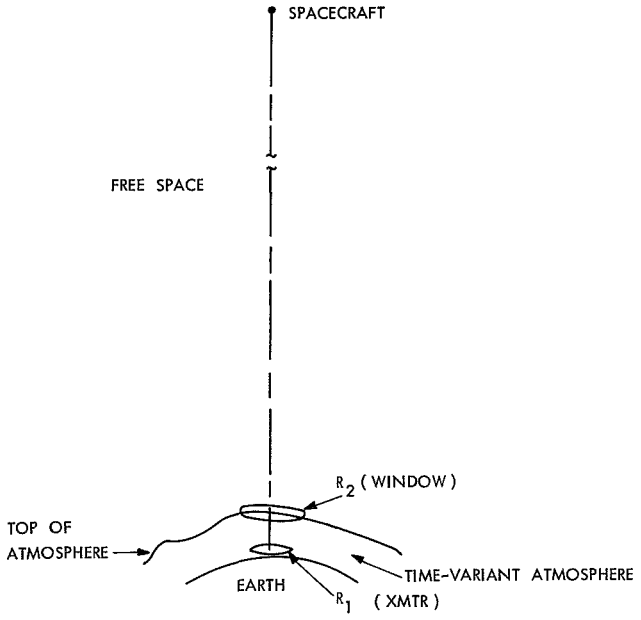

Fig. 10. Deep-space apodization problem.

atmospheric state be essentially fixed during a round-trip propagation time from R_2 to R_1 to R_2, a condition that cannot be satisfied with R_2 on the spacecraft.

A discussion of how long a path was a "deep-space" channel has been given in section 3.3. For the moment, let us only assume that the spacecraft is sufficiently far away that when a signal is sent from R_1 the field received at the spacecraft is proportional to the normally incident plane-wave component of the field at the window R_2 (under the assumption that the field is zero outside of R_2). In the light of this assumption, we shall consider the following apodization problem. A unit amplitude normally incident plane wave is transmitted from R_2 to R_1 as a beacon. On the ground we observe the received beacon field, and adapt our transmitter accordingly. The waveform transmitted from R_1 is constrained to have energy E_t, and we seek to maximize the energy in the normally incident plane-wave component of the field at R_2.

Let us see why this is a problem of interest. Subject to our path-length assumption, maximizing the energy in the normally incident plane wave component at R_2 maximizes the energy received at the apacecraft. Strictly speaking, this is not true unless the field at the top of the atmosphere is zero outside of R_2. This requirement may be eliminated by regarding R_2 as the infinite plane, and assuming an infinite plane wave beacon. It is convenient for several reasons to start with R_2 finite, and study the behavior of the resulting system as the size of R_2 is varied. Ultimately, we shall see that for most practical systems the beacon will be effectively of infinite extent. The optimal system that we seek distorts the waveform used at R_1 to account for the effects of the turbulence in such a way that the field leaving the atmosphere is a normally incident plane wave over the window R_2. In this sense, we are studying an adaptive equalization problem.

Note that the apodization problem specified above is identical to the two-way apodization problem that we studied earlier in section 2.3, with one exception. In the problem just specified the beacon waveform is not a parameter under the control of the system designer. It is interesting to note that in section 2.3 heterodyning at the receiver (R_2) was introduced rather arbitrarily, whereas heterodyning (extracting the normally incident plane-wave component) in the problem that we are now discussing arises naturally out of the propagation from R_2 to the spacecraft.

5.2 Q-Kernel Apodization System for a Single State

The great similarity between the problems described in sections 2.3, and 5.1, together with the results for reciprocal channels in Section III, lead us to examine a system that uses a conjugation ("turn around") transmitter at R_1 as a possible solution to our apodization problem. For such a system we may immediately evaluate the energy, E_r, in the normally incident plane-wave component of the field received at R_2 (for a single atmospheric state). We have

$$E_r = \frac{E_t \left| \iint_{R_2} Q(\vec{\rho}', \vec{r}')\, d\vec{\rho}' d\vec{r}' \right|^2}{A_2 \iint_{R_2} \underset{\leftrightarrow}{K}(\vec{\rho}', \vec{r}')\, d\vec{\rho}' d\vec{r}'}. \tag{55}$$

We shall spend considerable effort studying this energy expression.

5.21 Asymptotic Behavior of $\underset{\leftrightarrow}{K}$ and Q

We begin our evaluation of E_r by studying the asymptotic behavior of the $\underset{\leftrightarrow}{K}$ and Q kernels as D becomes infinite (R_1 becomes the entire plane). From their respective definitions (see Table 1) it is apparent that both of these kernels are functions of R_1. To make this dependence explicit, we use the notation $\underset{\leftrightarrow}{K}_{R_1}$ and Q_{R_1} to denote these kernels for a particular finite aperture R_1, and $\underset{\leftrightarrow}{K}_\infty$ and Q_∞ to denote the limit kernels that result as D approaches infinity. We shall prove the following lemma.

Lemma

Let $v(\vec{\rho}')$ be a unit energy signal on R_2, and $V(\vec{F}')$ be its spatial Fourier transform. Let ϵ be defined as

$$\epsilon = \int_{|\vec{F}| > \frac{1}{\lambda}} |V(\vec{F}')|^2 d\vec{F}'. \tag{56}$$

It follows then that

$$\iint_{R_2} v^*(\vec{\rho}')\, \underset{\leftrightarrow}{K}_\infty(\vec{\rho}', \vec{r}')\, v(\vec{r}')\, d\vec{\rho}' d\vec{r}' = 1 - \epsilon \tag{57}$$

$$\iint_{R_2} v^*(\vec{\rho}')\, Q_\infty(\vec{\rho}', \vec{r}')\, v(\vec{r}')\, d\vec{\rho}' d\vec{r}' = 1 - \epsilon. \tag{58}$$

Proof: Before getting into the details of the proof, let us examine the meaning of the lemma. The quantity ϵ is the energy in $v(\vec{\rho}')$ at spatial frequencies above $1/\lambda$. It is well known that these spatial frequencies correspond to waves that do not propagate, the so-called evanescent waves. These waves are exponentially attenuated in the z direction (R_2 to R_1 direction). Equation 57 says that all of the energy in the propagating waves falls on the infinite R_1 plane. Equation 58 says that a Q-kernel system with infinite D and $v(\vec{\rho}')$ as a beacon will return all of the energy in the propagating components of $v(\vec{\rho}')$ to R_2. Thus prepared, let us prove the lemma.

We shall prove (57) first. The energy received at R_1 when $v(\vec{\rho}')$ is transmitted from R_2 is

$$\int_{R_1} \left| \int_{R_2} v(\vec{\rho}')\, \underset{\leftrightarrow}{h}(\vec{\rho}, \vec{\rho}')\, d\vec{\rho}' \right|^2 d\vec{\rho} = \iint_{R_2} v^*(\vec{\rho}')\, \underset{\leftrightarrow}{K}_{R_1}(\vec{\rho}', \vec{r}')\, v(\vec{r}')\, d\vec{\rho}' d\vec{r}'. \tag{59}$$

It is known that the turbulence does not absorb any energy from an incident beam, nor is any energy scattered far out of the beam's initial direction.[22] Therefore the energy received at R_1 (the infinite plane) must be all of the energy in the propagating components of $v(\vec{\rho}')$ plus whatever energy from the evanescent waves that reaches R_1. For path lengths of kilometers (the case of interest) we may neglect any contribution to the received energy from evanescent waves; thus, as D becomes infinite

$$\iint_{R_2} v^*(\vec{\rho}')\, \underset{\leftrightarrow}{K}_{R_1}(\vec{\rho}', \vec{r}')\, v(\vec{r}')\, d\vec{\rho}' d\vec{r}' \longrightarrow 1 - \epsilon$$

which proves (57).

Equation 58 is proved as follows. Let $u(\vec{\rho})$ be the waveform received at R_1 when $v(\vec{\rho}')$ is transmitted from R_2. Let $\hat{v}^*(\vec{r}')$ be the field received over the infinite R_2 plane when $u^*(\vec{\rho})$ is transmitted from R_1. Then we have (see Table 1)

$$\iint_{R_2} v^*(\vec{\rho}')\, Q_{R_1}(\vec{\rho}', \vec{r}')\, v(\vec{r}')\, d\vec{\rho}' d\vec{r}' = \int_{R_2} \hat{v}^*(\vec{r}')\, v(\vec{r}')\, d\vec{r}'. \tag{60}$$

Let $\hat{V}(\vec{F}')$ be the spatial Fourier transform of $\hat{v}^*(\vec{r}')$. We shall prove that in the limit $D = \infty$

$$\hat{V}(\vec{F}') = \begin{cases} V^*(-\vec{F}') & |\vec{F}'| \leq \frac{1}{\lambda} \\ 0 & |\vec{F}'| > \frac{1}{\lambda} \end{cases} \tag{61}$$

Equation 61 and Parseval's theorem will then show that

$$\iint_{R_2} v^*(\vec{\rho}')\, Q_\infty(\vec{\rho}', \vec{r}')\, v(\vec{r}')\, d\vec{\rho}' d\vec{r}' = \int_{R_2} (\hat{v}(\vec{r}'))^*\, v(\vec{r}')\, d\vec{r}'$$

$$= \int_{|\vec{F}'| \leq \frac{1}{\lambda}} |V(\vec{F}')|^2\, d\vec{F}' = 1 - \epsilon,$$

which is Eq. 58.

Equation 61 is a consequence of the instantaneous time-reversibility of the atmosphere, defined as follows. Consider a single atmospheric state, and let $\underline{E}(\vec{r})$ be the complex-field amplitude at a point $\vec{r}$ in the turbulence that is due solely to the

propagating waves resulting from transmission of $v(\vec{\rho}')$ from R_2. Then the time reversibility of the atmosphere means that $\underline{E}^*(\vec{r})$ satisfies Maxwell's equations throughout the medium. We have not proved this assertion, we have only stated it. Before proving it let us observe how time reversibility implies (61). For the path lengths of interest we may assume that $u(\vec{\rho})$ is due solely to the propagating waves. Hence when we transmit $u^*(\vec{\rho})$ from the infinite R_1 plane the field that will result in the medium must be $\underline{E}^*(\vec{r})$, since it is a solution of Maxwell's equations that satisfies all of the boundary conditions (note that $\underline{E}(\vec{r})$ reduces to $u(\vec{\rho})$ for $\vec{r}$ in the R_1 plane). The definition of $\underline{E}(\vec{r})$ allows us to conclude that $\hat{v}^*(\vec{r}')$ must be $v^*(\vec{r}')$ bandlimited to spatial frequencies below $1/\lambda$, which is precisely the condition (61). Therefore to prove (58) it only remains to show that instantaneously the atmosphere is time-reversible.

5.22 Time Reversibility

To complete the proof of the asymptotic behavior of Q_{R_1} we must show that the atmosphere is time-reversible. First, let us see why this condition has been called time reversibility. As is shown in Appendix A, conjugation of a complex field amplitude reverses the direction of propagation of the wave. On the other hand, if we examine the time-domain fields, we find that conjugating the field amplitude is equivalent to using the original field amplitude with time running backwards; that is, $t_1 > t_2$ would then imply that t_1 occurs before t_2. For this statement to be true we must neglect the evanescent waves. We turn now to the proof.

Lemma (Time-Reversibility)

Consider any time-invariant, nonabsorbing, inhomogeneous medium with no sources. If the permittivity, $\epsilon(\vec{r})$, is a smoothly varying function of position, then the medium is time-reversible.

Proof: Maxwell's equations for the complex-field amplitudes in a source-free region are

$$\nabla \times \underline{\vec{E}}(\vec{r}) = -j\omega_c \mu_o \underline{\vec{H}}(\vec{r})$$

$$\nabla \times \underline{\vec{H}}(\vec{r}) = j\omega_c \epsilon(\vec{r})\, \underline{\vec{E}}(\vec{r})$$

$$\nabla \cdot \underline{\vec{H}}(\vec{r}) = 0$$

$$\nabla \cdot (\epsilon(\vec{r})\underline{\vec{E}}(\vec{r})) = 0. \qquad (62)$$

Since these are linear equations, the components of the complex-field amplitudes corresponding to the propagating waves and the evanescent waves must satisfy (62) independently. We shall assume in the rest of this proof that we are dealing only with the propagating components.

Since the medium is nonabsorbing $\epsilon(\vec{r})$ is real. It is clear, therefore, that $\underline{\vec{E}}^*(\vec{r})$ and $-\underline{\vec{H}}^*(\vec{r})$ are solutions to Maxwell's equations throughout the medium. Also, since $\epsilon(\vec{r})$

is smoothly varying, there are no internal boundary conditions to be considered. The medium is therefore time-reversible.

We know that the turbulence satisfies all of the assumptions of the lemma, on an instantaneous basis; therefore, we conclude that instantaneously the atmosphere is time-reversible.

Some of our results are known, in other notations, for the free-space channel. For instance, it is well-known that, in the absence of evanescent fields, the diffraction operator (in our terminology convolution with $\underset{\leftarrow}{h}$) from R_2 to R_1 is a unitary operator, a statement equivalent to (57). Time-reversibility has been investigated for the free-space channel under the title of inverse diffraction,[23,24] with conclusions that lead to results comparable to (58). We now continue our examination of the system performance, E_r, for a single atmospheric state.

5.23 Lower Bound to E_r for a Single Atmospheric State

From the results of sections 5.21 and 5.22 it is apparent that for $D = \infty$ the energy in the normally incident plane-wave component of the field received at R_2, E_r, given by Eq. 55, reduces to

$$E_r = \frac{E_t \left| \iint_{R_2} Q_\infty(\vec{\rho}', \vec{r}')\, d\vec{\rho}' d\vec{r}' \right|^2}{A_2 \iint_{R_2} \underset{\leftarrow}{K}_\infty(\vec{\rho}', \vec{r}')\, d\vec{\rho}' d\vec{r}'}$$

$$= E_t(1-\epsilon), \tag{63}$$

where

$$\epsilon = \int_{|\vec{F}'| > 1/\lambda} |V(\vec{F}')|^2 \, d\vec{F}'$$

and $V(\vec{F}')$ is now the spatial Fourier transform of the function

$$v(\vec{\rho}') = \begin{cases} \dfrac{1}{\sqrt{A_2}} & \vec{\rho} \in R_2 \\ 0 & \vec{\rho}' \notin R_2 \end{cases}$$

Note that $|V(\vec{F}')|^2$ is just the well-known Airy disk diffraction pattern. The parameter ϵ is a function of λ and d. It will be neglected in the rest of this section, since for typical values of λ and d (for example, $\lambda = 0.6328\mu$, d = 0.1 m), ϵ is no more than 10^{-10}. Therefore, we have from (63) that as D becomes infinite we can get essentially all of the energy transmitted from R_1 into the normally incident plane-wave component at R_2. Since we cannot build a transmitter with an infinite aperture, we would like to relate the rate of convergence of the Q_{R_1} integral to the rate of convergence of the

$\underset{\leftarrow}{K}_{R_1}$ integral to determine the performance of a system with D finite.

Let us examine some conditions under which the convergence relation is particularly simple. Suppose any one of the following conditions is true. (Note that 1 implies 2 and 2 implies 3.)

$$1.\quad \underset{\rightarrow}{h}(\vec{\rho}', \vec{\rho}) = \underset{\leftarrow}{h}(\vec{\rho}, \vec{\rho}') \qquad \forall\, \vec{\rho} \in R_1,\ \vec{\rho}' \in R_2$$

$$2.\quad Q_{R_1}(\vec{\rho}', \vec{r}') = \underset{\leftarrow}{K}_{R_1}(\vec{\rho}', \vec{r}') \qquad \forall\, \vec{\rho}', \vec{r}' \in R_2;\ \forall\, R_1$$

$$3.\quad \int_{R_2} \underset{\rightarrow}{h}(\vec{\rho}', \vec{\rho})\, d\vec{\rho}' = \int_{R_2} \underset{\leftarrow}{h}(\vec{\rho}, \vec{\rho}')\, d\vec{\rho}' \qquad \forall\, \vec{\rho} \in R_1 \tag{64}$$

From the definitions of the kernels (see Table 1), if any of the conditions in (64) is true, then

$$\iint_{R_2} Q_{R_1}(\vec{\rho}', \vec{r}')\, d\vec{\rho}' d\vec{r}' = \iint_{R_2} \underset{\leftarrow}{K}_{R_1}(\vec{\rho}', \vec{r}')\, d\vec{\rho}' d\vec{r}'. \tag{65}$$

The integral on the right is a readily measurable quantity; hence, proving any of the conditions in (64) immediately solves our convergence problem. Rather than address ourselves directly to that task, we shall obtain a lower bound to E_r for finite D.

Observe that we may write $\iint_{R_2} Q_{R_1}(\vec{\rho}', \vec{r}')\, d\vec{\rho}' d\vec{r}'$ in the form

$$\iint_{R_2} Q_{R_1}(\vec{\rho}', \vec{r}')\, d\vec{\rho}' d\vec{r}' = \int_{R_1} d\vec{\rho} \left(\int_{R_2} \underset{\rightarrow}{h}(\vec{r}', \vec{\rho})\, d\vec{r}' \right) \left(\int_{R_2} \underset{\leftarrow}{h}^*(\vec{\rho}, \vec{\rho}')\, d\vec{\rho}' \right)$$

$$= \int_{R_1} \underset{\rightarrow}{F}(\vec{\rho})\, \underset{\leftarrow}{F}^*(\vec{\rho})\, d\vec{\rho}, \tag{66}$$

where

$$\underset{\rightarrow}{F}(\vec{\rho}) = \int_{R_2} \underset{\rightarrow}{h}(\vec{r}', \vec{\rho})\, d\vec{r}'$$

$$\underset{\leftarrow}{F}(\vec{\rho}) = \int_{R_2} \underset{\leftarrow}{h}(\vec{\rho}, \vec{\rho}')\, d\vec{\rho}'.$$

Under the assumption that $\underset{\rightarrow}{F}$ and $\underset{\leftarrow}{F}$ have finite energies, (66) is a valid inner product on $L^2(R_1)$. From (58), as D becomes infinite

$$(\underset{\rightarrow}{F}, \underset{\leftarrow}{F})_{R_1} \triangleq \int_{R_1} \underset{\rightarrow}{F}(\vec{\rho})\, \underset{\leftarrow}{F}^{*}(\vec{\rho})\, d\vec{\rho} \longrightarrow A_2. \tag{67}$$

(The energy in the evanescent waves is so small that $A_2(1-\epsilon) \approx A_2$.)

Consider the quantity

$$\|\underset{\leftarrow}{F}\|_{R_1} \triangleq \left(\int_{R_1} |\underset{\rightarrow}{F}(\vec{\rho})|^2\, d\vec{\rho}\right)^{1/2}$$

$$= \left(\iint_{R_2} \underset{\leftarrow}{K}_{R_1}(\vec{\rho}', \vec{r}')\, d\vec{\rho}' d\vec{r}'\right)^{1/2}. \tag{68}$$

From Eq. 57 it is apparent that as D becomes infinite

$$\|\underset{\leftarrow}{F}\|_{R_1} \longrightarrow \sqrt{A_2}. \tag{69}$$

(Again, the energy in the evanescent waves is so small that $A_2(1-\epsilon) \approx A_2$.) Applying the Schwarz inequality to (66), we conclude that

$$|(\underset{\rightarrow}{F}, \underset{\leftarrow}{F})_{R_1}| \leq \|\underset{\rightarrow}{F}\|_{R_1}\, \|\underset{\leftarrow}{F}\|_{R_1}, \tag{70}$$

where

$$\|\underset{\rightarrow}{F}\|_{R_1} \triangleq \left(\int_{R_1} |\underset{\rightarrow}{F}(\vec{\rho})|^2\, d\vec{\rho}\right)^{1/2},$$

and using (67) and (69) in conjunction with (70), we have

$$\|\underset{\rightarrow}{F}\|_{R_1=\infty} \geq \sqrt{A_2}. \tag{71}$$

Note that equality holds in (71) if and only if $\underset{\rightarrow}{F}(\vec{\rho}) = \pm\underset{\leftarrow}{F}(\vec{\rho})$ (condition 3 in Eq. 64 is equivalent to $\underset{\rightarrow}{F}(\vec{\rho}) = \underset{\leftarrow}{F}(\vec{\rho})$). We assume that

$$\|\underset{\rightarrow}{F}\|_{R_1=\infty} = a\sqrt{A_2} \qquad \text{for some } a, \quad 1 \leq a < \infty.$$

Given $\epsilon > 0$, we can choose D_o large enough that

$$\|\underset{\leftarrow}{F}\|_{R_1} > \sqrt{A_2} - \epsilon \qquad \forall\, D \geq D_o. \tag{72}$$

Applying the triangle inequality, we have

$$|(\underset{\rightarrow}{F}, \underset{\leftarrow}{F})_{R_1=\infty}| \leq |(\underset{\rightarrow}{F}, \underset{\leftarrow}{F})_{R_1}| + |(\underset{\rightarrow}{F}, \underset{\leftarrow}{F})_{\infty-R_1}|, \tag{73}$$

where the inner product in the second term on the right is taken over the infinite region outside of some finite aperture R_1. From the Schwarz inequality and what we have proved concerning the norms and inner products of $\underset{\rightarrow}{F}$ and $\underset{\leftarrow}{F}$ as D becomes infinite, we obtain

$$A_2 = \left|(\underset{\rightarrow}{F}, \underset{\leftarrow}{F})_{R_1=\infty}\right| \leq \left|(\underset{\rightarrow}{F}, \underset{\leftarrow}{F})_{R_1}\right| + \left\|\underset{\rightarrow}{F}\right\|_{\infty-R_1} \left\|\underset{\leftarrow}{F}\right\|_{\infty-R_1}$$

$$\leq \left|(\underset{\rightarrow}{F}, \underset{\leftarrow}{F})_{R_1}\right| + \left\|\underset{\rightarrow}{F}\right\|_{R_1=\infty} \left\|\underset{\leftarrow}{F}\right\|_{\infty-R_1}$$

$$\leq \left|(\underset{\rightarrow}{F}, \underset{\leftarrow}{F})_{R_1}\right| + a\sqrt{A_2}\,\epsilon, \tag{74}$$

where the last inequality holds for all D such that $D \geq D_o$. We now substitute for $\underset{\rightarrow}{F}$ and $\underset{\leftarrow}{F}$ from their definitions in order to interpret the bound (74). The resulting expression is the following. Given $\epsilon > 0$, for all D such that

$$\left(\iint_{R_2} \underset{\leftarrow}{K}_{R_1}(\vec{\rho}', \vec{r}')\, d\vec{\rho}' d\vec{r}'\right)^{1/2} \geq \sqrt{A_2} - \epsilon, \tag{75}$$

we have

$$\left|\iint_{R_2} Q_{R_1}(\vec{\rho}', \vec{r}')\, d\vec{\rho}' d\vec{r}'\right| \geq \sqrt{A_2}\,(\sqrt{A_2} - a\epsilon). \tag{76}$$

Note that a is dimensionless, but ϵ must have dimension $(\text{area})^{1/2}$. We now use (76) to lower-bound E_r. If D is such that (75) is satisfied, then

$$E_r = \frac{E_t \left|\iint_{R_2} Q_{R_1}(\vec{\rho}', \vec{r}')\, d\vec{\rho}' d\vec{r}'\right|^2}{A_2 \iint_{R_2} \underset{\leftarrow}{K}_{R_1}(\vec{\rho}', \vec{r}')\, d\vec{\rho}' d\vec{r}'}$$

$$\geq \frac{E_t}{A_2^2}\left(\sqrt{A_2}\,(\sqrt{A_2} - a\epsilon)\right)^2$$

$$= E_t\left(1 - \frac{2\epsilon a}{\sqrt{A_2}} + \frac{\epsilon^2 a^2}{A_2}\right)$$

$$\geq E_t\left(1 - \frac{2\epsilon a}{\sqrt{A_2}}\right). \tag{77}$$

One crucial question remains to be answered, How large is a? In Appendix B it is argued that a is less than 10, typically from 3 to 5.

Note that for point-reciprocal channels $a = 1$, and our bound (77) reduces to

$$E_r \geq E_t\left(1 - \frac{2\epsilon}{\sqrt{A_2}}\right).$$

On the other hand, using (65), which is valid for reciprocal channels, we obtain

$$E_r \geq E_t\left(1 - \frac{\epsilon}{\sqrt{A_2}}\right)$$

as the tightest possible bound consistent with (75), so the bound (77) should be quite tight for small a and ϵ.

We shall extend the bound (77) to a probabilistic bound on the system performance for the time-variant atmosphere. This result will provide a way of picking an aperture diameter (for R_1) to insure a specified performance level.

5.3 INTERPRETATION OF THE Q-KERNEL SYSTEM PERFORMANCE

5.31 Performance Bound for the Time-Variant Atmosphere

The results of section 5.2 allow us to evaluate the performance, E_r, of a two-way (Q-kernel) communication system using a finite aperture, for any single state of the atmosphere. We shall now generalize these results to the time-variant atmosphere. We shall prove a performance bound of the following type. For a system operating during the time interval $(0, T)$, we would like the system to yield high energy transfer (from R_1 to R_2) with high probability during a substantial fraction β of $(0, T)$. In order to achieve this performance, D, the diameter of R_1, must be made sufficiently large. The actual bound is given in the next lemma.

Lemma (Performance Bound)

Given an operating interval $(0, T)$, for each $0 \leq \beta \leq 1$, $\epsilon > 0$, and $\delta > 0$, there exists a D_o ($D_o < \infty$) and an open set U in $(0, T)$ such that

$$\Pr\left[\left(\iint_{R_2} \underset{\leftarrow}{K}_{R_1}(\vec{\rho}', \vec{r}'; t)\, d\vec{\rho}' d\vec{r}'\right)^{1/2} > \sqrt{A_2} - \epsilon;\ \forall\, t \in U\right] > 1 - \delta \qquad \forall\, D \geq D_o \tag{78}$$

and the Lebesgue measure of U is greater than $T\beta$. Moreover, for any D such that (78) is satisfied, we have

$$\Pr\left[E_r(t) > E_t\left(1 - \frac{2\epsilon a}{\sqrt{A_2}}\right);\ \forall t \in U\right] > 1 - \delta. \tag{79}$$

Proof: We first show that given T, for each $0 \leq \beta \leq 1$, $\epsilon > 0$, and $\delta > 0$, there exists a finite D_o and an open set U of measure greater than $T\beta$ such that (78) is satisfied for all $D \geq D_o$. We partition (0, T) into coherence intervals of length τ_c ($\tau_c > 0$) such that

$$\iint_{R_2} \underset{\leftrightarrow}{K}_{R_1}(\vec{\rho}', \vec{r}'; t)\, d\vec{\rho}' d\vec{r}'$$

is constant for t in a coherence interval. This partition may always be made within the framework of our fixed-state model of the time-variant atmosphere, with τ_c approximately the reciprocal bandwidth of the turbulence process. Let I_i denote the i^{th} coherence interval, then, from section 5.23, there exists D_{o_i} ($D_{o_i} < \infty$) such that for all $D \geq D_{o_i}$

$$\Pr\left[\left(\iint_{R_2} \underset{\leftrightarrow}{K}_{R_1}(\vec{\rho}', \vec{r}'; t)\, d\vec{\rho}' d\vec{r}'\right)^{1/2} > \sqrt{A_2} - \epsilon; \quad \forall\, t \in I_i\right] > 1 - \delta_i, \tag{80}$$

where $\delta_i = \delta/N$, and N is the number of coherence intervals in (0, T). If the ensemble statistics of the channel do not change with time during (0, T), then all the D_{o_i} will be equal. The proof that we employ allows for the fact that the statistics of the channel will change with time. Let $\lceil \beta N \rceil$ denote the smallest integer larger than βN. If we order the coherence intervals in such a way that

$$D_{o_1} \leq D_{o_2} \leq D_{o_3} \leq \ldots$$

then choosing $D_o = D_{o\lceil \beta N \rceil}$ we have that for all $D \geq D_o$

$$\Pr\left[\left(\iint_{R_2} \underset{\leftrightarrow}{K}_{R_1}(\vec{\rho}', \vec{r}'; t)\, d\vec{\rho}' d\vec{r}'\right)^{1/2} > \sqrt{A_2} - \epsilon; \quad \forall\, t \in \bigcup_{i=1}^{\lceil \beta N \rceil} I_i\right]$$

$$\geq 1 - \sum_{i=1}^{\lceil \beta N \rceil} \Pr\left[\left(\iint_{R_2} \underset{\leftrightarrow}{K}_{R_1}(\vec{\rho}', \vec{r}'; t)\, d\vec{\rho}' d\vec{r}'\right)^{1/2} \leq \sqrt{A_2} - \epsilon; \quad \forall\, t \in I_i\right]$$

$$> 1 - \lceil \beta N \rceil\, \delta_i$$

$$\geq 1 - \delta, \tag{81}$$

where the first inequality follows from the union bound. If for each coherence interval D_{o_i} is chosen to be the infimum of all D that satisfy (80), then $D_o = D_{o\lceil \beta N \rceil}$ will be the infimum of all D that satisfy (81). Thus we have proved the first assertion of the lemma.

Using the results of section 5.23, we see that in each coherence interval if $D \geq D_{o_i}$, then

$$\Pr\left[E_r(t) > E_t\left(1 - \frac{2\epsilon a}{\sqrt{A_2}}\right);\ \forall\, t \in I_i\right] > 1 - \delta_i. \tag{82}$$

Hence, if $D_o = D_{o\lceil \beta N \rceil}$ as before, we have for all $D \geq D_o$

$$\begin{aligned}
&\Pr\left[E_r(t) > E_t\left(1 - \frac{2\epsilon a}{\sqrt{A_2}}\right);\ \forall\, t \in \bigcup_{i=1}^{\lceil \beta N \rceil} I_i\right] \\
&\geq 1 - \sum_{i=1}^{\lceil \beta N \rceil} \Pr\left[E_r(t) \leq E_t\left(1 - \frac{2\epsilon a}{\sqrt{A_2}}\right);\ \forall\, t \in I_i\right] \\
&> 1 - \lceil \beta N \rceil\, \delta_i \\
&\geq 1 - \delta
\end{aligned} \tag{83}$$

which proves the rest of the lemma.

Thus we have shown how the single-state performance bound of section 5.23 may be extended to the time-variant case. The entire problem of choosing an aperture diameter on the ground in order to achieve a desired performance level in terms of $E_r(t)$ has been reduced to studying the statistics of

$$\iint_{R_2} \underset{\leftarrow}{K}_{R_1}(\vec{\rho}', \vec{r}'; t)\, d\vec{\rho}' d\vec{r}',$$

the energy received at R_1 when a normally incident plane wave is transmitted from R_2.

Before proceeding to other issues, it is worth observing that the lemma that we have proved shows that our two-way apodization system does not exhibit a performance saturation as the transmitting aperture is enlarged (as a nonadaptive system would). To make this identification, it is necessary to evaluate the system performance in terms of $E_s(t)$, the energy received at the spacecraft. For convenience, we neglect the propagation delay between R_2 and the spacecraft; thus, our path-length assumption enables us to write

$$E_s(t) = CE_r(t). \tag{84}$$

From our path-length assumption, the field at the spacecraft is the spatial Fourier transform of the field at R_2 evaluated at zero spatial frequency (with the $1/r^2$ loss neglected), and since the Fourier transform of the normally incident plane-wave component on R_2 at zero frequency is proportional to $(A_2)^{1/2}$, we may write (84) in the form

$$E_s(t) = C'A_2E_r(t), \tag{85}$$

where C' is independent of d. Therefore we may rewrite the lemma just proved as follows.

Lemma (Performance Bound on $E_s(t)$)

For all D such that (78) is satisfied we have

$$\Pr\left[E_s(t) > E_t A_2 C' \left(1 - \frac{2\epsilon a}{\sqrt{A_2}}\right);\ \forall\, t \in U\right] > 1 - \delta. \tag{86}$$

Proof: Apply Eq. 85 to the previous performance lemma. (Because (85) is only true if the field received at the top of the atmosphere is zero outside of R_2, the performance bound on $E_s(t)$ is only true when ϵ is small enough.)

Hence we have verified that increasing d (enlarging R_2) and then increasing D until (78) is satisfied again continues to increase the energy received at the spacecraft (in proportion to d^2 for small enough ϵ) without performance saturation occurring. We have accomplished one of our major goals, demonstrating the existence of an adaptive spatially modulated system whose far-field beamwidth is not turbulence-limited as the relevant aperture size is increased.

5.32 Performance Limitation Caused by Turbulence

We shall compare the performance (in terms of $E_s(t)$) of a system of the type described above and a system transmitting a normally incident plane wave to the spacecraft through free space, both systems using the same transmitting aperture diameter, D_o. It is clear from our performance bound on $E_s(t)$ for the Q-kernel system, that if ϵ is small enough $E_s(t)$ increases in proportion to d^2, under the assumption that the atmospheric state is such that we are above threshold. That is,

$$\left(\iint_{R_2} \underset{\leftarrow}{K}_{R_1}(\vec{\rho}', \vec{r}'; t)\, d\vec{\rho}' d\vec{r}'\right)^{1/2} > \sqrt{A_2} - \epsilon. \tag{87}$$

For a system using an aperture of diameter D_o in the absence of turbulence, the energy received at the spacecraft will be proportional to D_o^2. Furthermore, since the path length to the spacecraft from the R_2 plane is essentially the same as the path length from the ground, the two proportionality constants that we have mentioned will be the same. Thus, when the atmospheric state is such that (87) is satisfied (for ϵ small), the ratio of the energy received at the spacecraft in the turbulent case (two-way system) to the energy received at the spacecraft in the nonturbulent case (one-way system) is $(d/D_o)^2$. It is convenient to define a parameter

$$\gamma^2 = \left(\frac{d}{D_o}\right)^2 \tag{88}$$

as a measure of the performance limitation imposed by the turbulence. We assume in (88) that γ^2 is a function only of d, and that D_o is chosen as the infimum of all D for

which (78) is satisfied, with $\beta = 1$ and $\delta \sim 0$. Since the one-way system using a normally incident plane wave over R_1 maximizes E_s for the given aperture diameter in the absence of turbulence, γ^2 upper-bounds the performance reduction (in terms of E_s) caused by the turbulence. (Since we have not proved that a Q-kernel system is optimal for the atmosphere, γ^2 is only an upper bound to the performance limitation.) Yet, interestingly enough, we can show that as d becomes infinite $\gamma^2(d)$ approaches unity; that is, in the limit of large d the turbulence causes no performance loss when going from the optimal one-way nonturbulnet system to the Q-kernel system that we have been studying (see section 5.43). Unfortunately, this result is only achieved when the aperture on the ground is infinite (see definition of D_o above).

5.4 EDGE EFFECTS PROBLEM

Thus far, in our discussion of two-way apodization systems for the turbulent channel we have ignored some important issues concerning the beacon signal. We shall now consider such problems. The first thing that we observe is that it is most likely that the beacon used at the top of the atmosphere will be infinite or practically infinite in extent; that is, it will be so large that the aperture on the ground (R_1) never sees the edges of the beam. This will lead us to study the performance of the infinite beacon system, and we shall compare this performance to that of a system using a finite beacon. When the R_1 aperture is large enough that it sometimes sees the edges of the finite beacon, but not so large that it always receives the entire beacon, we shall find that the performance lemma for $E_s(t)$ in section 5.31 leads to anomalous results. This is the edge effects problem. For R_1 as described we shall see that an assumption leading to the bound on $E_s(t)$ is violated, so the bound itself is invalid in this region.

5.41 Obtaining a Beacon Signal

Until now, we have not specified how the unit amplitude normally incident plane wave over R_2 (the beacon) is obtained. There are two practical options available, we can put the laser on the spacecraft itself, or we may use a laser located on a synchronous satellite (if we assume that the spacecraft is well beyond synchronous altitude) whose location is sufficiently close to the propagation path to provide a beacon of the required aiming accuracy. Since we shall assume that there are no ducting phenomena in the atmosphere to consider, we may assume that in either of the cases described above the beacon at the top of the atmosphere will be such that the aperture R_1 never sees the edges of the beacon; that is, the beacon is effectively an infinite plane wave (at R_2). If a finite beacon can be obtained, the results of section 5.3 apply directly. We only intend the present discussion as a rationale for investigating the infinite beacon case.

It is worth noting that in section 3.3 we proved that for a time-invariant point-reciprocal deep-space channel the optimal energy transfer from the ground to the spacecraft is achieved by a Q-kernel system in which the spacecraft transmits a normally

incident plane wave to the ground, which corresponds (in the present terminology) to using an infinite plane-wave beacon at the top of the atmosphere. We have not proved that the atmosphere is reciprocal yet, but this result should be kept in mind.

5.42 Infinite Beacon System

Suppose we have a two-way apodization system of the type under discussion here, using a unit amplitude normally incident infinite plane wave as the beacon. From Eqs. 55 and 85 we know that the energy received at the spacecraft will be

$$E_s(t) = \frac{C'E_t \left| \iint_{R_2=\infty} Q_{R_1}(\vec{\rho}', \vec{r}'; t)\, d\vec{\rho}' d\vec{r}' \right|^2}{\iint_{R_2=\infty} \underset{\leftrightarrow}{K}_{R_1}(\vec{\rho}', \vec{r}'; t)\, d\vec{\rho}' d\vec{r}'}. \tag{89}$$

For convenience, we assume that the channel is point-reciprocal instantaneously; therefore,

$$\iint_{R_2=\infty} Q_{R_1}(\vec{\rho}', \vec{r}'; t)\, d\vec{\rho}' d\vec{r}' = \iint_{R_2=\infty} \underset{\leftrightarrow}{K}_{R_1}(\vec{\rho}', \vec{r}'; t)\, d\vec{\rho}' d\vec{r}'$$

and (89) reduces to

$$E_s(t) = C'E_t \iint_{R_2=\infty} \underset{\leftrightarrow}{K}_{R_1}(\vec{\rho}', \vec{r}'; t)\, d\vec{\rho}' d\vec{r}'. \tag{90}$$

We now study the behavior of the double integral in (90) as D is increased. We have

$$\iint_{R_2=\infty} \underset{\leftrightarrow}{K}_{R_1}(\vec{\rho}', \vec{r}'; t)\, d\vec{\rho}' d\vec{r}' = \int_{R_1} \left| \int_{R_2=\infty} \underset{\leftrightarrow}{h}(\vec{\rho}, \vec{\rho}'; t)\, d\vec{\rho}' \right|^2 d\vec{\rho}$$

$$= \int_{R_1} |\underline{z}(\vec{\rho}, t)|^2\, d\vec{\rho}, \tag{91}$$

where the last equality follows from the $\underline{z}$ model for infinite plane-wave propagation through turbulence. Now we may apply some well-known results from the $\underline{z}$ model to our problem. We partition R_1 into nonoverlapping coherence areas (circular areas of diameter $2\rho_c$, where ρ_c is the distance at which the spatial correlation function of $|\underline{z}(\vec{\rho}, t)|^2$ has its first zero). We adapt the simplified model that $\underline{z}$ is completely correlated within a coherence distance ($2\rho_c$) and completely uncorrelated outside of this distance. Thus we have

$$\int_{R_1} |\underline{z}(\vec{\rho}, t)|^2 \, d\vec{\rho} = \sum_{i=1}^{N} |\underline{z}_i(t)|^2 A_c, \tag{92}$$

where $\underline{z}_i(t)$ is the value of $\underline{z}(\vec{\rho}, t)$ in the i^{th} coherence area, $A_c = \pi\rho_c^2$, and N is the number of coherence areas in R_1. From the $\underline{z}$ model, the sum in (92) is the sum of uncorrelated log-normal random variables whose ensemble average, $E[A_c |\underline{z}_i(t)|^2]$, is A_c.[18, 22] Consider the fluctuation about its mean of the sum in (92). That is,

$$\sigma_N(t) = \frac{\left(\text{VAR}\left[\sum_{i=1}^{N} |z_i(t)|^2 A_c\right]\right)^{1/2}}{E\left[\sum_{i=1}^{N} |\underline{z}_i(t)|^2 A_c\right]}. \tag{93}$$

Using the properties of the z_i, we have

$$\sigma_N(t) = \frac{\left(\text{VAR}\left(|z_i(t)|^2\right)\right)^{1/2}}{\sqrt{N}}. \tag{94}$$

The parameter σ_N is also the fluctuation of $E_s(t)$ about its mean; that is, from Eqs. 90-92, we have

$$\sigma_N(t) = \frac{(\text{VAR}\,(E_s(t)))^{1/2}}{E(E_s(t))}. \tag{95}$$

It is clear from (94) that $\sigma_N(t)$ is an increasing function of the intensity of the turbulence (through VAR $(|z_i(t)|^2)$), and a decreasing function of D (through $N = D^2/4\rho_c^2$). We have proved, therefore, that as D becomes infinite the fluctuation about its mean of the energy received at R_1 goes to zero, and similarly the fluctuation of $E_s(t)$ about its mean goes to zero.

Since the mean of $|z_i(t)|^2$ is also the value it achieves in the absence of turbulence, we have also proved for all D that the mean of $E_s(t)$ is the value that it achieves in the absence of turbulence. Also note that in the absence of turbulence the received beacon will be a normally incident plane wave, and so the field transmitted from R_1 will be a plane wave of energy E_t and diameter D, the optimum one-way result for deep-space apodization. In other words, $E(E_s(t))$ is equal to the optimum energy transfer that is possible in the absence of turbulence, that is, the diffraction-limited result for a lens of diameter D. Furthermore, since the fluctuation of $E_s(t)$ about its mean goes to zero as D becomes infinite, we see that in this limit the Q-kernel system achieves diffraction-limited performance with probability one.

The statements just made are important enough to warrant one more repetition. We have shown that for any size R_1, the turbulence does not reduce the average energy

transferred to the spacecraft. The turbulence does cause fading at the spacecraft, but as R_1 increases in size this fading decreases (relative to the mean), ultimately going to zero when R_1 becomes the entire plane.

We have reached some important conclusions in this section, but to obtain them we assumed that the atmosphere was point-reciprocal instantaneously. The reciprocity of the atmosphere is proved in Section VI. The rest of this section is devoted to comparing systems with finite beacons to the infinite beacon system.

5.43 Comparison with Finite Beacon Results

As in section 5.42 we shall assume a reciprocal channel. Consider a Q-kernel system using a plane-wave beacon of diameter d, and a transmitting aperture at R_1 of diameter D such that $D \ll d$. For d large enough (in the absolute sense) the radiation

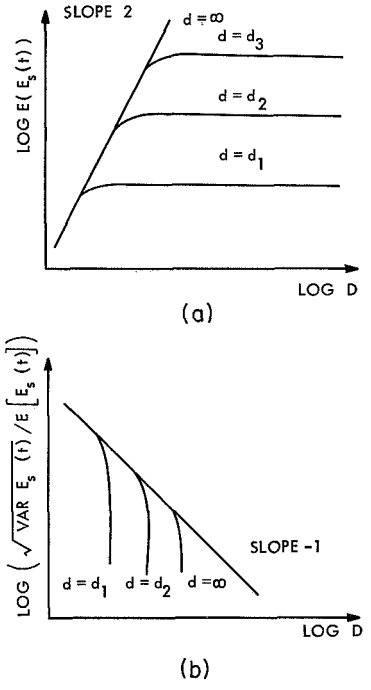

Fig. 11. $E_s(t)$ for Q-kernel systems.
(a) $d_1 < d_2 < d_3$. Saturation occurs when $d \ll D$, and the resulting energy is $E_s(t) = A_2 C' E_t$. Slope 2 behavior is only valid for $d \gg r_o$.
(b) $d_1 < d_2 < d_3$. For $d \ll D$, $\left((\text{VAR}\, E_s(t))^{1/2} / E(E_s(t))\right) \to 0$.

received over the aperture R_1 will come from the center of the beacon and its statistics will be well approximated by the infinite plane-wave $\underline{z}$ model. In particular, if d is large compared with the diameter at which the far-field beamwidth becomes turbulence-limited, then the results hold as stated. Thus the performance, $E_s(t)$, will be the same as that in section 5.42 for the infinite beacon. Now as D increases, $E_s(t)$ increases monotonically (for each atmospheric state) until D becomes comparable to d, and then a saturation effect begins to set in. This saturation arises out of the fact that we begin to receive the edges of the beam, and the energy received at R_1 (which for reciprocal channels is proportional to $E_s(t)$) cannot exceed A_2. In section 5.3 when we commented that performance saturation is avoided with a finite beacon system we had to keep increasing d. In the limit $D \gg d$ the performance of the finite beacon system has saturated at

$E_s(t) = E_t A_2 C'$. These results are shown in Fig. 11. It should be noted that in the region $D \sim d$, the finite beacon system seemingly outperforms the infinite beacon system for some atmospheric states. This is an anomalous result that is due to Eq. 85 not being valid (for all states) in this region. In section 6.2 we shall prove that, in terms of $E_s(t)$, the infinite beacon system always performs as well as or better than the finite beacon system.

There is one last result worth obtaining. In section 5.42 we proved that for an infinite beacon system, as D approaches infinity, $E_s(t)$ approaches the optimal one-way energy transfer possible in the nonturbulent case with probability one. Therefore $\gamma^2(d)$, the parameter that measures the performance limitation imposed by the turbulence (see Eq. 88), must approach one as d and D become infinite, since in this limit the turbulence does not reduce our ability to get energy to the spacecraft.

5.5 Summary of Deep-Space Apodization

We conclude our discussion of deep-space channels with a summary of the important results.

1. A Q-kernel system using a plane-wave beacon was investigated as a possible solution to a deep-space apodization problem.

2. An energy expression for $E_r(t)$, the energy received in the normally incident plane-wave component of the field at the window, R_2, at the top of the atmosphere, was obtained from the work in Sections II and III. This expression was lower-bounded in terms of

$$\iint_{R_2} \underset{\leftrightarrow}{K}_{R_1}(\vec{\rho}', \vec{r}')\, d\vec{\rho}' d\vec{r}',$$

the received beacon energy.

3. The results for single atmospheric states have been extended to probabilistic bounds on performance during a time interval (0, T).

4. It has been shown that it is quite likely that the beacon will be of infinite extent. The performance of infinite beacon systems has been studied, under the assumption that the atmosphere is point-reciprocal.

5. For the infinite beacon system we found that the average energy received at the spacecraft, $E(E_s(t))$, is the optimal one-way energy transfer possible (ground-to-spacecraft) in the absence of turbulence, and as the aperture on the ground becomes infinite the fluctuation about this mean energy goes to zero.

6. The performance of finite beacon systems was compared with the performance of the infinite beacon system, under the reciprocity assumption. For $D \ll d$ the two systems perform equally well. For $D \gg d$ the performance of the finite beacon system saturates (see Fig. 11).

7. Thus, although we have not yet proved the optimality of our Q-kernel system, we

have shown that it greatly improves the energy received at the spacecraft, compared with a nonadaptive system. In Section VI we shall prove the optimality of the Q-kernel system (for the atmosphere) by showing that the atmosphere is reciprocal.

VI. RECIPROCITY OF THE ATMOSPHERE

We shall now prove that the turbulent atmospheric channel is point-reciprocal on an instantaneous basis. Really, we shall prove that a model of the turbulence process satisfies instantaneous reciprocity. In the model that we use the following assumptions are made.

1. At a single instant in time the permittivity is a smoothly varying function of position.
2. The medium causes no depolarization.
3. No energy is scattered far out of an incident beam's direction.

These assumptions, which we have already used several times, are consistent with the properties of atmospheric turbulence.

We shall then examine some of the consequences of reciprocity for communication through the atmosphere.

6.1 POINT RECIPROCITY OF THE TURBULENT CHANNEL

We assume the atmosphere may be modeled as undergoing a succession of fixed states (see Section IV). We shall show that

$$\underset{\rightarrow}{h}(\vec{\rho}', \vec{\rho}; t) = \underset{\leftarrow}{h}(\vec{\rho}, \vec{\rho}'; t) \qquad \forall\, \vec{\rho} \in R_1,\ \vec{\rho}' \in R_2, t. \tag{96}$$

For convenience, we suppress the time dependence of the impulse responses, $\underset{\rightarrow}{h}$ and $\underset{\leftarrow}{h}$, where it is understood that we are always referring to a single fixed state of the turbulence.

Two proofs of (96) are given, one under the assumption of Kirchhoff boundary conditions, and the other of Rayleigh-Sommerfeld boundary conditions.[25] The first proof is presented primarily because of its relative simplicity. The second proof, with a more consistent set of boundary conditions, is significantly more involved.

6.11 Proof with Kirchhoff Boundary Conditions

This proof is an application of Green's theorem for scalar fields, and is based on an argument presented by Morse and Feshbach.[26]

Green's theorem states that for any well-behaved complex functions of position U, W

$$\int_S (U \nabla W - W \nabla U) \cdot d\vec{A} = \int_V (U \nabla^2 W - W \nabla^2 U)\, dv, \tag{97}$$

where S is a closed surface enclosing a volume V, and the functions U and W have no singularities on S. We shall apply this theorem to the case in which U and W are the two impulse responses, $\underset{\rightarrow}{h}$ and $\underset{\leftarrow}{h}$. We know that the impulse responses satisfy the following Helmholtz equations[26]

$$\nabla^2 \underset{\rightarrow}{h}(\vec{r}, \vec{\rho}) + k^2 n^2(\vec{r})\, \underset{\rightarrow}{h}(\vec{r}, \vec{\rho}) = -\delta(\vec{r} - \vec{\rho}) \tag{98}$$

$$\nabla^2 \underset{\leftarrow}{h}(\vec{r}, \vec{\rho}') + k^2 n^2(\vec{r})\, \underset{\leftarrow}{h}(\vec{r}, \vec{\rho}') = -\delta(\vec{r}-\vec{\rho}'), \tag{99}$$

where k is the wave number, $n(\vec{r})$ is the index of refraction at a point $\vec{r}$, ∇ operates only on the observational $(\vec{r})$ coordinates, and $\delta(\cdot)$ is the volume impulse function. We

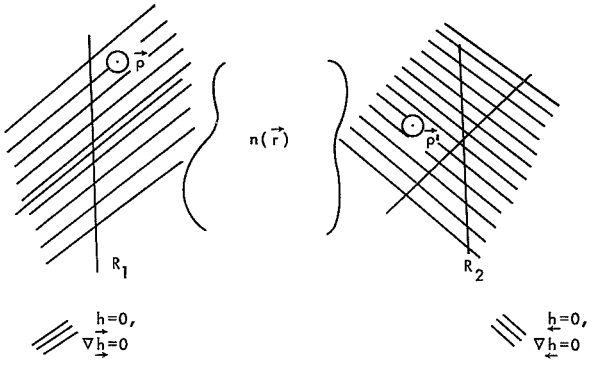

Fig. 12. Kirchhoff boundary conditions.

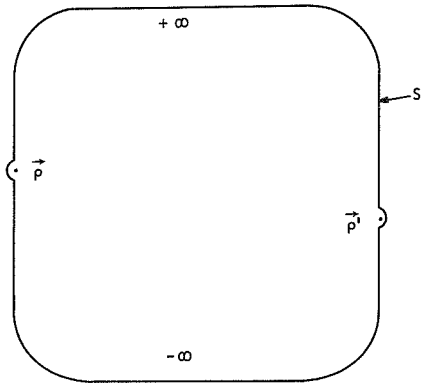

Fig. 13. Closed-surface S.

must specify the boundary conditions that the impulse responses satisfy. The boundary conditions that we wish to impose are shown in Fig. 12. In the plane of R_1, $\underset{\rightarrow}{h}$ and $\nabla \underset{\rightarrow}{h}$ are zero everywhere except in a small neighborhood of the source point; similarly, $\underset{\leftarrow}{h}$ and $\nabla \underset{\leftarrow}{h}$ are zero everywhere in the R_2 plane except in some small neighborhood of the source point. These conditions are the Kirchhoff boundary conditions for a medium in which there is no backscatter.[22, 25] We form a closed surface S by closing the R_1 and R_2 planes at infinity, and taking two small (spherical) caps behind the source points (see Fig. 13). On the surfaces at infinity both impulse responses are assumed to be zero, which is equivalent to assuming that the impulse responses vanish at least as fast as a diverging spherical wave as the distance between the observation and source points becomes infinite. We shall also assume that each impulse response and its gradient is zero on the cap behind its respective source point. This assumption depends upon two conditions: (i) there is no backscatter from the turbulence; and (ii) since the impulse responses are Green's functions for diffraction through apertures, they may be regarded as the fields of anisotropic point sources where the anisotropy is such that no energy is radiated behind the diffracting screen in the absence of turbulence.

Now that our boundary conditions are completely specified we may proceed rapidly. Multiplying Eq. 98 by $\underset{\leftarrow}{h}(\vec{r}, \vec{\rho}')$ and Eq. 99 by $\underset{\rightarrow}{h}(\vec{r}, \vec{\rho})$ and subtracting, we obtain

$$\underset{\leftarrow}{h}(\vec{r}, \vec{\rho}')\, \nabla^2 \underset{\rightarrow}{h}(\vec{r}, \vec{\rho}) - \underset{\rightarrow}{h}(\vec{r}, \vec{\rho})\, \nabla^2 \underset{\leftarrow}{h}(\vec{r}, \vec{\rho}') = -(\delta(\vec{r}-\vec{\rho})\underset{\leftarrow}{h}(\vec{r}, \vec{\rho}')-\delta(\vec{r}-\vec{\rho}')\underset{\rightarrow}{h}(\vec{r}, \vec{\rho})). \tag{100}$$

Integrating (100) over the volume V enclosed by S, we have

$$\int_V (\underset{\rightarrow}{h}(\vec{r}, \vec{\rho}')\nabla^2\underset{\rightarrow}{h}(\vec{r}, \vec{\rho}) - \underset{\rightarrow}{h}(\vec{r}, \vec{\rho})\nabla^2\underset{\leftarrow}{h}(\vec{r}, \vec{\rho}'))\, dv = (\underset{\rightarrow}{h}(\vec{\rho}', \vec{\rho}) - \underset{\leftarrow}{h}(\vec{\rho}, \vec{\rho}')). \tag{101}$$

Since $\underset{\rightarrow}{h}$ and $\underset{\leftarrow}{h}$ are well-behaved functions on the surface S, we may apply Green's theorem to change the volume integral to a surface integral. Thus

$$\int_S (\underset{\rightarrow}{h}(\vec{r}, \vec{\rho}')\nabla\underset{\rightarrow}{h}(\vec{r}, \vec{\rho}) - \underset{\rightarrow}{h}(\vec{r}, \vec{\rho})\nabla\underset{\leftarrow}{h}(\vec{r}, \vec{\rho}')) \cdot d\vec{A} = (\underset{\rightarrow}{h}(\vec{\rho}', \vec{\rho}) - \underset{\leftarrow}{h}(\vec{\rho}, \vec{\rho}')). \tag{102}$$

Applying our boundary conditions to (102), we see that the surface integral is zero. Therefore

$$\underset{\rightarrow}{h}(\vec{\rho}', \vec{\rho}) = \underset{\leftarrow}{h}(\vec{\rho}, \vec{\rho}') \qquad \forall\, \vec{\rho} \in R_1,\ \vec{\rho}' \in R_2;$$

hence, the atmosphere is point-reciprocal on an instantaneous basis.

6.12 Proof with Rayleigh-Sommerfeld Boundary Conditions

The internal inconsistency in the Kirchhoff boundary conditions is well known. We shall now prove point reciprocity, using more consistent boundary conditions. We wish to remove the necessity of specifying the values of both an impulse response and its gradient on an open surface. Our revised proof is somewhat more complicated than the proof with Kirchhoff boundary conditions; it is a series of three lemmas.

Lemma 1

For a fixed state of the atmosphere let $G(\vec{r}, \vec{r}_o)$ be the field at a point $\vec{r}$ that results from a unit-amplitude isotropic point source located at point $\vec{r}_o$, where $\vec{r}$ and $\vec{r}_o$ are points within the turbulence. Then G is a symmetric function of its two variables. That is, for any $\vec{r}_o, \vec{r}_1$

$$G(\vec{r}_1, \vec{r}_o) = G(\vec{r}_o, \vec{r}_1). \tag{103}$$

Proof: This lemma will show that the atmosphere is reciprocal for isotropic point sources, on an instantaneous basis.

The function G satisfies the same Helmholtz equation as the functions $\underset{\rightarrow}{h}$ and $\underset{\leftarrow}{h}$,[26]

$$\nabla^2 G(\vec{r}, \vec{r}_o) + k^2 n^2(\vec{r})\, G(\vec{r}, \vec{r}_o) = -\delta(\vec{r} - \vec{r}_o). \tag{104}$$

Also, G satisfies a homogeneous boundary condition at infinity. That is,

$$G(\vec{r}, \vec{r}_o) \longrightarrow 0 \quad \text{as} \quad |\vec{r} - \vec{r}_o| \longrightarrow \infty.$$

Let S denote the surface of the sphere of infinite radius centered at $\vec{r}_o$, and V denote the volume enclosed by S. Since G satisfies the same Helmholtz equation that the impulse responses $\underset{\rightarrow}{h}$ and $\underset{\leftarrow}{h}$ do, we may use the argument of section 6.11 to show that

$$G(\vec{r}, \vec{r}_1)\,\nabla^2 G(\vec{r}, \vec{r}_o) - G(\vec{r}, \vec{r}_o)\,\nabla^2 G(\vec{r}, \vec{r}_1) = -(\delta(\vec{r}-\vec{r}_o)G(\vec{r}, \vec{r}_1) - \delta(\vec{r}-\vec{r}_1)G(\vec{r}, \vec{r}_o)). \tag{105}$$

Thus, by integrating (105) over the volume V enclosed by S, we obtain

$$\int_V (G(\vec{r}, \vec{r}_1)\nabla^2 G(\vec{r}, \vec{r}_o) - G(\vec{r}, \vec{r}_o)\nabla^2 G(\vec{r}, \vec{r}_1))\, dv = (G(\vec{r}_1, \vec{r}_o) - G(\vec{r}_o, \vec{r}_1)). \tag{106}$$

Using Green's theorem, we transform the volume integral into a surface integral. Therefore,

$$\int_S (G(\vec{r}, \vec{r}_1)\nabla G(\vec{r}, \vec{r}_o) - G(\vec{r}, \vec{r}_o)\nabla G(\vec{r}, \vec{r}_1)) \cdot d\vec{A} = (G(\vec{r}_1, \vec{r}_o) - G(\vec{r}_o, \vec{r}_1)) \tag{107}$$

and from our boundary conditions on S we conclude that

$$G(\vec{r}_1, \vec{r}_o) = G(\vec{r}_o, \vec{r}_1).$$

Lemma 2

Consider a small aperture in the R_1 plane centered on point $\vec{\rho}$, and let $\vec{\rho}'$ be a point in the R_2 plane. We define the function $\underset{\rightarrow}{G}$ in terms of the isotropic impulse response G by

$$\underset{\rightarrow}{G}(\vec{r}, \vec{\rho}') = G(\vec{r}, \vec{\rho}') - G(\vec{r}, \overset{\wedge}{\vec{\rho}}'), \tag{108}$$

where $\overset{\wedge}{\vec{\rho}}'$ is the mirror image of point $\vec{\rho}'$ with respect to the R_1 plane, the medium behind R_1 is assumed to be the mirror image (in terms of the index of refraction) of the medium in front of the plane, and G is calculated when the diffracting screen is not present (see Fig. 14). For $\underset{\rightarrow}{G}$ thus defined it follows that

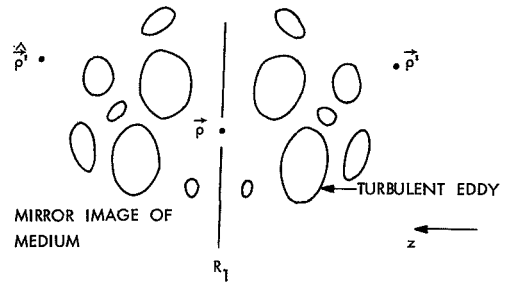

Fig. 14.
The function $\underset{\rightarrow}{G}(\vec{r}, \vec{\rho}')$. ($G(\vec{r}, \vec{\rho}')$ and $G(\vec{r}, \overset{\wedge}{\vec{\rho}}')$ are isotropic point-source Green's functions computed in the absence of the diffracting screen.)

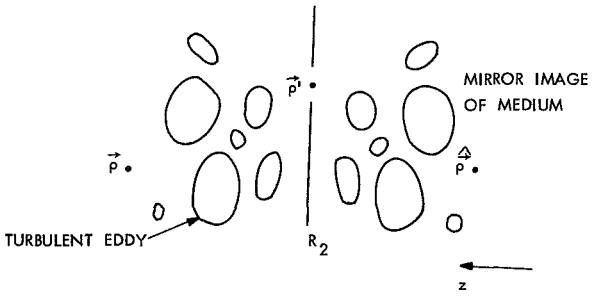

Fig. 15.
The function $\underset{\rightarrow}{G}(\vec{r}, \vec{\rho})$. ($G(\vec{r}, \vec{\rho})$ and $G(\vec{r}, \overset{\wedge}{\vec{\rho}})$ are isotropic point-source Green's functions computed in the absence of the diffracting screen.)

$$\underline{\underline{h}}(\vec{\rho}', \vec{\rho}) = \left.\frac{\partial \underline{\underline{G}}(\vec{r}, \vec{\rho}')}{\partial z}\right|_{\vec{r}=\vec{\rho}}. \tag{109}$$

In this expression and in Eq. 111 the z axis is the line from the origin of R_2 to the origin of R_1. The partial derivatives are taken with respect to the observational $(\vec{r})$ coordinates of $\underline{\underline{G}}$ and $\underline{\underline{G}}$.

Similarly, we define

$$\underline{\underline{G}}(\vec{r}, \vec{\rho}) = G(\vec{r}, \vec{\rho}) - G(\vec{r}, \hat{\vec{\rho}}), \tag{110}$$

where $\hat{\vec{\rho}}$ is the mirror image of the point $\vec{\rho}$ with respect to the R_2 plane, the region behind R_2 (see Fig. 15) is assumed to be the mirror image of the region in front of R_2, and G is calculated when the diffracting screen is not present. It follows that

$$\underline{\underline{h}}(\vec{\rho}, \vec{\rho}') = \left.\frac{-\partial \underline{\underline{G}}(\vec{r}, \vec{\rho})}{\partial z}\right|_{\vec{r}=\vec{\rho}'}. \tag{111}$$

Proof: We shall prove (109) first. The proof of (111) will be the same. From (104) and (108), $\underline{\underline{G}}$ satisfies the equation

$$\nabla^2 \underline{\underline{G}}(\vec{r}, \vec{\rho}') + k^2 n^2(\vec{r})\, \underline{\underline{G}}(\vec{r}, \vec{\rho}') = -(\delta(\vec{r}-\vec{\rho}') - \delta(\vec{r}-\hat{\vec{\rho}}')). \tag{112}$$

Let $U(\vec{r})$ be the solution of the Helmholtz equation that corresponds to diffraction through the aperture in R_1 shown in Fig. 14. We have

$$\nabla^2 U(\vec{r}) + k^2 n(\vec{r})\, U(\vec{r}) = 0. \tag{113}$$

Therefore from (112) we conclude that

$$\underline{\underline{G}}(\vec{r}, \vec{\rho}')\, \nabla^2 U(\vec{r}) - U(\vec{r})\, \nabla^2 \underline{\underline{G}}(\vec{r}, \vec{\rho}') = U(\vec{r})\, (\delta(\vec{r}-\vec{\rho}') - \delta(\vec{r}-\hat{\vec{\rho}}')). \tag{114}$$

Let S be the surface obtained by closing the R_1 plane at infinity to the right

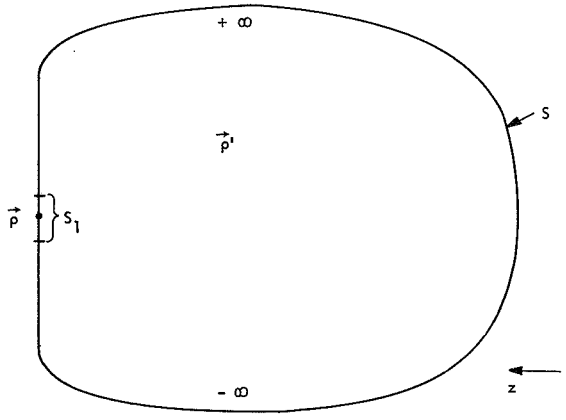

Fig. 16. Closed-surface S for proof of Lemma 2.

(see Fig. 16), and let V be the volume enclosed by S. Integrating (114) over V, we have

$$\int_V (\underline{G}(\vec{r}, \vec{\rho}')\nabla^2 U(\vec{r}) - U(\vec{r})\nabla^2 \underline{G}(\vec{r}, \vec{\rho}')) \, dv = U(\vec{\rho}'). \tag{115}$$

Using Green's theorem to change the volume integral to a surface integral, we obtain

$$\int_S (\underline{G}(\vec{r}, \vec{\rho}')\nabla U(\vec{r}) - U(\vec{r})\nabla \underline{G}(\vec{r}, \vec{\rho}')) \cdot d\vec{A} = U(\vec{\rho}'). \tag{116}$$

On the surface at infinity both U and $\underline{G}$ are zero, and in the R_1 plane outside of the aperture we assume that U is zero. From (108) we know that $\underline{G}(\vec{r}, \vec{\rho}')$ is zero for all $\vec{r}$ in the R_1 plane (really this is the purpose of defining $\underline{G}$ by Eq. 108). Therefore, if S_1 denotes the aperture in the R_1 plane shown in Fig. 14, then (116) reduces to

$$\int_{S_1} (U(\vec{r})\nabla \underline{G}(\vec{r}, \vec{\rho}')) \cdot d\vec{A} = U(\vec{\rho}'). \tag{117}$$

If we let S_1 become vanishingly small and on S_1 let U approach a unit-amplitude point source at $\vec{\rho}$, then (117) reduces to

$$\left.\frac{\partial \underline{G}(\vec{r}, \vec{\rho}')}{\partial z}\right|_{\vec{r}=\vec{\rho}} = \underline{h}(\vec{\rho}', \vec{\rho}) \tag{118}$$

which proves Eq. 109. Equation 111 is proved in a similar manner. The minus sign arises from the fact that the z axis will be antiparallel to the outward normal from the aperture in the R_2 plane.

The important thing to remember is that in this lemma we have only placed a boundary condition on the values of the impulse responses, $\underline{h}$ and $\underline{h}$; their gradients have not been constrained.

Lemma 3

For any $\vec{\rho} \in R_1$ and $\vec{\rho}' \in R_2$ we have

$$\underline{G}(\vec{\rho}+(dz)\vec{i}_z, \vec{\rho}') = \underline{G}(\vec{\rho}'-(dz)\vec{i}_z, \vec{\rho}) \tag{119}$$

for sufficiently small dz.

Proof: The proof of this lemma is straightforward. For dz sufficiently small we may write

$$\underline{G}(\vec{\rho}+(dz)\vec{i}_z, \vec{\rho}') = \exp[-jk(dz)(\cos\theta)n(\vec{\rho})] \, G(\vec{\rho}, \vec{\rho}') - \exp[+jk(dz)(\cos\theta)n(\vec{\rho})] \, G(\vec{\rho}, \hat{\vec{\rho}}'), \tag{120}$$

where θ is the angle between the z axis and the vector from $\vec{\rho}$ to $\vec{\rho}'$ (see Fig. 17).

Equation 120 follows from the fact that for small dz the only perturbation in $\underset{\rightarrow}{\underset{\leftarrow}{G}}$ is a differential phase delay. Similarly, we can show that for dz sufficiently small

$$\underset{\rightarrow}{\underset{\leftarrow}{G}}(\vec{\rho}'-(dz)\vec{i}_z, \vec{\rho}) = \exp[-jk(dz)(\cos\theta)n(\vec{\rho}')]\,\underset{\rightarrow}{\underset{\leftarrow}{G}}(\vec{\rho}', \vec{\rho}) - \exp[+jk(dz)(\cos\theta)n(\hat{\vec{\rho}}')]\,\underset{\rightarrow}{\underset{\leftarrow}{G}}(\vec{\rho}', \hat{\vec{\rho}}). \tag{121}$$

Since dz can be made arbitrarily small, and the perturbations in the index of refraction caused by the turbulence are typically only a few parts in 10^6, we may assume n = 1 in all the phase terms in both (120) and (121). We now have

$$(\underset{\rightarrow}{\underset{\leftarrow}{G}}(\vec{\rho}+(dz)\vec{i}_z, \vec{\rho}')-\underset{\rightarrow}{\underset{\leftarrow}{G}}(\vec{\rho}'-(dz)\vec{i}_z, \vec{\rho}))$$

$$= \exp[-jk(dz)(\cos\theta)]\,(G(\vec{\rho}, \vec{\rho}')-G(\vec{\rho}', \vec{\rho})) - \exp[+jk(dz)(\cos\theta)]\,(G(\vec{\rho}, \hat{\vec{\rho}}')-G(\vec{\rho}', \hat{\vec{\rho}})). \tag{122}$$

From Lemma 1, the first term on the right in (122) must be zero. Furthermore, by the construction of our mirror images in the hypothesis of Lemma 2, we have

$$G(\vec{\rho}, \hat{\vec{\rho}}') = G(\vec{\rho}, \vec{\rho}')$$

$$G(\vec{\rho}', \hat{\vec{\rho}}) = G(\vec{\rho}', \vec{\rho}). \tag{123}$$

Thus, applying Lemma 1 and Eq. 123, we see that the second term on the right in (122) is zero, which proves the lemma.

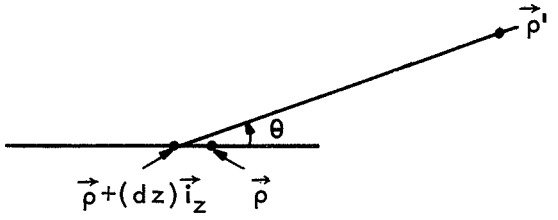

Fig. 17. Geometry of Lemma 3.

We are now ready to prove that the channel is point-reciprocal. From (109), we have

$$\underset{\rightarrow}{\underset{\leftarrow}{h}}(\vec{\rho}', \vec{\rho}) = \lim_{dz\to 0} \frac{\underset{\rightarrow}{\underset{\leftarrow}{G}}(\vec{\rho}+(dz)\vec{i}_z, \vec{\rho}') - \underset{\rightarrow}{\underset{\leftarrow}{G}}(\vec{\rho}, \vec{\rho}')}{dz}, \tag{124}$$

and substituting from (119) and (103), we have

$$\underset{\rightarrow}{\underset{\leftarrow}{h}}(\vec{\rho}', \vec{\rho}) = \lim_{dz\to 0} \frac{\underset{\rightarrow}{\underset{\leftarrow}{G}}(\vec{\rho}'-(dz)\vec{i}_z, \vec{\rho}) - \underset{\rightarrow}{\underset{\leftarrow}{G}}(\vec{\rho}', \vec{\rho})}{dz}. \tag{125}$$

Applying (111) to (125), we conclude that

$$\underset{\rightarrow}{h}(\vec{\rho}', \vec{\rho}) = \underset{\leftarrow}{h}(\vec{\rho}, \vec{\rho}'),$$

and the atmosphere is point reciprocal (instantaneously).

6.2 OPTIMALITY OF A TWO-WAY Q-KERNEL COMMUNICATION SYSTEM

Now that we have proved that the atmosphere is reciprocal, we may show that a Q-kernel system, as described in Section V, is an optimal system for deep-space apodization. We may conclude directly that if the spacecraft is sufficiently far away (see the path-length assumption in section 3.3) a Q-kernel system as described in Section V achieves the maximum energy transfer to the spacecraft that would be possible if the channel were known to the transmitter at R_1. This optimal system uses an infinite plane wave at the top of the atmosphere as a beacon.

Now that we have proved the reciprocity of the atmosphere it is instructive to consider another (rather simple) proof of the optimality statement above. Let R_1 be the aperture on the ground, R_2 the infinite plane tangent to the top of the atmosphere, and the impulse responses $\underset{\rightarrow}{h}$ and $\underset{\leftarrow}{h}$ describe the propagation between these two planes for a single atmospheric state. Let us evaluate the impulse response, $h(\vec{\xi}, \vec{\rho})$, associated with transmission from R_1 to R_3, the spacecraft antenna aperture. This is the impulse response for a single atmospheric state. For the path lengths of interest, by assumption, we have

$$h(\vec{\xi}, \vec{\rho}) = \sqrt{\frac{C'}{A_3}} \int_{R_2=\infty} \underset{\rightarrow}{h}(\vec{\rho}', \vec{\rho})\, d\vec{\rho}'\, e^{ja} \qquad \forall\, \vec{\xi} \in R_3,\ \vec{\rho} \in R_1, \tag{126}$$

where A_3 is the area of the aperture R_3, a is a constant phase delay, and C' is the proportionality constant defined in Eq. 85.

We define a kernel

$$K_{DS}(\vec{\rho}, \vec{r}) = \int_{R_3} h^*(\vec{\xi}, \vec{\rho})\, h(\vec{\xi}, \vec{r})\, d\vec{\xi}. \tag{127}$$

From our discussion of one-way apodization (see Table 1) we know that the eigenfunction of K_{DS} with maximum eigenvalue is the optimum waveform for transferring energy from the ground to the spacecraft. Combining (126) and (127) we have

$$K_{DS}(\vec{\rho}, \vec{r}) = C' \left(\int_{R_2=\infty} \underset{\rightarrow}{h}(\vec{\rho}', \vec{\rho})\, d\vec{\rho}' \right)^* \left(\int_{R_2=\infty} \underset{\rightarrow}{h}(\vec{\rho}', \vec{r})\, d\vec{\rho}' \right). \tag{128}$$

Since the kernel $K_{DS}(\vec{\rho}, \vec{r})$ may be written in the form[14]

$$K_{DS}(\vec{\rho}, \vec{r}) = \sum_{i=1}^{\infty} \beta_i \gamma_i(\vec{\rho})\, \gamma_i^*(\vec{r}), \tag{129}$$

where $\gamma_i(\vec{\rho})$ and β_i are the eigenfunctions and eigenvalues of K_{DS}, Eq. 128 implies that K_{DS} has only one eigenfunction, $\gamma_1(\vec{\rho})$, of nonzero eigenvalue, and that the eigenfunction is

$$\gamma_1(\vec{\rho}) = \frac{\left(\int_{R_2=\infty} \underset{\rightarrow}{h}(\vec{\rho}', \vec{\rho})\, d\vec{\rho}'\right)^*}{\left(\int_{R_1} \left| \int_{R_2=\infty} \underset{\rightarrow}{h}(\vec{\rho}', \vec{\rho})\, d\vec{\rho}' \right|^2 d\vec{\rho}\right)^{1/2}}. \tag{130}$$

The reciprocity of the atmosphere shows that

$$\gamma_1(\rho) = \frac{\left(\int_{R_2=\infty} \underset{\leftarrow}{h}(\vec{\rho}, \vec{\rho}')\, d\vec{\rho}'\right)^*}{\left(\int_{R_1} \left| \int_{R_2=\infty} \underset{\leftarrow}{h}(\vec{\rho}, \vec{\rho}')\, d\vec{\rho}' \right|^2 d\vec{\rho}\right)^{1/2}} \tag{131}$$

which is precisely the conjugated received beacon signal (normalized to unit energy) that results when we use an infinite plane-wave beacon at the top of the atmosphere. Thus, we have proved that the infinite beacon Q-kernel system is optimum for deep-space apodization.

Equation 128 also verifies the comment made in section 3.3 that for deep-space applications (through a reciprocal channel) there is only one branch to the parallel-channel model (for transmission between the ground and the spacecraft) with nonzero gain.

Finally, let us observe that the optimality proofs presented here guarantee that the performance in terms of $E_s(t)$ of an infinite beacon system cannot be exceeded by the performance of any finite beacon system for deep-space applications.

6.3 COMPARISON OF ADAPTIVE AND NONADAPTIVE APODIZATION SYSTEMS

We shall compare the optimal adaptive apodization system for deep-space applications (the Q-kernel system with infinite plane-wave beacon) to the optimal nonadaptive system. We begin by deriving the optimum nonadaptive system for a general apodization problem, and then apply the results obtained to the deep-space channel through turbulence.

6.31 Nonadaptive Apodization

Let R_1 and R_2 be the transmitting and receiving apertures, respectively, and let $\underset{\rightarrow}{h}(\vec{\rho}', \vec{\rho}; t)$ be the time-variant spatial impulse response that governs propagation from R_1 to R_2. We shall assume that the medium between R_1 and R_2 may be modeled as a succession of fixed states; that is, if $u(\vec{\rho})$ is the input field at R_1, then the output field at R_2 is

$$v(\vec{\rho}';t) = \int_{R_1} u(\vec{\rho})\, \underline{h}(\vec{\rho}', \vec{\rho}; t)\, d\vec{\rho}. \tag{132}$$

The energy in the field received at R_2 is therefore

$$E(t) = \int_{R_2} |v(\vec{\rho}';t)|^2\, d\vec{\rho}'$$

$$= \iint_{R_1} u^*(\vec{\rho})\, \underline{K}(\vec{\rho}, \vec{r}; t)\, u(\vec{r})\, d\vec{\rho} d\vec{r}, \tag{133}$$

where $\underline{K}(\vec{\rho}, \vec{r}; t)$ is the usual one-way propagation kernel (see Table 1) at time t. We wish to find the unit-energy waveform $u(\vec{\rho})$ on R_1 that maximizes the time-average energy received at R_2, $\langle E(t) \rangle$. In other words, we seek $u(\vec{\rho})$ such that

$$\int_{R_1} |u(\vec{\rho})|^2\, d\vec{\rho} = 1$$

and

$$\langle E(t) \rangle = \left\langle \iint_{R_1} u^*(\vec{\rho})\, \underline{K}(\vec{\rho}, \vec{r}; t)\, u(\vec{r})\, d\vec{\rho} d\vec{r} \right\rangle \tag{134}$$

is a maximum. We assume that we may bring the time average operation within the integral, and that the atmosphere is ergodic in the sense that the time average of $\underline{K}$ is the same as the ensemble average. That is,

$$\langle \underline{K}(\vec{\rho}, \vec{r}; t) \rangle = E[\underline{K}(\vec{\rho}, \vec{r}; t)]. \tag{135}$$

We may now rewrite (134) in the form

$$\langle E(t) \rangle = \iint_{R_1} u^*(\vec{\rho})\, E[\underline{K}(\vec{\rho}, \vec{r}; t)]\, u(\vec{r})\, d\vec{\rho} d\vec{r}. \tag{136}$$

The waveform $u(\vec{\rho})$ is the unit-energy waveform that maximizes (136). By analogy with the results of Section II, we see that $u(\vec{\rho})$ must be the eigenfunction of the kernel $E[\underline{K}(\vec{\rho}, \vec{r}; t)]$ of maximum eigenvalue.

The result just obtained is not new.[27,28] We shall discuss the performance of this optimum nonadaptive system for deep-space communication through the turbulent channel.

6.32 Applications to the Deep-Space Turbulent Channel

For the deep-space channel, the time-dependent one-way propagation kernel is

$$K_{DS}(\vec{\rho}, \vec{r}; t) = C'\left(\int_{R_2=\infty} \underset{\rightarrow}{h}(\vec{\rho}', \vec{\rho}; t)\, d\vec{\rho}'\right)^* \left(\int_{R_2=\infty} \underset{\rightarrow}{h}(\vec{\rho}', \vec{r}; t)\, d\vec{\rho}'\right), \tag{137}$$

where R_2 is now the infinite plane at the top of the atmosphere, and $\underset{\rightarrow}{h}(\vec{\rho}', \vec{\rho}; t)$ is the impulse response that applies to propagation from the ground to the top of the atmosphere. Since the channel is point-reciprocal, we have

$$K_{DS}(\vec{\rho}, \vec{r}; t) = C'\left(\int_{R_2=\infty} \underset{\leftarrow}{h}(\vec{\rho}, \vec{\rho}'; t)\, d\vec{\rho}'\right)^* \left(\int_{R_2=\infty} \underset{\leftarrow}{h}(\vec{r}, \vec{\rho}'; t)\, d\vec{\rho}'\right) \tag{138}$$

and from the $\underline{z}$ model for infinite plane-wave propagation through turbulence (see Section IV), we may conclude that

$$K_{DS}(\vec{\rho}, \vec{r}; t) = C'\underline{z}^*(\vec{\rho}, t)\, \underline{z}(\vec{r}, t). \tag{139}$$

Hence the ensemble average of the kernel of interest is

$$E[K_{DS}(\vec{\rho}, \vec{r}; t)] = C'E[\underline{z}^*(\vec{\rho}, t)\underline{z}(\vec{r}, t)] \tag{140}$$

which has been evaluated theoretically with the following result[29]

$$E[K_{DS}(\vec{\rho}, \vec{r}; t)] = C' \exp\left[-3.44\left(\frac{|\vec{\rho}-\vec{r}|}{r_o}\right)^{5/3}\right], \tag{141}$$

where r_o is determined by the strength of the turbulence and the optical wavelength. Moreland and Collins[27] have solved the resulting Fredholm integral equation numerically for the optimum eigenfunction and eigenvalue for several values of D (R_1 diameter) up to $D = 4r_o$. The optimum $u(\vec{\rho})$ has uniform phase over R_1, but its amplitude decreases monotonically with $|\vec{\rho}|$. More important, they show that the time-average energy received at the spacecraft when $u(\vec{\rho})$ is transmitted only slightly exceeds the average energy received if a plane wave $\left(u(\vec{\rho}) = \frac{1}{\sqrt{A_1}}\ \vec{\rho} \in R_1\right)$ were used, and in both cases increasing D beyond r_o does not significantly improve the performance of the system.

Thus, for the deep-space application, the optimum nonadaptive (one-way) system has an energy performance that saturates with increasing aperture diameter. On the other hand, the Q-kernel system of Section V with infinite plane-wave beacon (which, as we have seen, is the optimum deep-space system for all atmospheric states) does not exhibit this energy saturation with increasing D. We conclude that for large D as compared with r_o there is no nonadaptive system whose performance approximates the performance of the optimal Q-kernel adaptive system for the deep-space channel.

VII. POINT-TO-POINT COMMUNICATION THROUGH TURBULENCE

7.1 PROBLEM SPECIFICATION

We shall now apply the results of Section III for point-to-point communication through a reciprocal channel to the turbulent atmospheric channel. The system that we shall study is shown in Fig. 18. The regions R_1 and R_2 are circular apertures of diameters D and d, respectively, whose centers lie along a perpendicular between the R_1 and R_2

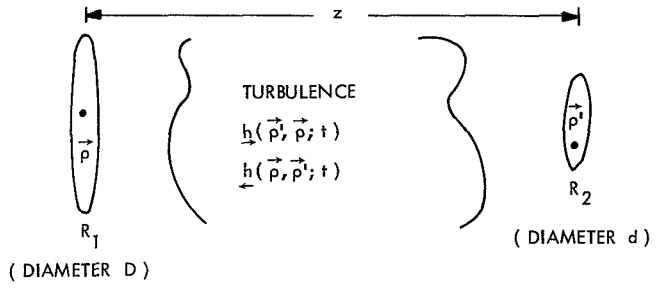

Fig. 18. Point-to-point Q-kernel system geometry.

planes. We denote the path length (perpendicular distance) from R_1 to R_2 by z. The medium between the two planes is the turbulent atmosphere, characterized by the two impulse responses, $\underset{\rightarrow}{h}(\vec{\rho}', \vec{\rho}; t)$ and $\underset{\leftarrow}{h}(\vec{\rho}, \vec{\rho}'; t)$. We assume that z is short enough that the atmosphere may be assumed to be "frozen" for at least one round trip, R_2 to R_1 to R_2, propagation time.

We shall study the energy performance of some adaptive systems of the Q-kernel type. In this study we shall make frequent use of the properties of the various channel kernels that are valid for reciprocal channels; hence, the reader may find it helpful to review Tables 1 and 3.

7.2 Optimal Spatial Modulation for Point-to-Point Channels

Let us study the following system. A unit-energy beacon, $v(\vec{\rho}')$, is transmitted from R_2, the transmitter at R_1 then sends a turned-around (conjugation operation) renormalized (to energy E_t) version of the received beacon field, and at R_2 the received field is heterodyned with $v(\vec{\rho}')$. It has been shown that for maximizing the energy received by the heterodyne receiver at R_2, the optimal beacon waveform for any single state of the atmosphere is $\phi_1(\vec{\rho}')$, the eigenfunction of $\underset{\leftarrow}{K}(\vec{\rho}', \vec{r}')$ for the particular state with maximum eigenvalue. We have observed that although it was not possible to calculate $\phi_1(\vec{\rho}')$ a priori, for time-invariant channels, it was possible to approximate an optimal beacon signal to any degree of approximation by using an adaptively updated beacon system. We shall now show how that result can be extended to the time-variant atmosphere.

Let the round-trip propagation time from R_2 to R_1 to R_2 be τ_p, where τ_p includes all of the necessary processing time at the transmitter. Let the coherence time of the

atmosphere be τ_c; that is, τ_c is the maximum length of time for which the atmosphere may be regarded as fixed. We define the parameter M to be the largest integer in τ_c/τ_p. Thus the atmosphere is essentially "frozen" for M round-trip propagation times.

Consider the adaptive beacon system described here. At time zero an initial beacon, $v_o(\vec{\rho}')$, is sent from R_2 to R_1. When this beacon is received at R_1 it is conjugated, normalized, and transmitted back to R_2. At R_2 the received field is heterodyned with $v_o(\vec{\rho}')$ as in a nonadaptive beacon system, but the received field is also conjugated,

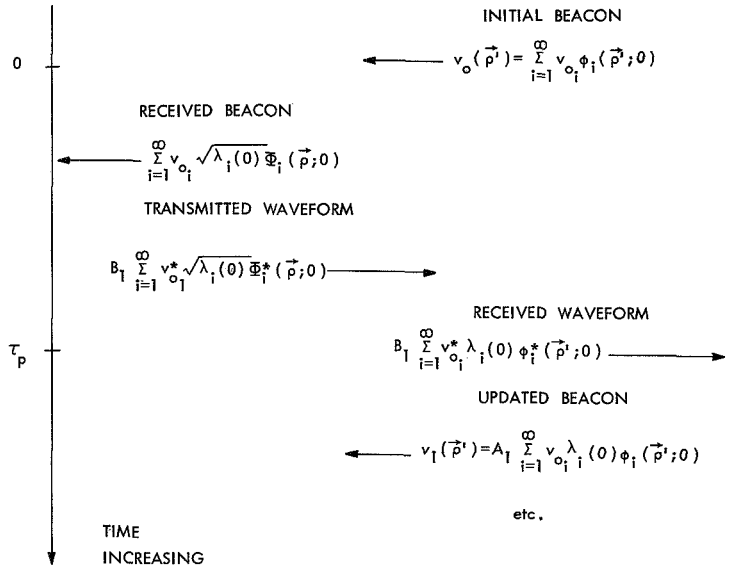

Fig. 19. Adaptive beacon system. Arrows denote direction of propagation. The adaptation process may continue as shown for M round trips before the atmosphere changes significantly.

renormalized, and used as an updated beacon, $v_1(\vec{\rho}')$. This process can be continued for M round trips before the atmosphere changes significantly (see Fig. 19).

Let $\phi_i(\vec{\rho}';t)$ and $\lambda_i(t)$ be the eigenfunctions and eigenvalues of the kernel $Q(\vec{\rho}', \vec{r}';t)$. From our assumptions, ϕ_i and λ_i are essentially constant during the time interval $(O, M\tau_p)$. Thus if the initial beacon is expanded in the form

$$v_o(\vec{\rho}') = \sum_{i=1}^{\infty} v_{o_i} \phi_i(\vec{\rho}';0), \tag{142}$$

then we may write the j^{th} updated version of the beacon in the form

$$v_j(\vec{\rho}') = A_j \sum_{i=1}^{\infty} v_{o_i} \lambda_i^j(0)\, \phi_i(\vec{\rho}';0) \qquad j = 1, 2, 3, \ldots, M, \tag{143}$$

where A_j is a normalizing constant. The performance of this adaptive beacon system (in terms of the output energy of the heterodyne receiver) increases monotonically (as long as the channel may be regarded as time-invariant) with time, and converges toward the optimal energy transfer possible (under the assumption that $v_{o_1} \neq 0$). Again if

$$\lambda_i \approx 1 \quad \forall\, i \leq D_f, \qquad \lambda_i \approx 0 \quad \forall\, i > D_f,$$

where D_f is the number of degrees of freedom of the channel as discussed in section 2.4, then the convergence will be essentially complete in one or two round trips, and the energy performance thereafter virtually optimum.

Since the atmospheric state is a smoothly varying quantity (in time), the eigenfunctions and eigenvalues, ϕ_i and λ_i, should also be smoothly varying time functions. Thus if $\tau_p \ll \tau_c$ (M large), the adaptive beacon system should be able to track the changes in the atmospheric state and, therefore, after some initial turn-on transient, the adaptive beacon system should achieve near-optimal performance for all ensuing atmospheric states.

To achieve this optimality, we had to make M large, and to do this we must restrict ourselves to short path lengths, and be able to rapidly process the incoming fields at R_1 and R_2. With the present technology it appears that the processing time restriction will be the more stringent of the two.

The adaptive beacon system that we have just described is an optimal spatial modulation system for the point-to-point channel when $\tau_c \gg \tau_p$. The rest of this discussion is devoted to a simpler system that places less stringent requirements on our processing times, but for large enough apertures achieves the same performance as the adaptive beacon system.

We use the same geometry as in the adaptive beacon system, but we now assume that the beacon is constrained to be a unit-energy normally incident plane wave. We assume that $\tau_c > \tau_p$ ($M \geq 1$); so, we may employ a fixed-state model for a single round-trip propagation time. The transmitter at R_1 is still a conjugation operation transmitter (with renormalization to energy E_t), and the receiver at R_2 heterodynes the field received there with the beacon signal (now a plane wave). Except that the transmission path is horizontal, rather than vertical, this system is the same as the ground-to-"window" system discussed in Section V, when the window (R_2) at the top of the atmosphere is finite. Thus, for the point-to-point system, the output energy of the heterodyne detector at R_2 must be given by

$$E_r(t) = \frac{E_t \left| \iint_{R_2} Q(\vec{\rho}', \vec{r}'; t)\, d\vec{\rho}' d\vec{r}' \right|^2}{A_2 \iint_{R_2} \underset{\leftarrow}{K}(\vec{\rho}', \vec{r}'; t)\, d\vec{\rho}' d\vec{r}'}. \tag{144}$$

Since the channel is point-reciprocal, we have $Q = \underset{\leftarrow}{K}$; therefore, (144) reduces to

$$E_r(t) = E_t \iint_{R_2} \frac{1}{\sqrt{A_2}} \underset{\leftarrow}{K}(\vec{\rho}', \vec{r}'; t) \frac{1}{\sqrt{A_2}} \, d\vec{\rho}' d\vec{r}' \tag{145}$$

which is the received beacon energy times E_t.

We can now apply the lemma of section 5.21 to show that given $\epsilon > 0$, for each atmospheric state there exists a D_o ($D_o < \infty$) such that

$$E_t \iint_{R_2} \frac{1}{\sqrt{A_2}} \underset{\leftarrow}{K}(\vec{\rho}', \vec{r}'; t) \frac{1}{\sqrt{A_2}} \, d\vec{\rho}' d\vec{r}' > E_t(1-\epsilon) \qquad \forall \; D \geq D_o, \tag{146}$$

where D is the diameter of the R_1 aperture. Recall that $\underset{\leftarrow}{K}$ depends implicitly upon R_1. Furthermore, we can apply the probabilistic bound of section 5.31 to show that there exist finite R_1 apertures that achieve a given level of performance during a substantial fraction of a given operating interval with high probability.

Although the system just considered achieves near-optimal performance for large enough transmitting apertures, the system is inefficient compared with the adaptive beacon system (when M is large). This inefficiency is the following. An adaptive beacon system will deliver good energy performance if the aperture areas are large enough that at least one eigenvalue, $\lambda_1(t)$, is always near unity. The plane-wave beacon system just considered will in general require that more than one of the $\lambda_i(t)$ be "always" near unity, and to achieve this condition the R_1 aperture must be enlarged from the minimum value for which the adaptive beacon system performs well. On the other hand, the plane-wave beacon system requires much less processing than the adaptive beacon system, so we are trading increased aperture diameter for decreased complexity. This is especially important in view of the processing time constraint set by the coherence time of the turbulence.

7.3 Remarks

We conclude the discussion of point-to-point communication with some comments on the possible uses of two-way communication systems. We shall restrict ourselves to the adaptive beacon system of section 7.2, although what we say may be related to the plane-wave beacon system, too.

Suppose in the adaptive beacon system shown in Fig. 19 the beacon used has energy E_t, and at R_1 there is a receiver, in addition to the adaptive transmitter, which heterodynes the received beacon field with a stored version of the previous received beacon field. Temporal modulation may then be employed at both terminals, R_1 and R_2, and information transmitted in both directions simultaneously. The received carrier energy for propagation in either direction, by the very nature of the system, will be near the optimal value of energy transfer (if M is large) for all atmospheric states, and since transmission of information occurs in both directions, there is no energy used purely for channel measurement, as there would be if the beacon were not temporally modulated.

This concludes our discussion of point-to-point channels, the last topic in our investigation of the turbulent channel in the noise-free case.

VIII. APODIZATION IN THE PRESENCE OF NOISE

8.1 INTRODUCTION

Thus far in our study of adaptive spatially modulated communication systems we have made two implicit assumptions: (i) the beacon signal is received in the absence of noise, and (ii) the adaptive transmitter is capable of generating the conjugate of an arbitrary incident field amplitude. We shall now remove these assumptions, and focus our attention upon the problems of beacon estimation and approximate transmitter implementation.

We begin by proving two general performance lemmas for Q-kernel systems, one for point-to-point channels, and one for deep-space channels. These lemmas will both summarize the previous work and set a firm foundation for the rest. Next, we shall develop a model for the noisy estimation problem, and derive the maximum-likelihood estimator. Then we shall study the optimal use of spatial bandwidth in a Q-kernel system, and conclude by examining the performance of a class of approximate transmitter implementations in the absence of noise.

8.2 PERFORMANCE LEMMAS

We shall study the performance of some Q-kernel communication systems operating in the turbulent atmosphere. We begin with the point-to-point channel.

8.21 Point-to-Point Channel

Consider the geometry shown in Fig. 20. We have two finite apertures, R_1 and R_2, separated by the turbulent atmosphere. We assume that the path length between these apertures is short enough that the coherence time of the turbulence is less than a round-trip

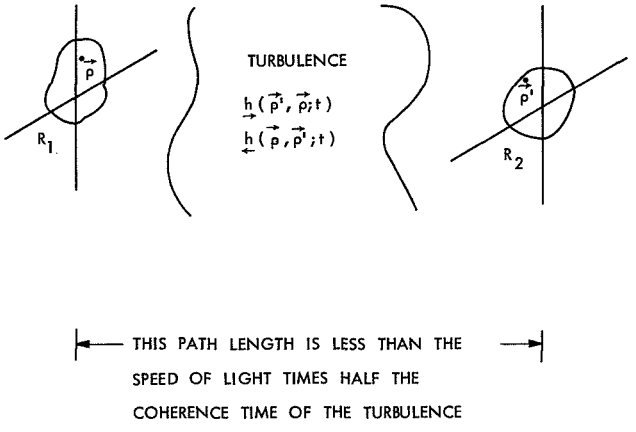

Fig. 20.
Point-to-point system geometry.

$(R_2\text{-}R_1\text{-}R_2)$ propagation time. Thus we may apply the fixed-state model of Section IV, and describe the system by two impulse responses: $\underset{\rightarrow}{h}(\vec{\rho}', \vec{\rho}; t)$ governing propagation from R_1 to R_2 and $\underset{\leftarrow}{h}(\vec{\rho}, \vec{\rho}'; t)$ governing propagation from R_2 to R_1. We restrict ourselves to considering a single atmospheric state, and, for convenience, we suppress the time dependence of the impulse responses.

We wish to evaluate the performance of the following system. A beacon, $\sqrt{E_b}\, v(\vec{\rho}')$,

of energy E_b is transmitted from R_2. We denote the received beacon field at R_1 by $u_o(\vec{\rho})$. That is,

$$u_o(\vec{\rho}) = \int_{R_2} \sqrt{E_b}\, v(\vec{\rho}')\, \underline{\underline{h}}(\vec{\rho}, \vec{\rho}')\, d\vec{\rho}'. \tag{147}$$

The transmitter at R_1 transmits $\tilde{u}^*(\vec{\rho})$, and at R_2 the received field is heterodyned with the beacon waveform $v(\vec{\rho}')$. We denote the energy in the output of this heterodyne detector by E_r. That is,

$$E_r = \left| \int_{R_2} \left(\int_{R_1} \tilde{u}^*(\vec{\rho})\, \underline{\underline{h}}(\vec{\rho}', \vec{\rho})\, d\vec{\rho} \right) v(\vec{\rho}')\, d\vec{\rho}' \right|^2. \tag{148}$$

Note that if we had

$$\tilde{u}(\vec{\rho}) = \sqrt{\frac{E_t}{\int_{R_1} |u_o(\vec{\rho})|^2\, d\vec{\rho}}}\; u_o(\vec{\rho}), \tag{149}$$

then the system just described would be our usual Q-kernel system. By leaving $\tilde{u}(\vec{\rho})$ arbitrary, the system described above may be used to model the noisy estimation or approximate transmitter problems.

Having set the stage, let us proceed with the lemma to be proved.

Lemma (Point-to-Point System Performance)

If the number of degrees of freedom of the channel D_f has the following properties: (i) $D_f > 1$, (ii) $\lambda_i \approx 1\ \forall\ i \leq D_f$, and (iii) $\lambda_i \approx 0\ \forall\ i > D_f$, then the output energy of the heterodyne detector at R_2 is given by

$$E_r = \left| \iint_{R_2} \sqrt{E_b}\, v^*(\vec{\rho}')\, Q(\vec{\rho}', \vec{r}')\, v(\vec{r}')\, d\vec{\rho}'\, d\vec{r}' \right|^2 \frac{\left| \int_{R_1} \tilde{u}(\vec{\rho})\, u_o^*(\vec{\rho})\, d\vec{\rho} \right|^2}{\left(\int_{R_1} |u_o(\vec{\rho})|^2\, d\vec{\rho} \right)^2}$$

$$= \frac{\left| \int_{R_1} \tilde{u}(\vec{\rho})\, u_o^*(\vec{\rho})\, d\vec{\rho} \right|^2}{E_b}. \tag{150}$$

Proof: First let us interpret what we are proving. Condition (i) of the lemma means that the two apertures are in the near-field region. Conditions (ii) and (iii) are properties of D_f that we have used from time to time, and they will be assumed to be true here. Let us examine the first equality in (150). From Table 1 we know that when $\tilde{u}(\vec{\rho}) = u_o(\vec{\rho})$ the output energy is given by

$$E_r = \left| \iint_{R_2} \sqrt{E_b}\, v^*(\vec{\rho}')\, Q(\vec{\rho}', \vec{r}')\, v(\vec{r}')\, d\vec{\rho}' d\vec{r}' \right|^2 .$$

Thus the lemma asserts that the effect of having $\tilde{u}(\vec{\rho}) \neq u_o(\vec{\rho})$ is a multiplicative term,

$$\frac{\left| \int_{R_1} \tilde{u}(\vec{\rho})\, u_o^*(\vec{\rho})\, d\vec{\rho} \right|^2}{\left(\int_{R_1} |u_o(\vec{\rho})|^2\, d\vec{\rho} \right)^2},$$

in the resulting energy expression. This term is precisely the energy in the $u_o(\vec{\rho})$ component of $\tilde{u}(\vec{\rho})$. Now let us begin the proof.

We first show that

$$\left| \iint_{R_2} \sqrt{E_b}\, v^*(\vec{\rho}')\, Q(\vec{\rho}', \vec{r}')\, v(\vec{r}')\, d\vec{\rho}' d\vec{r}' \right|^2 \frac{\left| \int_{R_1} \tilde{u}(\vec{\rho})\, u_o^*(\vec{\rho})\, d\vec{\rho} \right|^2}{\left(\int_{R_1} |u_o(\vec{\rho})|^2\, d\vec{\rho} \right)^2}$$

$$= \frac{\left| \int_{R_1} \tilde{u}(\vec{\rho})\, u_o^*(\vec{\rho})\, d\vec{\rho} \right|^2}{E_b}. \tag{151}$$

Since $u_o(\vec{\rho})$ is the received beacon field, $\int_{R_1} |u_o(\vec{\rho})|^2\, d\vec{\rho}$ is the energy in the received beacon field. But from the properties of the $\underset{\leftarrow}{K}$ kernel (see Table 1), the energy in the received beacon field is

$$E_b \iint_{R_2} v^*(\vec{\rho}')\, \underset{\leftarrow}{K}(\vec{\rho}', \vec{r}')\, v(\vec{r}')\, d\vec{\rho}' d\vec{r}'.$$

Furthermore, atmospheric reciprocity implies $Q = \underset{\leftarrow}{K}$; therefore,

$$\left| \iint_{R_2} \sqrt{E_b}\, v^*(\vec{\rho}')\, Q(\vec{\rho}', \vec{r}')\, v(\vec{r}')\, d\vec{\rho}' d\vec{r}' \right|^2 = \frac{\left(\int_{R_1} |u_o(\vec{\rho})|^2\, d\vec{\rho} \right)^2}{E_b}$$

which proves (151). To complete the proof, we need only show that

$$E_r = \frac{\left| \int_{R_1} \tilde{u}(\vec{\rho})\, u_o^*(\vec{\rho})\, d\vec{\rho} \right|^2}{E_b}.$$

We proceed as follows. We expand the beacon waveform in terms of $\{\phi_i\}$, the input

eigenfunctions of the $\underset{\leftarrow}{K}$ kernel. That is,

$$v(\vec{\rho}') = \sum_{i=1}^{\infty} v_i \phi_i(\vec{\rho}'), \tag{152}$$

where

$$v_i = \int_{R_2} v(\vec{\rho}')\ \phi_i^*(\vec{\rho}')\ d\vec{\rho}'.$$

From the properties of $\{\phi_i\}$ (see Table 1), we have

$$u_o(\vec{\rho}) = \sqrt{E_b} \sum_{i=1}^{\infty} v_i \sqrt{\lambda_i}\ \Phi_i(\vec{\rho}). \tag{153}$$

We now express $\tilde{u}(\vec{\rho})$ in the form

$$\tilde{u}(\vec{\rho}) = \frac{a u_o(\vec{\rho})}{\left(\int_{R_1} |u_o(\vec{\rho})|^2\ d\vec{\rho}\right)^{1/2}} + \omega(\vec{\rho}), \tag{154}$$

where

$$a = \int_{R_1} \tilde{u}(\vec{\rho})\ \frac{u_o^*(\vec{\rho})}{\left(\int_{R_1} |u_o(\vec{\xi})|^2\ d\vec{\xi}\right)^{1/2}}\ d\vec{\rho}$$

and

$$\int_{R_1} \omega(\vec{\rho})\ u_o^*(\vec{\rho})\ d\vec{\rho} = 0. \tag{155}$$

In terms of $\{\Phi_i\}$, the output eigenfunctions of the $\underset{\leftarrow}{K}$ kernel (154) may be written in the form

$$\tilde{u}(\vec{\rho}) = \sum_{i=1}^{\infty} \frac{\sqrt{E_b}\, a v_i \sqrt{\lambda_i}}{\left(\sum_{i=1}^{\infty} E_b |v_i|^2 \lambda_i\right)^{1/2}}\ \Phi_i(\vec{\rho}) + \sum_{i=1}^{\infty} \omega_i \Phi_i(\vec{\rho}), \tag{156}$$

where a is as given above, and $\omega_i = \int_{R_1} \omega(\vec{\rho})\ \Phi_i^*(\vec{\rho})\ d\vec{\rho}$. From the properties of $\{\Phi_i\}$

(see Table 3), $\hat{v}^*(\vec{\rho}')$, the field received at R_2, is

$$\hat{v}^*(\vec{\rho}') = \sum_{i=1}^{\infty} \left(\frac{a^* v_i^* \lambda_i \sqrt{E_b}}{\left(\sum_{i=1}^{\infty} E_b |v_i|^2 \lambda_i \right)^{1/2}} + \omega_i^* \sqrt{\lambda_i} \right) \phi_i^*(\vec{\rho}').$$

Thus the output energy of the heterodyne detector at R_2 is

$$E_r = \left| \int_{R_2} \hat{v}^*(\vec{\rho}')\, v(\vec{\rho}')\, d\vec{\rho}' \right|^2$$

$$= \left| \frac{\sum_{i=1}^{\infty} a^* \sqrt{E_b}\, \lambda_i |v_i|^2}{\left(\sum_{i=1}^{\infty} E_b |v_i|^2 \lambda_i \right)^{1/2}} + \sum_{i=1}^{\infty} \omega_i^* v_i \sqrt{\lambda_i} \right|^2$$

$$= \left| a^* \left(\sum_{i=1}^{\infty} |v_i|^2 \lambda_i \right)^{1/2} + \sum_{i=1}^{\infty} \omega_i^* v_i \sqrt{\lambda_i} \right|^2 . \tag{157}$$

We now use the assumed properties of D_f to reduce (157) to

$$E_r = \left| a^* \left(\sum_{i=1}^{D_f} |v_i|^2 \right)^{1/2} + \sum_{i=1}^{D_f} \omega_i^* v_i \right|^2 . \tag{158}$$

From (155),

$$0 = \int_{R_1} \omega(\vec{\rho})\, u_o^*(\vec{\rho})\, d\vec{\rho} = \sum_{i=1}^{D_f} \sqrt{E_b}\, \omega_i v_i^* .$$

Therefore

$$E_r = \left| a^* \left(\sum_{i=1}^{D_f} |v_i|^2 \right)^{1/2} \right|^2$$

$$= \left| \int_{R_1} \tilde{u}(\vec{\rho})\, u_o^*(\vec{\rho})\, d\vec{\rho} \right|^2 \frac{\sum_{i=1}^{D_f} |v_i|^2}{\int_{R_1} |u_o(\vec{\rho})|^2 \, d\vec{\rho}}$$

$$= \frac{\left| \int_{R_1} \tilde{u}(\vec{\rho})\, u_o^*(\vec{\rho})\, d\vec{\rho} \right|^2}{E_b},$$

which proves the lemma.

As we have mentioned, the essence of this lemma is that E_r is given by the performance when $\tilde{u}(\vec{\rho}) = u_o(\vec{\rho})$ times the energy in the $u_o(\vec{\rho})$ component of $\tilde{u}(\vec{\rho})$. The proof that we have presented hinges on the fact that since $u_o^*(\vec{\rho})$ and $\omega^*(\vec{\rho})$ are orthogonal on R_1, they are also orthogonal on R_2 after propagation through the channel. The assumption that the eigenvalues $\{\lambda_i\}$ are either zero or one implies that any two orthogonal functions on R_1 have this property.

In apodization problems we are concerned with maximizing the received energy for a fixed transmitted energy, so we now prove the following corollary.

Corollary. If the conditions of the previous lemma are satisfied, then the fraction of the transmitted energy that is in the output of the heterodyne detector at R_2 is given by

$$\frac{E_r}{E_{in}} = \frac{\left| \int_{R_1} \tilde{u}(\vec{\rho})\, u_o^*(\vec{\rho})\, d\vec{\rho} \right|^2}{E_b \int_{R_1} |\tilde{u}(\vec{\rho})|^2\, d\vec{\rho}}$$

$$= \left(\iint_{R_2} v^*(\vec{\rho}')\, \underline{\underline{K}}(\vec{\rho}', \vec{r}')\, v(\vec{r}')\, d\vec{\rho}' d\vec{r}' \right) \cos^2(\tilde{u}, u_o), \tag{159}$$

where $E_{in} = \int_{R_1} |\tilde{u}(\vec{\rho})|^2\, d\vec{\rho}$ is the transmitted energy, and

$$\cos(\tilde{u}, u_o) = \frac{\left| \int_{R_1} \tilde{u}(\vec{\rho})\, u_o^*(\vec{\rho})\, d\vec{\rho} \right|}{\left(\int_{R_1} |\tilde{u}(\vec{\rho})|^2\, d\vec{\rho} \right)^{1/2} \left(\int_{R_1} |u_o(\vec{\rho})|^2\, d\vec{\rho} \right)^{1/2}}.$$

Proof: The first equality follows directly from (150) and the definition of E_{in}. The second equality follows from the fact that

$$\int_{R_1} |u_o(\vec{\rho})|^2\, d\vec{\rho} = E_b \iint_{R_2} v^*(\vec{\rho}')\, \underline{\underline{K}}(\vec{\rho}', \vec{r}')\, v(\vec{r}')\, d\vec{\rho}' d\vec{r}'$$

and the definition of $\cos(\tilde{u}, u_o)$.

The interpretation of this corollary is much more important than its proof. Equation 159 says that the fraction of the transmitted energy in the output is the fraction of the beacon energy received at R_1 times $\cos^2(\tilde{u}, u_o)$. The term $\cos(\tilde{u}, u_o)$ is the magnitude of the cosine of the angle between the functions $\tilde{u}(\vec{\rho})$ and $u_o(\vec{\rho})$ in $L^2(R_1)$. The Schwarz inequality shows that $0 \leq \cos^2(\tilde{u}, u_o) \leq 1$, and $\cos^2(\tilde{u}, u_o) = 1$ if and only if $\tilde{u}(\vec{\rho}) = b u_o(\vec{\rho})$, where b is some scalar. We now turn to the deep-space channel.

8.22 Deep-Space Channel

The geometry of interest is shown in Fig. 21. The R_1 aperture is still a finite transmitting aperture on the ground, but R_2 is now the infinite plane at the top of the atmosphere perpendicular to the line connecting R_1 with the spacecraft aperture R_3. We

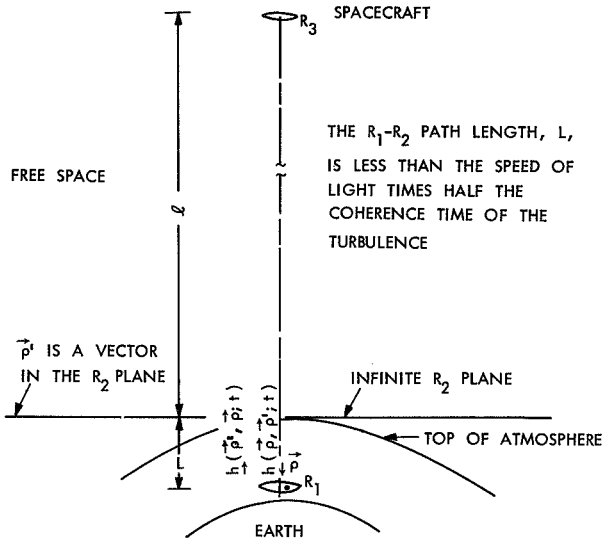

Fig. 21. Deep-space system geometry.

assume that the zenith angle of the R_1-R_3 path is small enough that the round-trip propagation time (R_2-R_1-R_2) is less than the coherence time of the turbulence; thus we may use the fixed-state model of Section IV. We work with a single atmospheric state, suppressing the time dependence of the impulse responses.

The system that we wish to consider is the following. A normally incident uniform plane wave of amplitude B is transmitted from R_2 to R_1. We denote the received beacon field $u_o(\vec{\rho})$ as in section 8.21, only in this case we have

$$u_o(\vec{\rho}) = \int_{R_2=\infty} B \, \underline{h}(\vec{\rho}, \vec{\rho}') \, d\vec{\rho}'. \tag{160}$$

The transmitter at R_1 transmits $\tilde{u}^*(\vec{\rho})$. We assume that the path length from R_2 to R_3 is sufficiently large that the field received at R_3 when $\tilde{u}^*(\vec{\rho})$ is transmitted from R_1 is a normally incident plane wave whose amplitude is

$$\frac{e^{jb}}{\lambda \ell} \int_{R_2=\infty} \left(\int_{R_1} \tilde{u}^*(\vec{\rho}) \, \underline{h}(\vec{\rho}', \vec{\rho}) \, d\vec{\rho} \right) d\vec{\rho}', \tag{161}$$

where ℓ is the R_2-R_3 path length, and b is a constant phase delay. This assumption is the same path-length assumption that we made when discussing deep-space channels

before. From 161, E_s, the energy received over R_3, is

$$E_s = \frac{A_3}{(\lambda \ell)^2} \left| \int_{R_2=\infty} \left(\int_{R_1} \tilde{u}^*(\vec{\rho}) \, \underline{\underline{h}}(\vec{\rho}', \vec{\rho}) \, d\vec{\rho} \right) d\vec{\rho}' \right|^2, \tag{162}$$

where A_3 is the area of the aperture R_3. Note that if $\tilde{u}(\vec{\rho}) = u_o(\vec{\rho})$, then (162) reduces to the energy received at the spacecraft from a Q-kernel system.

We now prove the following lemma.

Lemma (Deep-Space System Performance)

For the deep-space system described above we have

$$E_s = \frac{A_3}{(\lambda \ell)^2} \left| \iint_{R_2=\infty} BQ(\vec{\rho}', \vec{r}') \, d\vec{\rho}' d\vec{r}' \right|^2 \frac{\left| \int_{R_1} \tilde{u}(\vec{\rho}) \, u_o^*(\vec{\rho}) \, d\vec{\rho} \right|^2}{\left(\int_{R_1} |u_o(\vec{\rho})|^2 \, d\vec{\rho} \right)^2}$$

$$= \frac{A_3}{(\lambda \ell)^2} \frac{\left| \int_{R_1} \tilde{u}(\vec{\rho}) \, u_o^*(\vec{\rho}) \, d\vec{\rho} \right|^2}{B^2}. \tag{163}$$

Proof: First let us note that the definition of the Q kernel and Eq. 162 imply that when $\tilde{u}(\vec{\rho}) = u_o(\vec{\rho})$ the enery received at the spacecraft is

$$E_s = \frac{A_3}{(\lambda \ell)^2} \left| \iint_{R_2=\infty} BQ(\vec{\rho}', \vec{r}') \, d\vec{\rho}' d\vec{r}' \right|^2.$$

Thus (163) says that E_s is given by the performance when $\tilde{u}(\vec{\rho}) = u_o(\vec{\rho})$ times the energy in the $u_o(\vec{\rho})$ component of $\tilde{u}(\vec{\rho})$. Since R_2 is infinite, however, we cannot use the eigenfunction expansion argument of section 8.21 to prove the lemma above. Instead we proceed as follows.

From the properties of the $\underline{\underline{K}}$ kernel and reciprocity we immediately conclude that

$$\int_{R_1} |u_o(\vec{\rho})|^2 \, d\vec{\rho} = \iint_{R_2=\infty} B^2 \underline{\underline{K}}(\vec{\rho}', \vec{r}') \, d\vec{\rho}' d\vec{r}'$$

$$= \iint_{R_2=\infty} B^2 Q(\vec{\rho}', \vec{r}') \, d\vec{\rho}' d\vec{r}'.$$

Therefore, we have

$$\left| \iint_{R_2=\infty} BQ(\vec{\rho}', \vec{r}') \, d\vec{\rho}' d\vec{r}' \right|^2 = \frac{\left(\int_{R_1} |u_o(\vec{\rho})|^2 \, d\vec{\rho} \right)^2}{B^2},$$

so we need only show that

$$E_s = \frac{A_3}{(\lambda \ell)^2} \frac{\left| \int_{R_1} \tilde{u}(\vec{\rho})\, u_o^*(\vec{\rho})\, d\vec{\rho} \right|^2}{B^2}$$

to complete the proof of the lemma.

From (162) we have

$$E_s = \frac{A_3}{(\lambda \ell)^2} \left| \int_{R_2=\infty} \left(\int_{R_1} \tilde{u}^*(\vec{\rho})\, \underset{\leftrightarrows}{h}(\vec{\rho}', \vec{\rho})\, d\vec{\rho} \right) d\vec{\rho}' \right|^2 .$$

Interchanging the orders of integration and using the reciprocity of the atmosphere, we obtain

$$E_s = \frac{A_3}{(\lambda \ell)^2} \left| \int_{R_1} \tilde{u}^*(\vec{\rho}) \left(\int_{R_2=\infty} \underset{\leftrightarrows}{h}(\vec{\rho}, \vec{\rho}')\, d\vec{\rho}' \right) d\vec{\rho} \right|^2 .$$

Next we substitute for $\int_{R_2=\infty} \underset{\leftrightarrows}{h}(\vec{\rho}, \vec{\rho}')\, d\vec{\rho}'$ from (160) to obtain

$$E_s = \frac{A_3}{(\lambda \ell)^2} \frac{\left| \int_{R_1} \tilde{u}^*(\vec{\rho})\, u_o(\vec{\rho})\, d\vec{\rho} \right|^2}{B^2}$$

$$= \frac{A_3}{(\lambda \ell)^2} \frac{\left| \int_{R_1} \tilde{u}(\vec{\rho})\, u_o^*(\vec{\rho})\, d\vec{\rho} \right|^2}{B^2},$$

which proves the lemma.

The fact that the energy received at the spacecraft is due solely to the energy in the $u_o(\vec{\rho})$ component of $\tilde{u}(\vec{\rho})$ should come as no surprise at this point. In Section VI we showed that the apodization kernel for propagation from R_1 to R_3 had only one eigenfunction with nonzero eigenvalue, and that eigenfunction was proportional to the conjugate of the received beacon field, that is, $u_o(\vec{\rho})$ in our present notation.

We now prove a simple corollary concerning the fraction of the transmitted energy that reaches the spacecraft.

Corollary. For the deep-space system under consideration the fraction of the transmitted energy that is received at the spacecraft is

$$\frac{E_s}{E_{in}} = \frac{A_3}{(\lambda \ell)^2} \frac{\left| \int_{R_1} \tilde{u}(\vec{\rho})\, u_o^*(\vec{\rho})\, d\vec{\rho} \right|^2}{B^2 \int_{R_1} |\tilde{u}(\vec{\rho})|^2\, d\vec{\rho}}$$

$$= \frac{A_3}{(\lambda \ell)^2} \left(\iint_{R_2=\infty} \underset{\leftrightarrows}{K}(\vec{\rho}', \vec{r}')\, d\vec{\rho}' d\vec{r}' \right) \cos^2(\tilde{u}, u_o), \tag{164}$$

where $E_{in} = \int_{R_1} |\tilde{u}(\vec{\rho})|^2 \, d\vec{\rho}$ is the transmitted energy, and

$$\cos(\tilde{u}, u_o) = \frac{\left| \int_{R_1} \tilde{u}(\vec{\rho}) \, u_o^*(\vec{\rho}) \, d\vec{\rho} \right|}{\left(\int_{R_1} |\tilde{u}(\vec{\rho})|^2 \, d\vec{\rho} \right)^{1/2} \left(\int_{R_1} |u_o(\vec{\rho})|^2 \, d\vec{\rho} \right)^{1/2}}.$$

Proof: The first equality follows directly from the lemma and the definition of E_{in}. The second equality follows from

$$\int_{R_1} |u_o(\vec{\rho})|^2 \, d\vec{\rho} = \iint_{R_2=\infty} B^2 \, \underset{\leftarrow}{K}(\vec{\rho}', \vec{r}') \, d\vec{\rho}' d\vec{r}'$$

and the definition of $\cos(\tilde{u}, u_o)$.

The interpretation of this corollary is similar to that of section 8.21. The term

$$\frac{A_3}{(\lambda \ell)^2} \iint_{R_2=\infty} \underset{\leftarrow}{K}(\vec{\rho}', \vec{r}') \, d\vec{\rho}' d\vec{r}'$$

is the fraction of the transmitted energy that reaches the spacecraft when $\tilde{u}(\vec{\rho}) = u_o(\vec{\rho})$. Note that for R_1 large (see section 5.4) this term is approximately $A_1 A_3/(\lambda \ell)^2$ with high probability. Although it might appear that we can make this term arbitrarily large by increasing A_3 or A_1, the path-length assumption implies that $A_1 A_3/(\lambda \ell)^2 \ll 1$. (Remember that $A_1 A_3/(\lambda \ell)^2$ is the number of degrees of freedom of the R_1-R_3 system in the absence of turbulence.) The $\cos^2(\tilde{u}, u_o)$ term measures how much performance is lost because $\tilde{u}(\vec{\rho})$ has energy in components orthogonal to $u_o(\vec{\rho})$.

8.23 Remarks

Let us emphasize one aspect of the results just proved. The ratio of the output energy to the transmitted energy, that is, E_r/E_{in} for point-to-point channels and E_s/E_{in} for deep-space channels, is the gain of the system. Our results show that these gains are equal to the values they take on when $\tilde{u}(\vec{\rho}) = u_o(\vec{\rho})$ times a gain reduction factor $g \triangleq \cos^2(\tilde{u}, u_o)$. This gain reduction factor lies between zero and one, and it is one if and only if $\tilde{u}(\vec{\rho})$ is proportional to $u_o(\vec{\rho})$. The gain reduction factor measures how much gain is lost because $\tilde{u}(\vec{\rho})$ has components orthogonal to $u_o(\vec{\rho})$, and it will be the center of our attention in discussing beacon estimation and approximate transmitter implementations. We shall begin this work by developing a model for the relevant noise sources in our system.

A final word is in order. None of the proofs in this section depended in any way upon special properties of the atmospheric channel (other than the fixed-state model and reciprocity), so all of our results are in fact valid for any time-invariant point-reciprocal spatially modulated channel.

8.3 NOISE MODEL

When a beacon is transmitted from R_2 to R_1, whether in a point-to-point channel or a deep-space channel, the signal is received at R_1 in a noisy environment. Let us consider the sources of noise in the receiver at R_1. In general there will be a number of different noise contributions: background noise from scattered sunlight, black-body and other radiation sources, shot noise from energy detectors, and thermal noise from amplifier circuits in the receiver, to name a few. We shall concentrate on the background noise and quantum shot noise as the principal noise sources in our system.

8.31 Background Noise

When a beacon is transmitted from R_2 the received beacon field is

$$u_o(\vec{\rho}) = \begin{cases} \int_{R_2} \sqrt{E_b}\, v(\vec{\rho}')\, \underset{\leftrightarrows}{h}(\vec{\rho}, \vec{\rho}')\, d\vec{\rho}' & \text{for point-to-point channels} \\ \int_{R_2=\infty} B \underset{\leftrightarrows}{h}(\vec{\rho}, \vec{\rho}')\, d\vec{\rho}' & \text{for deep-space channels} \end{cases} \tag{165}$$

The quantity $u_o(\vec{\rho})$ is the complex-field amplitude of the linearly polarized wave that would be received at R_1 were there no noise present. The actual field amplitude received at R_1 is

$$\vec{u}(\vec{\rho}, t) = u_o(\vec{\rho})\, \vec{i}_x + \vec{n}_B(\vec{\rho}, t), \tag{166}$$

where $\vec{n}_B(\vec{\rho},t)$ is the complex-field amplitude of the background noise, and $\vec{i}_x$ is a unit vector in the direction of polarization of the transmitted beacon field. We are describing the complex-field amplitude of the noise process by $\vec{n}_B(\vec{\rho}, t)$. The actual background noise waveform is

$$\text{Re}\left[\vec{n}_B(\vec{\rho}, t)\, e^{j\omega_c t}\right].$$

The reader should keep in mind that when we speak of noise fields here we shall always be concerned with the complex amplitude of the noise.

For light from incoherent sources the background noise may modeled as a zero-mean Gaussian random process whose two polarizations are statistically independent.[22, 30] Thus no loss in optimality results from passing the field received at R_1 through a polarizer that selects the $\vec{i}_x$ polarization. The output of such a polarizer is

$$u(\vec{\rho}, t) = u_o(\vec{\rho}) + n_B(\vec{\rho}, t), \tag{167}$$

where $u(\vec{\rho}, t) = \vec{u}(\vec{\rho}, t) \cdot \vec{i}_x$, and $n_B(\vec{\rho}, t) = \vec{n}_B(\vec{\rho}, t) \cdot \vec{i}_x$. For receivers with large fields of view $n_B(\vec{\rho}, t)$ has the following properties.[4,22]

1. Let $\{u_i^*\}$ be a complete set of orthonormal functions defined on R_1. We define

the processes

$$n_{B_i}(t) = \int_{R_1} n_B(\vec{\rho}, t)\, u_i^*(\vec{\rho})\, d\vec{\rho}. \tag{168}$$

The processes $\{n_{B_i}(t)\}$ are then statistically independent identically distributed zero-mean Gaussian processes, whose real and imaginary parts are statistically independent and identically distributed.

2. Suppose that $R_{B_i}(\tau)$ is the correlation function of $n_{B_i}(t)$, and let $S_{B_i}(f)$ be the Fourier transform of $R_{B_i}(\tau)$. That is,

$$R_{B_i}(\tau) = E\left[n_{B_i}(t+\tau)\, n_{B_i}^*(t) \right] \tag{169}$$

and

$$S_{B_i}(f) = \int_{-\infty}^{\infty} R_{B_i}(\tau)\, e^{-j2\pi f\tau}\, d\tau. \tag{170}$$

Then $S_{B_i}(f)$, the power spectral density of $n_{B_i}(t)$, is constant in a large region about zero frequency. Properties 1 and 2 imply that the background noise is well approximated by a Gaussian process that is "white" in both time and space. The power spectral density of this noise depends on both the time of day and the center frequency $(\omega_c/2\pi)$ of the radiation. For the present, we shall assume that

$$S_{B_i}(f) = N_o, \tag{171}$$

where $S_{B_i}(f)$ is defined by (170). (This value of $S_{B_i}(f)$ implies that the average power in a 1-Hz bandwidth (bilateral) of the noise field

$$\mathrm{Re}\left[n_{B_i}(t)\, e^{j\omega_c t} \right]$$

is N_o.)

8.32 Quantum Shot Noise

Since we must estimate the spatial variations of $u(\vec{\rho}, t)$, some sort of coherent-field detection is required. In particular, it will be assumed eventually that heterodyne detection is employed to measure the components of $u(\vec{\rho}, t)$ along a set of N spatial modes. Thus we now consider the quantum shot noise of such systems.

Suppose that $u(\vec{\rho}, t)$ is heterodyned with the waveform $\sqrt{E_o}\, u_1^*(\vec{\rho})\, \exp(+j\Delta\omega t)$ (see Fig. 22), where $\Delta\omega/2\pi$ is the intermediate (offset) frequency, and $u_1(\vec{\rho})$ is assumed to have unit energy. The complex envelope of the output of the photodetector in some bandwidth W about the intermediate frequency will have three components, a signal

proportional to

$$\sqrt{E_o} \int_{R_1} u_o(\vec{\rho})\, u_1^*(\vec{\rho})\, d\vec{\rho},$$

a contribution from the background noise proportional to

$$\sqrt{E_o} \int_{R_1} [n_B(\vec{\rho}, t)]_{BL}\, u_1^*(\vec{\rho})\, d\vec{\rho},$$

where $[n_B(\vec{\rho}, t)]_{BL}$ is the noise process $n_B(\vec{\rho}, t)$ limited to a bandwidth W about zero frequency, and a shot-noise term that arises from the quantum nature of light. Helstrom[31] has shown that in the limit

$$E_o \gg \int_{R_1} |u_o(\vec{\rho})|^2\, d\vec{\rho} + 2N_o W \tag{172}$$

the shot noise is a Gaussian random process, whose real and imaginary parts are statistically independent and identically distributed, and whose spectral density is flat over

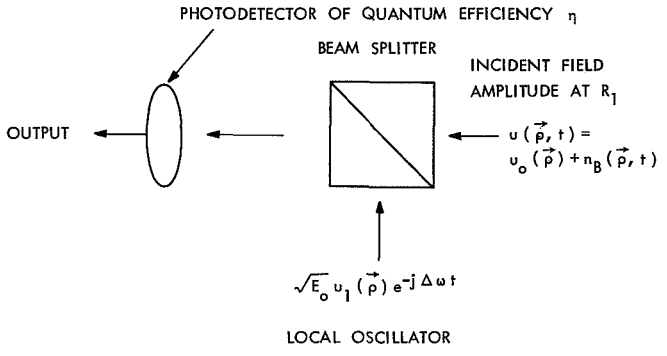

Fig. 22. Single heterodyne detection system. The photodetector covers the region R_1. The output of the detector is at the offset frequency $\Delta\omega/2\pi$, and has bandwidth W.

the bandwidth W. Furthermore, the value of the spectral density depends only on the local oscillator power, the center frequency of the incident light, and the quantum efficiency of the photodetector used. The inequality (172) implies that the local oscillator is much stronger than the received beacon plus average background noise, over the bandwidth of interest. When (172) is satisfied the shot noise in the output of the photodetector may be represented by an equivalent noise field amplitude, $n_S(\vec{\rho}, t)$, with the quantum nature of the detection process ignored. This noise field has the following properties.[32, 33]

1. $n_s(\vec{\rho}, t)$ is a zero-mean Gaussian process that is statistically independent of $n_B(\vec{\rho}, t)$.

2. The process $n_s(\vec{\rho}, t)$ may be written in the form

$$n_s(\vec{\rho}, t) = n_{s_1}(t)\, u_1(\vec{\rho}),$$

where $n_{s_1}(t)$ is a Gaussian random process whose real and imaginary parts are statistically independent and identically distributed, and whose spectral density is $\hbar\omega_c/2\eta$ over a bandwidth about zero frequency that is large compared with W, where η is the quantum efficiency of the photodetector in Fig. 22.

Now let us suppose that $u(\vec{\rho}, t)$ is heterodyned with N local oscillators

$$\sqrt{E_o}\, u_1^*(\vec{\rho})\, e^{+j\Delta\omega t},\ \sqrt{E_o}\, u_2^*(\vec{\rho})\, e^{+j\Delta\omega t},\ \ldots,\ \sqrt{E_o}\, u_N^*(\vec{\rho})\, e^{+j\Delta\omega t},$$

where $\{u_i^*;\ 1 \leq i \leq N\}$ is a set of orthonormal functions on R_1, and E_o satisfies (172) (see Fig. 23). The complex envelope of the output of each photodetector will contain

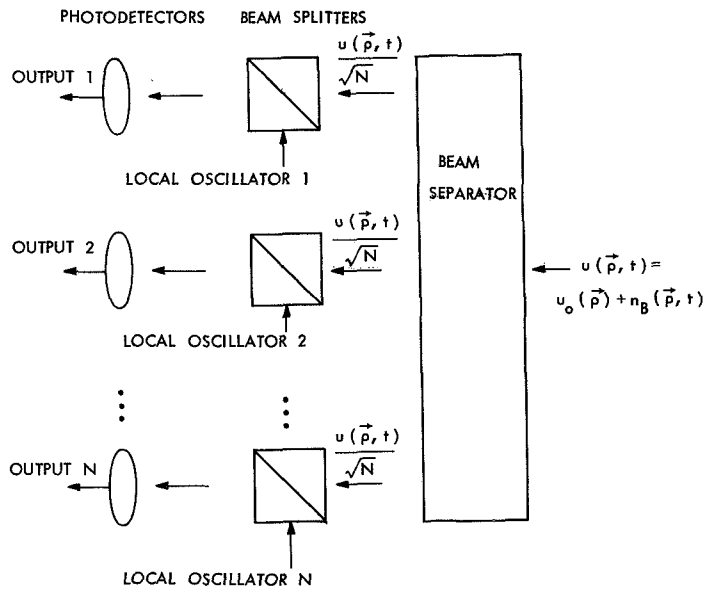

Fig. 23. Array of heterodyne detectors. L. O. i is the i^{th} local oscillator = $\sqrt{E_o/N}\, u_i(\vec{\rho})\, e^{-j\Delta\omega t}$. The photodetectors have areas congruent to R_1, and are all of quantum efficiency η. The outputs are at the offset frequency $\Delta\omega/2\pi$, and have bandwidth W.

a signal component, a contribution from the background noise, and a "white" Gaussian shot noise over the bandwidth W. Since each local oscillator-photodetector pair is independent (physically) of all other such pairs, it is reasonable to assume that the shot noises are independent processes. Moreover, if we use an equivalent shot-noise field,

$n_s(\vec{\rho}, t)$, to account for the shot noise in the photodetector outputs, then $n_s(\vec{\rho}, t)$ has the following properties.

1. $n_s(\vec{\rho}, t)$ is a zero-mean Gaussian process that is statistically independent of $n_B(\vec{\rho}, t)$.

2. The process $n_s(\vec{\rho}, t)$ may be written in the form

$$n_s(\vec{\rho}, t) = \sum_{i=1}^{N} n_{s_i}(t)\, u_i(\vec{\rho}), \tag{173}$$

where $\{n_{s_i}(t)\}$ is a set of statistically independent Gaussian noise processes whose real and imaginary parts are statistically independent and identically distributed, and whose spectral densities are constant at $\hbar\omega_c/2\eta$ over a bandwidth about zero frequency that is large compared with W.

Although the description of $n_s(\vec{\rho}, t)$ in Eq. 173 is complete with respect to the shot noise in the outputs of the photodetectors in Fig. 23, it is not the description that we shall use now. Let $\{u_i^*\}$ be a complete orthonormal set of functions on R_1, where

$$u_1^*(\vec{\rho}),\ u_2^*(\vec{\rho}),\ \ldots,\ u_N^*(\vec{\rho})$$

are the spatial waveforms used in Fig. 23. Consider the expression

$$n_s(\vec{\rho}, t) = \sum_{i=1}^{\infty} n_{s_i}(t)\, u_i(\vec{\rho}), \tag{174}$$

where $\{n_{s_i}(t)\}$ is as in condition 2. It is clear that as far as the outputs of the N photodetectors in Fig. 23 are concerned, Eq. 174 may be used instead of Eq. 173 as a description of the equivalent shot-noise field. Equation 174 is the description of a Gaussian process that is essentially white in both time and space, and it is the description of the shot noise that we use.

From our discussions, we conclude that the reception of the beacon signal at R_1 may be modeled as occurring in the presence of an additive noise-field amplitude

$$n(\vec{\rho}, t) = n_B(\vec{\rho}, t) + n_s(\vec{\rho}, t),$$

where $n_B(\vec{\rho}, t)$ is the background noise as described in section 8.31, and $n_s(\vec{\rho}, t)$ is the equivalent shot noise field described by Eq. 174. We have seen that both $n_B(\vec{\rho}, t)$ and $n_s(\vec{\rho}, t)$ are white Gaussian noise processes in time and space. Since the two noises are statistically independent, $n(\vec{\rho}, t)$ is a white Gaussian process also. In particular, if $\{\xi_i\}$ is some arbitrary complete orthonormal set of functions on R_1, then the processes

$$n_i(t) = \int_{R_1} n(\vec{\rho}, t)\, \xi_i(\vec{\rho})\, d\vec{\rho} \tag{175}$$

are statistically independent identically distributed white Gaussian noise processes with spectral densities $N_o + \hbar\omega_c/2\eta$. This result follows from the Karhunen-Loève expansion of white Gaussian noise.

Before continuing, let us emphasize the importance of this result. Although we are concerned with the noise in the output of an array of N heterodyne detectors using a particular set of local oscillator waveforms, we have shown that it is equivalent to assuming an additive white Gaussian noise at the input and ignoring the quantum nature of the detection process and the particular set of local-oscillator waveforms used.

8.4 MAXIMUM-LIKELIHOOD TRANSMITTER

We are now ready to study apodization in the presence of noise. Consider the following maximization problem. A spatial waveform $u_o(\vec{\rho})$ is received over some finite aperture R_1 in the presence of an additive noise $n(\vec{\rho}, t)$. The noise-corrupted waveform

$$u(\vec{\rho}, t) = u_o(\vec{\rho}) + n(\vec{\rho}, t)$$

is detected by an array of N heterodyne detectors (as in Fig. 23) using spatial waveforms

$$\sqrt{E_o}\, u_1^*(\vec{\rho})\, e^{+j\Delta\omega t},\ \sqrt{E_o}\, u_2^*(\vec{\rho})\, e^{+j\Delta\omega t},\ \ldots,\ \sqrt{E_o}\, u_N^*(\vec{\rho})\, e^{+j\Delta\omega t},$$

where $\{u_i^*:\ 1 \leq i \leq N\}$ is a set of orthonormal functions on R_1. The outputs of the N heterodyne detectors are observed over a time interval $(0, \tau)$, and from this observation an estimate, $\tilde{u}(\vec{\rho})$, of $u_o(\vec{\rho})$ is made. We seek to find the estimation rule that maximizes

$$E\left[\frac{\left|\int_{R_1} \tilde{u}(\vec{\rho})\, u_o^*(\vec{\rho})\, d\vec{\rho}\right|^2}{\int_{R_1} |u_o(\vec{\rho})|^2\, d\vec{\rho} \int_{R_1} |\tilde{u}(\vec{\rho})|^2\, d\vec{\rho}}\right], \tag{176}$$

subject to the constraint

$$\tilde{u}(\vec{\rho}) = \sqrt{\frac{E_t}{\sum_{i=1}^{N} |\hat{a}_i|^2}} \sum_{i=1}^{N} \hat{a}_i u_i(\vec{\rho}), \tag{177}$$

where the expectation is over the noise ensemble.

Let us see why this is a problem of interest. Suppose $u_o(\vec{\rho})$ is the received beacon field in a point-to-point or deep-space two-way communication system (as in section 8.2). From the results of section 8.2 we find that the solution to the estimation problem above maximizes the average gain of the system, subject to an energy constraint at the transmitter. We shall begin the solution of this problem.

8.41 Apodization in the Presence of Weak Noise

We shall solve the maximization problem posed above in the weak-noise limit, using the noise model developed in section 8.3. That is, we assume

$$\left\{ n_i(t) = \int_{R_1} n(\vec{\rho}, t)\, u_i^*(\vec{\rho})\, d\vec{\rho}: \quad 1 \leq i \leq N \right\}$$

is a set of statistically independent identically distributed white Gaussian noise processes with spectral densities $\frac{2N_o + \hbar\omega_c/\eta}{2}$. It is convenient to define the parameters

$$a_i = \int_{R_1} u_o(\vec{\rho})\, u_i^*(\vec{\rho})\, d\vec{\rho} \qquad 1 \leq i \leq N \tag{178}$$

in terms of which the gain reduction factor may be written

$$\frac{\left| \int_{R_1} \tilde{u}(\vec{\rho})\, u_o^*(\vec{\rho})\, d\vec{\rho} \right|^2}{\int_{R_1} |u_o(\vec{\rho})|^2\, d\vec{\rho} \int_{R_1} |\tilde{u}(\vec{\rho})|^2\, d\vec{\rho}} = \frac{\sum_{i=1}^{N} |a_i|^2}{\int_{R_1} |u_o(\vec{\rho})|^2\, d\vec{\rho}} \left[\frac{\left| \sum_{i=1}^{N} \hat{a}_i a_i^* \right|^2}{\sum_{i=1}^{N} |a_i|^2 \sum_{i=1}^{N} |\hat{a}_i|^2} \right], \tag{179}$$

where we have used (177) for $\tilde{u}(\vec{\rho})$. Equation 179 has the following important interpretation. The term

$$\frac{\sum_{i=1}^{N} |a_i|^2}{\int_{R_1} |u_o(\vec{\rho})|^2\, d\vec{\rho}}$$

is the gain reduction factor that would result from using

$$\tilde{u}(\vec{\rho}) = \sum_{i=1}^{N} a_i u_i(\vec{\rho})$$

as an approximation to $u_o(\vec{\rho})$. The key word here is approximation, rather than estimate, since we can only measure $u_o(\vec{\rho})$ when there is no noise. We shall return to discuss noise-free approximate transmitter implementations. For the moment, we are interested only in the effects of the noise. The term in brackets in Eq. 179,

$$\frac{\left| \sum_{i=1}^{N} \hat{a}_i a_i^* \right|^2}{\sum_{i=1}^{N} |a_i|^2 \sum_{i=1}^{N} |\hat{a}_i|^2},$$

measures how much performance is lost (in addition to the noise-free gain reduction)

because of the presence of noise. Note that this term has the form of the gain-reduction factor when

$$u_o(\vec{\rho}) = \sum_{i=1}^{N} a_i u_i(\vec{\rho}).$$

Since we have assumed a fixed set of heterodyne waveforms, our original maximization problem reduces to the following form. From the observation

$$\{a_i + n_i(t): \quad 1 \leq i \leq N \quad 0 \leq t \leq \tau\}$$

find the estimate, $\hat{a}_i$, of a_i that maximizes

$$E\left[\frac{\left|\sum_{i=1}^{N} \hat{a}_i a_i^*\right|^2}{\sum_{i=1}^{N} |a_i|^2 \sum_{i=1}^{N} |\hat{a}_i|^2}\right].$$

(Note that since we are working with a fixed atmospheric state, we have implicitly assumed that τ is less than the coherence time of the turbulence minus the round-trip $(R_2\text{-}R_1\text{-}R_2)$ propagation time.)

Observe that no loss in optimality is incurred by time-averaging the observation $\{a_i + n_i(t): \ 1 \leq i \leq N, \ 0 \leq t \leq \tau\}$ over the interval $(0, \tau)$. This assertion can be proved as follows. The time-average of the observation is

$$\left\{\frac{1}{\tau}\int_0^{\tau} (a_i + n_i(t))\ dt = a_i + \frac{1}{\tau}\int_0^{\tau} n_i(t)\ dt: \ 1 \leq i \leq N\right\}$$

and, since $\{n_i(t)\}$ is a set of independent white Gaussian noise processes, the noise components whose time averages are zero are irrelevant. Let us define the random variables

$$n_i = \frac{1}{\tau}\int_0^{\tau} n_i(t)\ dt \qquad 1 \leq i \leq N.$$

The set $\{n_i\}$ is therefore a collection of statistically independent identically distributed zero-mean Gaussian random variables, whose real and imaginary parts are statistically independent and identically distributed, and whose variances are $\frac{2N_o + \hbar\omega_c/\eta}{2\tau}$. Our problem is now to maximize

$$E\left[\frac{\left|\sum_{i=1}^{N} \hat{a}_i a_i^*\right|^2}{\sum_{i=1}^{N} |a_i|^2 \sum_{i=1}^{N} |\hat{a}_i|^2}\right]$$

by choice of $\hat{a}_i$, given the observation $\{a_i + n_i: \ 1 \leq i \leq N\}$.

The problem just posed is easily solved in the weak-noise limit. Remember that

$$\frac{\left| \sum_{i=1}^{N} \hat{a}_i a_i^* \right|^2}{\sum_{i=1}^{N} |a_i|^2 \sum_{i=1}^{N} |\hat{a}_i|^2}$$

is the square of the cosine of the angle between the vectors $\sum_{i=1}^{N} \hat{a}_i u_i(\vec{\rho})$ and $\sum_{i=1}^{N} a_i u_i(\vec{\rho})$ in the function space spanned by $\{u_i(\vec{\rho}): \ 1 \leq i \leq N\}$. Consider the error vector

$$\sum_{i=1}^{N} (\hat{a}_i - a_i) \, u_i(\vec{\rho}).$$

As shown in Fig. 24, this vector has a component along $\sum_{i=1}^{N} a_i u_i(\vec{\rho})$ (the in-phase error) and a component perpendicular to $\sum_{i=1}^{N} a_i u_i(\vec{\rho})$ (the out-of-phase error). If

$$\sum_{i=1}^{N} |\hat{a}_i - a_i|^2 \ll \sum_{i=1}^{N} |a_i|^2 \tag{180}$$

(the percentage square error is quite small), then the angle between $\sum_{i=1}^{N} \hat{a}_i u_i(\vec{\rho})$ and $\sum_{i=1}^{N} a_i u_i(\vec{\rho})$ will also be quite small. Furthermore, this angle will then be approximately the ratio of the length of the out-of-phase error vector to the length of the signal vector $\sum_{i=1}^{N} a_i u_i(\vec{\rho})$. Thus, if (180) is satisfied, then the error angle, the angle α between the

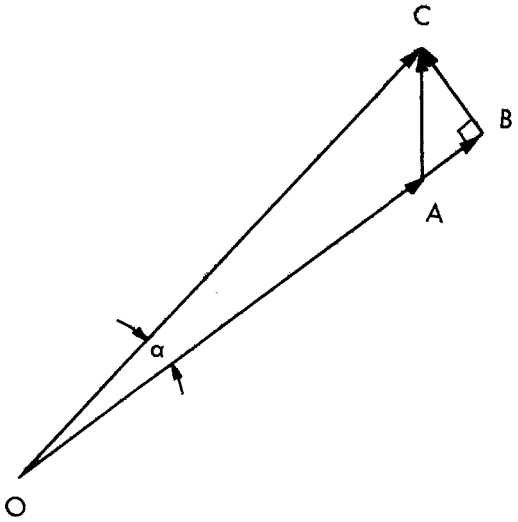

Fig. 24.

Error angle α. This plot is in the space spanned by $\{u_i(\vec{\rho}): \ 1 \leq i \leq N\}$.

OA is the signal vector, $\sum_{i=1}^{N} a_i u_i(\vec{\rho})$

OC is the estimate vector, $\sum_{i=1}^{N} \hat{a}_i u_i(\vec{\rho})$

AC is the error vector, $\sum_{i=1}^{N} (\hat{a}_i - a_i) \, u_i(\vec{\rho})$

AB is the in-phase error, and BC is the out-of-phase error.

vectors $\sum_{i=1}^{N} \hat{a}_i u_i(\vec{\rho})$ and $\sum_{i=1}^{N} a_i u_i(\vec{\rho})$, is given by

$$\alpha \approx \frac{\left(\sum_{k=1}^{N} \left| \hat{a}_k - a_k \left(\frac{\sum_{j=1}^{N} \hat{a}_j a_j^*}{\sum_{j=1}^{N} |a_j|^2} \right) \right|^2 \right)^{1/2}}{\left(\sum_{k=1}^{N} |a_k|^2 \right)^{1/2}}, \tag{181}$$

where we have evaluated the length of the out-of-phase error vector. In terms of α we have

$$\frac{\left| \sum_{i=1}^{N} \hat{a}_i a_i^* \right|^2}{\sum_{i=1}^{N} |a_i|^2 \sum_{i=1}^{N} |\hat{a}_i|^2} = \cos^2 \alpha \tag{182}$$

and, since α is small compared with one, (182) reduces to

$$\frac{\left| \sum_{i=1}^{N} \hat{a}_i a_i^* \right|^2}{\sum_{i=1}^{N} |a_i|^2 \sum_{i=1}^{N} |\hat{a}_i|^2} \approx 1 - \alpha^2. \tag{183}$$

Therefore in the weak-noise limit the average gain reduction factor is maximized by minimizing $E(\alpha^2)$. From the discussion leading to (181) we see that $E(\alpha^2)$ is minimized, in the weak-noise limit, by minimizing the mean-square out-of-phase error. It is well-known[13] that the minimum mean-square error unbiased estimator for the unknown mean of a white Gaussian process with equal variances in each dimension is the maximum-likelihood estimator

$$\hat{a}_{i_{ML}} = a_i + n_i = \frac{1}{\tau} \int_0^{\tau} \left(\int_{R_1} u(\vec{\rho}, t)\, u_i^*(\vec{\rho})\, d\vec{\rho} \right) dt \qquad 1 \leq i \leq N. \tag{184}$$

The Cramer-Rao bound shows that there is no estimator with a fixed bias, a bias independent of $\sum_{i=1}^{N} a_i u_i(\vec{\rho})$, which has a lower mean-square error than the maximum-likelihood estimator. A variable bias system might exist that would outperform the maximum-likelihood system, but to find such a system we would need some a priori information concerning $\sum_{i=1}^{N} a_i u_i(\vec{\rho})$. Thus we have restricted ourselves to unbiased estimators.

The resulting mean-square out-of-phase error, when maximum-likelihood estimation is used, is

$$(N-1)\,\frac{(2N_o+\hbar\omega_c/\eta)}{2\tau}.$$

Thus the average gain-reduction factor is maximized by the maximum-likelihood rule given in (184), and when this rule is used the resulting average gain-reduction factor is

$$\begin{aligned} E(g) &= E(\cos^2(\tilde{u}, u_o)) \\ &= \frac{\sum_{i=1}^{N} |a_i|^2}{\int_{R_1} |u_o(\vec{\rho})|^2\, d\vec{\rho}} \left(1 - \frac{(N-1)(2N_o+\hbar\omega_c/\eta)}{2\tau \sum_{i=1}^{N} |a_i|^2}\right) \\ &= \frac{\sum_{i=1}^{N} \left|\int_{R_1} u_o(\vec{\rho})\, u_i^*(\vec{\rho})\, d\vec{\rho}\right|^2}{\int_{R_1} |u_o(\vec{\rho})|^2\, d\vec{\rho}} \left(1 - \frac{(N-1)(2N_o+\hbar\omega_c/\eta)}{2\tau \sum_{i=1}^{N} \left|\int_{R_1} u_o(\vec{\rho})\, u_i^*(\vec{\rho})\, d\vec{\rho}\right|^2}\right) \end{aligned} \tag{185}$$

The result that we have obtained is quite important, and to emphasize it we state it as a lemma.

Lemma (Performance in Weak-Noise)

At R_1 we receive

$$u(\vec{\rho}, t) = u_o(\vec{\rho}) + n(\vec{\rho}, t),$$

where $u_o(\vec{\rho})$ is the received beacon field in a two-way adaptive communication system, and $n(\vec{\rho}, t)$ is the white Gaussian noise discussed in section 8.3. The field at R_1 is detected by an array of N heterodyne detectors using a set of N orthonormal waveforms, $\{u_i^*(\vec{\rho}):\ 1 \leq i \leq N\}$, as local oscillators, and the outputs of these detectors are observed over a time interval $(0, \tau)$. The average gain of a communication system using an unbiased estimator at R_1 is maximized by the maximum-likelihood transmitter

$$\tilde{u}(\vec{\rho}) = \sqrt{\frac{E_t}{\sum_{i=1}^{N} \left|\hat{a}_{i_{ML}}\right|^2}} \sum_{i=1}^{N} \hat{a}_{i_{ML}}\, u_i(\vec{\rho}),$$

where $\hat{a}_{i_{ML}} = \frac{1}{\tau}\int_0^\tau \left(\int_{R_1} u(\vec{\rho}, t)\, u_i^*(\vec{\rho})\, d\vec{\rho}\right) dt$, $1 \leq i \leq N$ when the noise is weak enough that

$$\frac{N(2N_o+\hbar\omega_c/\eta)}{2\tau} \ll \sum_{i=1}^{N} \left|\int_{R_1} u_o(\vec{\rho})\, u_i^*(\vec{\rho})\, d\vec{\rho}\right|^2.$$

(Note that we have substituted a bound on the ratio of the average length of the error vector to the length of the signal vector for the condition in (180). The resulting average gain-reduction factor under the conditions above is

$$E(g) = E\left[\frac{\left|\int_{R_1} \tilde{u}(\vec{\rho})\, u_o^*(\vec{\rho})\, d\vec{\rho}\right|^2}{\int_{R_1} |u_o(\vec{\rho})|^2\, d\vec{\rho} \int_{R_1} |\tilde{u}(\vec{\rho})|^2\, d\vec{\rho}}\right]$$

$$= \frac{\sum_{i=1}^{N} \left|\int_{R_1} u_o(\vec{\rho})\, u_i^*(\vec{\rho})\, d\vec{\rho}\right|^2}{\int_{R_1} |u_o(\vec{\rho})|^2\, d\vec{\rho}} \left(1 - \frac{(N-1)(2N_o + \hbar\omega_c/\eta)}{2\tau \sum_{i=1}^{N} \left|\int_{R_1} u_o(\vec{\rho})\, u_i^*(\vec{\rho})\, d\vec{\rho}\right|^2}\right).$$

We shall continue the study of apodization in the presence of noise by discussing the optimal use of spatial bandwidth in the weak-noise limit.

8.42 Optimal Use of Spatial Bandwidth in Weak Noise

The maximum-likelihood transmitter and the resulting gain-reduction factor performance are the complete solution of the weak-noise apodization problem when the N heterodyne waveforms used at R_1 are fixed. We shall now discuss what can be done when $\{u_i^*: 1 \leq i \leq N\}$ may be chosen to maximize the average gain-reduction factor. From Eq. 179, if $u_1(\vec{\rho}) = u_o(\vec{\rho})$ and $N = 1$, then the gain-reduction factor would be one regardless of the noise. This choice of heterodyne waveforms is equivalent to knowing $u_o(\vec{\rho})$ a priori, which is not possible. It was precisely because we did not know the channel state a priori that we began to consider two-way communication systems.

We shall study the following problem. Given a complete orthonormal set of functions on R_1, $\{\xi_k^*\}$, which subset of $\{\xi_k^*\}$ achieves the largest average gain-reduction factor when used as the heterodyne waveforms in a weak-noise maximum-likelihood estimator. Our results are stated in the following lemma.

Lemma (Optimal Use of Spatial Bandwidth in Weak-Noise)

Consider a maximum-likelihood estimator operating in a weak-noise environment using some subset of $\{\xi_k^*\}$ as heterodyne waveforms. Let

$$u_i^*(\vec{\rho}) = \xi_{k_i}^*(\vec{\rho}) \qquad i = 1, 2, 3, \ldots,$$

where

$$\left|\int_{R_1} u_o(\vec{\rho})\, u_1^*(\vec{\rho})\, d\vec{\rho}\right|^2 \geq \left|\int_{R_1} u_o(\vec{\rho})\, u_2^*(\vec{\rho})\, d\vec{\rho}\right|^2 \geq \ldots, \tag{186}$$

and let N be such that

$$\left| \int_{R_1} u_o(\vec{\rho})\, u_N^*(\vec{\rho})\, d\vec{\rho} \right|^2 \geq \frac{2N_o + \hbar\omega_c/\eta}{2\tau}$$

$$\left| \int_{R_1} u_o(\vec{\rho})\, u_{N+1}^*(\vec{\rho})\, d\vec{\rho} \right|^2 < \frac{2N_o + \hbar\omega_c/\eta}{2\tau}. \tag{187}$$

Then the optimum subset of $\left\{\xi_k^*\right\}$ for maximizing the average gain-reduction factor is $\{u_i^*: \ 1 \leq i \leq N\}$.

Proof: In the presence of weak noise the average gain-reduction factor achieved by a maximum-likelihood system using heterodyne waveforms $\{u_i^*: \ 1 \leq i \leq M\}$ is

$$E(g) = \frac{\sum_{i=1}^{M} \left| \int_{R_1} u_o(\vec{\rho})\, u_i^*(\vec{\rho})\, d\vec{\rho} \right|^2 - (M-1)\, \frac{2N_o + \hbar\omega_c/\eta}{2\tau}}{\int_{R_1} |u_o(\vec{\rho})|^2\, d\vec{\rho}}.$$

If $\left\{u_i^*\right\}$ are constrained to be chosed from a given complete orthonormal set, $\left\{\xi_k^*\right\}$, then for any M the choice given in (186) maximizes

$$\frac{\sum_{i=1}^{M} \left| \int_{R_1} u_o(\vec{\rho})\, u_i^*(\vec{\rho})\, d\vec{\rho} \right|^2}{\int_{R_1} |u_o(\vec{\rho})|^2\, d\vec{\rho}}.$$

Furthermore, when $\left\{u_i^*\right\}$ is chosen in this manner, E(g) is maximized by M = N, where N satisfies (187), which proves the lemma.

This lemma has an important interpretation in terms of "matching" spatial bandwidths within the system. It asserts that the optimal subset of a given complete orthonormal set of spatial modes is the set of modes in which the signal energy exceeds the average noise energy. In other words, it tells us to match the spatial bandwidth of the transmitter at R_1 to the bandwidth over which the signal energy density exceeds the noise spectral density.

In general, this lemma is the only spatial bandwidth result that we can obtain. For the point-to-point channel, however, there is another lemma that can be proved.

Lemma (Spatial Bandwidth for Point-to-Point Channels)

The average gain of a point-to-point two-way communication system using a maximum-likelihood transmitter in the presence of weak noise with heterodyne waveforms chosen from a given complete orthonormal set, $\left\{\xi_k^*\right\}$, is a maximum under the following conditions.

1. When the number of degrees of freedom of the channel, D_f, is such that

$$\iint_{R_2} v^*(\vec{\rho}')\, \underline{\underline{K}}(\vec{\rho}', \vec{r}')\, v(\vec{r}')\, d\vec{\rho}' d\vec{r}' \approx 1. \tag{188}$$

2. When the heterodyne waveforms are chosen from $\left\{\xi_k^*\right\}$ in accordance with the previous lemma.

Proof: From the corollary of section 8.21, the average gain of the point-to-point channel is

$$\left(\iint_{R_2} v^*(\vec{\rho}')\, \underline{\underline{K}}(\vec{\rho}', \vec{r}')\, v(\vec{r}')\, d\vec{\rho}' d\vec{r}' \right) E(g)$$

and, since $v(\vec{\rho}')$ has unit energy, we have

$$0 \leq \iint_{R_2} v^*(\vec{\rho}')\, \underline{\underline{K}}(\vec{\rho}', \vec{r}')\, v(\vec{r}')\, d\vec{\rho}' d\vec{r}' \leq 1.$$

Thus applying (188) and the previous lemma completes the proof.

Let us see what interpretation we can attach to this lemma. Condition (188) says that the beacon signal $v(\vec{\rho}')$ must propagate through the channel with essentially no attenuation. How does this result relate to spatial bandwidth? Using the notation of section 8.21, we have

$$\iint_{R_2} v^*(\vec{\rho}')\, \underline{\underline{K}}(\vec{\rho}', \vec{r}')\, v(\vec{r}')\, d\vec{\rho}' d\vec{r}' = \sum_{i=1}^{\infty} |v_i|^2 \lambda_i$$

$$\approx \sum_{i=1}^{D_f} |v_i|^2,$$

where

$$\sum_{i=1}^{\infty} |v_i|^2 = \int_{R_2} |v(\vec{\rho}')|^2 \, d\vec{\rho}' = 1.$$

In section 2.4 we observed that the number of degrees of freedom of the channel is in essence a spatial bandwidth constraint imposed upon signals propagating through the channel medium. Thus Eq. 188 says that we must make the channel spatial bandwidth larger than the spatial bandwidth of the beacon that we are using. Conversely, if the aperture sizes are fixed, we must choose a beacon whose spatial bandwidth is less than the bandwidth of the channel. (Remember that D_f is an increasing function of A_1 and A_2.)

We have seen that the spatial bandwidth of the transmitter at R_1 must be matched to the bandwidth over which the signal energy density exceeds the noise spectral density. For point-to-point channels we have just seen that the signal spatial bandwidth must be less than the channel spatial bandwidth. Thus in the point-to-point case, performance is optimum when the spatial bandwidths of the beacon and the transmitter at R_1 are properly matched to the spatial bandwidth of the channel.

8.43 System Performance in Strong Noise

The results of sections 8.41 and 8.42 were predicated upon a weak-noise assumption. We shall now derive some performance results that are valid regardless of the strength of the noise. Rather than attack the problem of maximizing the average gain-reduction factor, which is a difficult problem when we cannot make a weak-noise assumption, we shall study the performance of a particular two-way system that reduces to the maximum-likelihood system of section 8.41 when the noise is weak.

Consider the system shown in Fig. 25. The field received at R_1 is

$$u(\vec{\rho}, t) = u_o(\vec{\rho}) + n(\vec{\rho}, t)$$

as in section 8.41. The field transmitted from R_1, however, now is

$$\tilde{u}^*(\vec{\rho}) = \sqrt{\frac{E_t}{\sum_{i=1}^{N} \left(|a_i|^2 + \frac{2N_o + \hbar\omega_c/\eta}{2\tau} \right)}} \sum_{i=1}^{N} \hat{a}^*_{i_{ML}} u_i^*(\vec{\rho}), \tag{189}$$

where

$$\hat{a}_{i_{ML}} = \frac{1}{\tau} \int_0^\tau \left(\int_{R_1} u(\vec{\rho}, t)\, u_i^*(\vec{\rho})\, d\vec{\rho} \right) dt$$

and

$$a_i = \int_{R_1} u_o(\vec{\rho})\, u_i^*(\vec{\rho})\, d\vec{\rho}.$$

This transmitter is the same as the maximum-likelihood transmitter of section 8.41,

except for the fact that in the system of Fig. 25 the average transmitted energy

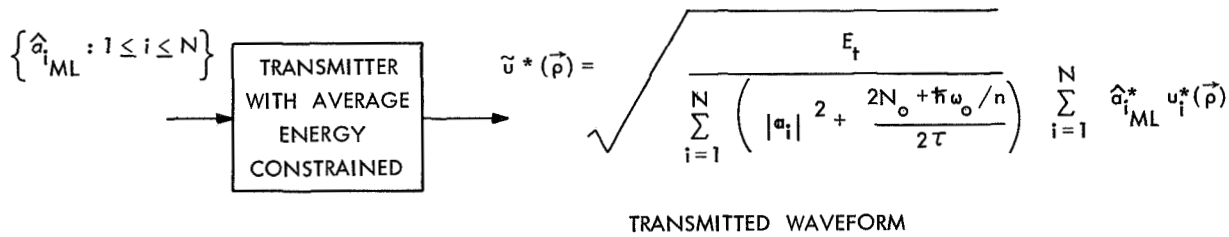

Fig. 25. Maximum-likelihood transmitter with average energy constrained.

is constrained, rather than the actual transmitted energy. This normalization is convenient for the calculations that we shall make.

In Appendix C it is shown that for $\tilde{u}(\vec{\rho})$ as defined above

$$E\left[\left|\int_{R_1} \tilde{u}(\vec{\rho})\, u_o^*(\vec{\rho})\, d\vec{\rho}\right|^2\right] = \frac{E_t \sum_{i=1}^{N} |a_i|^2 \left(\sum_{i=1}^{N} |a_i|^2 + \frac{2N_o + \hbar\omega_c/\eta}{2\tau}\right)}{\sum_{i=1}^{N} |a_i|^2 + \frac{N(2N_o + \hbar\omega_c/\eta)}{2\tau}} \tag{190}$$

and

$$\mathrm{VAR}\left[\left|\int_{R_1} \tilde{u}(\vec{\rho})\, u_o^*(\vec{\rho})\, d\vec{\rho}\right|^2\right] =$$

$$2\left(\frac{E_t \sum_{i=1}^{N} |a_i|^2}{\sum_{i=1}^{N} |a_i|^2 + \frac{N(2N_o + \hbar\omega_c/\eta)}{2\tau}}\right)^2 \left(\frac{2N_o + \hbar\omega_c/\eta}{2\tau}\right)\left(\sum_{i=1}^{N} |a_i|^2 + \frac{2N_o + \hbar\omega_c/\eta}{4\tau}\right), \tag{191}$$

where the expectations are over the noise ensemble. Using these results, we can prove the following lemmas.

Lemma (Point-to-Point System Performance)

Let $u_o(\vec{\rho})$ be the received beacon field in a point-to-point system using a beacon, $\sqrt{E_b}\, v(\vec{\rho}')$, of energy E_b. Then the performance of the system that transmits $\tilde{u}^*(\vec{\rho})$, given by (189), is as follows.

1. The average energy over the noise ensemble in the output of the heterodyne detector at R_2 is

$$E(E_r) = \frac{E_t}{E_b} \sum_{i=1}^{N} |a_i|^2 \left(\frac{1 + \dfrac{2N_o + \hbar\omega_c/\eta}{2\tau \sum_{i=1}^{N} |a_i|^2}}{1 + \dfrac{N(2N_o + \hbar\omega_c/\eta)}{2\tau \sum_{i=1}^{N} |a_i|^2}} \right). \tag{192}$$

2. The variance of the output energy of the heterodyne detector at R_2 is

$$VAR(E_r) = \frac{2\left(\dfrac{E_t}{E_b}\right)^2 \left(\sum_{i=1}^{N} |a_i|^2 \right)^2 \left(\dfrac{2N_o + \hbar\omega_c/\eta}{2\tau \sum_{i=1}^{N} |a_i|^2} \right) \left(1 + \dfrac{2N_o + \hbar\omega_c/\eta}{4\tau \sum_{i=1}^{N} |a_i|^2} \right)}{\left(1 + \dfrac{N(2N_o + \hbar\omega_c/\eta)}{2\tau \sum_{i=1}^{N} |a_i|^2} \right)^2}. \tag{193}$$

3. The fractional fluctuation of E_r about its mean, that is, the ratio of the standard deviation of E_r to its mean, is

$$\frac{(VAR(E_r))^{1/2}}{E(E_r)} = \left(\frac{2 - \left(1 + \dfrac{2\tau \sum_{i=1}^{N} |a_i|^2}{2N_o + \hbar\omega_c/\eta} \right)^{-1}}{1 + \dfrac{2\tau \sum_{i=1}^{N} |a_i|^2}{2N_o + \hbar\omega_c/\eta}} \right)^{1/2}. \tag{194}$$

Proof: Equations 192 and 193 follow immediately from Eqs. 190 and 191 and the Lemma of section 8.21. Equation 194 is obtained by taking the square root of Eq. 193 and dividing by Eq. 192.

We shall comment on these results after proving the next lemma.

Lemma (Deep-Space System Performance)

Let $u_o(\vec{\rho})$ be the received beacon field in a deep-space system using an infinite plane-wave beacon of amplitude B. Then the performance of the system that transmits $\tilde{u}^*(\vec{\rho})$, given by (189), is as follows.

1. The average energy (over the noise ensemble) received at the space-craft is

$$E(E_s) = \frac{A_3 E_t \sum_{i=1}^{N} |a_i|^2}{(\lambda \ell)^2 B^2} \left(\frac{1 + \dfrac{2N_o + \hbar\omega_c/\eta}{2\tau \sum_{i=1}^{N} |a_i|^2}}{1 + \dfrac{N(2N_o + \hbar\omega_c/\eta)}{2\tau \sum_{i=1}^{N} |a_i|^2}} \right). \tag{195}$$

2. The variance of the energy received at the spacecraft is

$$\mathrm{VAR}\,(E_s) = \frac{2\left(\dfrac{A_3 E_t \sum_{i=1}^{N} |a_i|^2}{(\lambda \ell)^2 B^2}\right)^2 \left(\dfrac{2N_o + \hbar\omega_c/\eta}{2\tau \sum_{i=1}^{N} |a_i|^2}\right)\left(1 + \dfrac{2N_o + \hbar\omega_c/\eta}{4\tau \sum_{i=1}^{N} |a_i|^2}\right)}{\left(1 + \dfrac{N(2N_o + \hbar\omega_c/\eta)}{2\tau \sum_{i=1}^{N} |a_i|^2}\right)^2}. \tag{196}$$

3. The ratio of the standard deviation of E_s to its mean is

$$\frac{(\mathrm{VAR}\,(E_s))^{1/2}}{E(E_s)} = \left(\frac{2 - \left(1 + \dfrac{2\tau \sum_{i=1}^{N} |a_i|^2}{2N_o + \hbar\omega_c/\eta}\right)^{-1}}{1 + \dfrac{2\tau \sum_{i=1}^{N} |a_i|^2}{2N_o + \hbar\omega_c/\eta}} \right)^{1/2}. \tag{197}$$

Proof: Apply Eqs. 190 and 191 to the Lemma of section 8.22.

The results that we have just obtained are valid regardless of the strength of the noise relative to the received beacon energy. It can be seen that they reduce to the weak-noise results of section 8.41 when

$$\frac{N(2N_o + \hbar\omega_c/\eta)}{2\tau} \ll \sum_{i=1}^{N} |a_i|^2.$$

Let us consider what happens when we are not in this weak-noise limit. From our results we see that the noise has had two effects on the system.

1. The noise in the $u_o(\vec{\rho})$ component of the field at R_1 causes fading at the receiver, that is, the variances of E_r and E_s are nonzero.

2. The noise causes the transmitter at R_1 to waste energy on spatial modes orthogonal to $u_o(\vec{\rho})$.

Consider the following special case. Suppose that

$$\frac{2N_o + \hbar\omega_c/\eta}{2\tau \sum_{i=1}^{N} |a_i|^2} \ll 1 \lesssim \frac{N(2N_o + \hbar\omega_c/\eta)}{2\tau \sum_{i=1}^{N} |a_i|^2}.$$

Since N may be quite large, we may often find ourselves in this situation. In this case the in-phase noise is negligible, but the total noise is still not weak enough to use the results of section 8.41. From the lemmas just proved we note that although the fraction of the average transmitted energy that is received will not be close to one, there will be little or no fading caused by the noise. That is,

$$\frac{(\mathrm{VAR}(E_r))^{1/2}}{E(E_r)} = \frac{(\mathrm{VAR}(E_s))^{1/2}}{E(E_s)} \approx 0.$$

(Remember that we are working with a fixed atmospheric state; changes in the atmospheric state will produce fading at the receiver even if there were no noise in the system. See section 5.4 for a discussion of this type of fading.) Thus the maximum-likelihood transmitter delivers good energy performance, that is, little fading, for a single atmospheric state, as long as the average noise energy per spatial mode is small compared with the signal energy at R_1, and its performance is optimum if the total average noise energy is small compared with the signal energy at R_1.

We shall leave the question of performance in the presence of noise and study the behavior of some approximate transmitter implementations in the absence of noise.

8.5 APPROXIMATE TRANSMITTER IMPLEMENTATIONS

In the absence of noise the optimal transmitter for maximizing the gain of a two-way adaptive communication system transmits a scaled version of the conjugate of the received beacon field $u_o(\vec{\rho})$. At present, there does not seem to be a device capable of generating the conjugate of an arbitrary received beacon field, so we now address ourselves to the theoretical problem of approximating the conjugation operation in the absence of noise. In this matter we shall find the lemmas of section 8.2 quite helpful.

We shall restrict ourselves to considering systems that heterodyne $u_o(\vec{\rho})$ with a set of N orthonormal waveforms $\{u_i^*: 1 \leq i \leq N\}$ and transmit a scaled version of the conjugate of

$$\tilde{u}(\vec{\rho}) = \sum_{i=1}^{N} a_i u_i(\vec{\rho}), \tag{198}$$

where

$$a_i = \int_{R_1} u_o(\vec{\rho})\, u_i^*(\vec{\rho})\, d\vec{\rho}.$$

From the results of section 8.2, we know that the system gain for point-to-point or deep-space channels is proportional to the gain reduction factor

$$g = \frac{\left| \int_{R_1} \tilde{u}(\vec{\rho})\, u_o^*(\vec{\rho})\, d\vec{\rho} \right|^2}{\int_{R_1} |\tilde{u}(\vec{\rho})|^2\, d\vec{\rho} \int_{R_1} |u_o(\vec{\rho})|^2\, d\vec{\rho}}$$

and for the case of interest here we have

$$g = \frac{\sum_{i=1}^{N} |a_i|^2}{\int_{R_1} |u_o(\vec{\rho})|^2\, d\vec{\rho}}. \tag{199}$$

If $\{u_i^*: 1 \leq i \leq N\}$ is such that

$$\sum_{i=1}^{N} |a_i|^2 \approx \int_{R_1} |u_o(\vec{\rho})|^2\, d\vec{\rho}, \tag{200}$$

then no performance has been lost by going to an approximate transmitter.

As an example of an approximate transmitter implementation, let us consider the Taylor series arrays. We partition the R_1 aperture into nonoverlapping circular array elements of radius r. Over the i^{th} array element an n^{th}-order Taylor series transmitter makes an n^{th}-order Taylor series approximation of the complex phase of $u_o(\vec{\rho})$, and $\tilde{u}(\vec{\rho})$ is taken to be the component of $u_o(\vec{\rho})$ parallel to the approximate phasor. That is, if

$$u_o(\vec{\rho}) = e^{\underline{a}(\vec{\rho})},$$

then

$$\tilde{u}(\vec{\rho}) = \frac{a_{i,n}\, e^{\underline{a}_{i,n}(\vec{\rho})}}{\sqrt{\pi r^2}} B_{i,n} \qquad \vec{\rho} \in A_i \qquad 1 \leq i \leq N, \tag{201}$$

where A_i denotes the i^{th} array element, $\underline{a}_{i,n}(\vec{\rho})$ is the n^{th}-order Taylor series approximation of $\underline{a}(\vec{\rho})$ on A_i, $B_{i,n}$ is a normalizing constant, and

$$a_{i,n} = \int_{A_i} u_o(\vec{\rho}) \frac{\exp[\underline{a}_{i,n}^*(\vec{\rho})]}{\sqrt{\pi r^2}} B_{i,n}\, d\vec{\rho}.$$

In the n = 0 case, $\tilde{u}(\vec{\rho})$ is a piecewise plane wave normally incident on R_1, whose absolute phase delay varies from array element to array element. In the n = 1 case, $\tilde{u}(\vec{\rho})$ is a piecewise plane wave, whose direction of propagation and absolute phase delay

varies from array element to array element. In the n = 2 case, $\tilde{u}(\vec{\rho})$ is compensated for the spherical and hyperbolic aberrations in the phase of $u_o(\vec{\rho})$.

The n^{th}-order Taylor series transmitters fall within the framework set up previously with

$$u_i^*(\vec{\rho}) = \begin{cases} \dfrac{e^{\underline{\alpha}_{i,n}^*(\vec{\rho})}}{\sqrt{\pi r^2}} B_{i,n} & \vec{\rho} \in A_i \quad \vec{\rho} \notin A_i \quad 1 \leq i \leq N, \\ 0 \end{cases} \tag{202}$$

where N is now the number of array elements in R_1. Fried[2] has studied the Taylor series approximation that we are discussing for the deep-space channel. For the n^{th}-order Taylor series system he has calculated a maximum array element radius ρ_n, such that if $r < \rho_n$, then

$$E\left(\sum_{i=1}^{N} |a_{i,n}|^2\right) \approx E\left(\int_{R_1} |u_o(\vec{\rho})|^2 \, d\vec{\rho}\right).$$

That is, $g \approx 1$ on the average, and if $r > \rho_n$, then

$$\frac{E\left(\sum_{i=1}^{N} |a_{i,n}|^2\right)}{E\left(\int_{R_1} |u_o(\vec{\rho})|^2 \, d\vec{\rho}\right)}$$

decreases monotonically as r increases, where the expectations are over the turbulence ensemble.

This completes our discussion of approximate transmitter implementations. We have only dealt with the noise-free case. The performance of array systems in the presence of noise was considered in section 8.4. But, since the heterodyne waveforms used by a Taylor series array depend upon the field received at R_1, the results of section 8.4 can only be applied to the Taylor series arrays in the weak-noise limit.

8.6 SUMMARY

We have covered a great deal of material, and it is worth reviewing what we have accomplished. The principal results are as follows.

1. The performance of a general two-way spatially modulated communication system was evaluated for both point-to-point and deep-space channels. It was shown that the system gain, the ratio of the output energy to the input energy, is given by the gain of an ideal Q-kernel system times a gain-reduction factor.

2. The performance of Q-kernel systems in the presence of noise was examined. The noise was modeled as a white Gaussian process in space and time, and the maximum-likelihood estimator for the received beacon field was derived.

3. The maximum-likelihood transmitter was shown to be the unbiased estimator that maximizes the average system gain (over the noise ensemble) in the presence of weak noise.

4. The energy performance of the maximum-likelihood system in the presence of strong noise was derived.

5. The optimal matching of spatial bandwidths between the beacon, channel, and transmitter at R_1 was discussed.

6. A class of approximate transmitters was investigated in the absence of noise. The performance of such systems, compared with the ideal conjugation transmitter, is determined by a gain-reduction factor.

The result of greatest importance is that neither the presence of noise, nor the use of an approximate transmitter implementation in the absence of noise, changes the essential fact that a two-way Q-kernel system achieves good energy performance through the turbulent atmosphere.

IX. HYPOTHETICAL DEEP-SPACE COMMUNICATION SYSTEM

We shall now specify the parameters of a hypothetical deep-space Q-kernel communication system, and calculate its energy performance. The system will contain a beacon at synchronous altitude, an adaptive transmitter on the ground, and a receiver on a spacecraft approximately 80 million miles from Earth (typical Mars range). We shall calculate the following quantities:

1. energy performance when an ideal conjugation transmitter is used on the ground, in the absence of noise,

2. number of elements needed by a Taylor series transmitter (of orders zero or one) to achieve near-ideal performance in the absence of noise, that is, a gain reduction factor of approximately one,

3. performance of a Taylor series system, with a noise-free gain reduction factor of unity in the presence of noise, and

4. comparison of Q-kernel energy performance with the performance of nonadaptive optical and microwave systems.

The geometry of the problem is shown in Fig. 26. The beacon is a 0.01 W laser operating at 0.6328μ, with a diffraction-limited aperture, 0.2 m in diameter. The beacon is located on a synchronous satellite at zero zenith angle, and the field across the beacon aperture, R_3, is assumed to be a uniform plane wave whose direction of

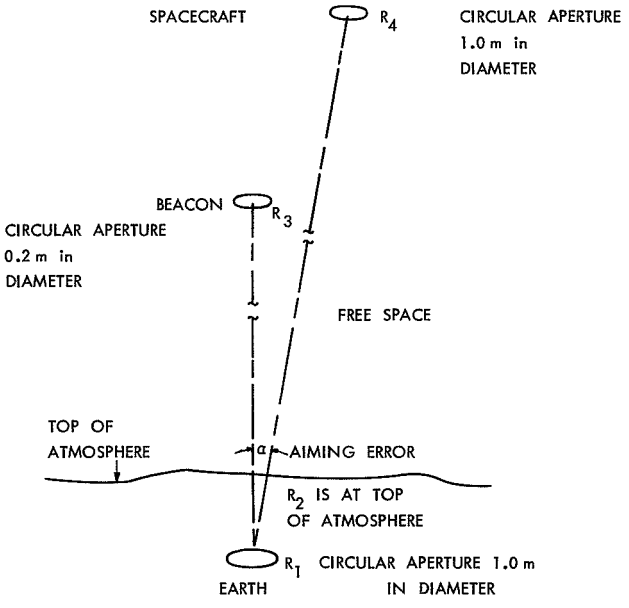

Fig. 26. Hypothetical deep-space Q-kernel system. The beacon is at zero zenith angle: power is $P_B = 0.01$ W; the wavelength is $\lambda = 0.6328\mu$. The transmitter power at R_1 is $P_t = 0.1$ W; the wavelength at R_1 is $\lambda = 0.6328\mu$. The R_2-R_3 path length is z_1; z_2 is the R_2-R_4 path length.

propagation is parallel to the center-to-center perpendicular from the beacon antenna (R_3) to the Earth antenna (R_1). The aperture on the ground, R_1, is a circular aperture, 1.0 m in diameter, and the transmitter power used at R_1 is nominally 0.1 W. The wavelength used at R_1 is also 0.6328μ. The spacecraft is at a distance 1.29×10^{11} m (80 million miles) from the Earth, and it has a circular receiving aperture (R_4), 1.0 m in diameter. The angular displacement between the R_4-R_1 and R_3-R_1 lines is α, the beacon aiming error (see Fig. 26). We begin our calculations with the energy performance in the absence of noise.

9.1 SYSTEM PERFORMANCE IN THE ABSENCE OF NOISE

Before proceeding, some preliminary comments are in order. First, let us note an implicit assumption in the system specification. We have placed the beacon on a synchronous satellite, and we assume that the field received at the top of the atmosphere (R_2) is, as far as R_1 is concerned, an infinite plane wave whose amplitude is proportional to the spatial Fourier transform of the beacon waveform at zero spatial frequency. In the absence of atmospheric ducting, this assumption is satisfied for a 1-m aperture on the ground and a 20-cm aperture at synchronous altitude.

Our second comment concerns what we mean by energy. Heretofore, we have adopted the convention that $\int_{R_1} |u(\vec{\rho})|^2 \, d\vec{\rho}$ is the energy in the spatial waveform $u(\vec{\rho})$ over R_1. We must now give up this fiction. If c and ϵ_o denote the speed of light and the permittivity of free-space, respectively, then the power in the electric field over R_1 whose complex-field amplitude is $u(\vec{\rho})$ is

$$\frac{c\epsilon_o}{2} \int_{R_1} |u(\vec{\rho})|^2 \, d\vec{\rho} \text{ W}.$$

This is the convention that we shall now use.

When a plane-wave beacon of power P_B is transmitted from R_3 the field at the top of the atmosphere is a plane wave whose amplitude is

$$\frac{e^{ja}}{\lambda z_1} \int_{R_3} \left(\frac{2P_B}{c\epsilon_o A_3}\right)^{1/2} d\vec{x},$$

where a is a phase delay, z_1 is the path length from R_3 to R_2, λ is the wavelength of the radiation, and A_3 is the area of the aperture R_3. Thus, if the constant phase delay is neglected, the field received at R_1, for a single atmospheric state, is

$$u_o(\vec{\rho}) = \frac{1}{\lambda z_1} \left(\frac{2P_B A_3}{c\epsilon_o}\right)^{1/2} \int_{R_2=\infty} \underline{h}(\vec{\rho}, \vec{\rho}') \, d\vec{\rho}'$$

$$= \frac{1}{\lambda z_1} \left(\frac{2P_B A_3}{c\epsilon_o}\right)^{1/2} \underline{z}(\vec{\rho}), \tag{203}$$

where $\underline{z}(\vec{\rho})$ is the perturbation from the $\underline{z}$ model for infinite plane-wave propagation through turbulence. The power received over R_1 therefore is

$$P_1 = \frac{P_B A_3}{(\lambda z_1)^2} \int_{R_1} |\underline{z}(\vec{\rho})|^2 \, d\vec{\rho}. \tag{204}$$

If, in the absence of noise, the transmitter at R_1 transmits $\sqrt{P_t/P_1}\, u_o^*(\vec{\rho})$, (this waveform has power P_t), then, under the assumption that the aiming error a is sufficiently small, the field received at R_4 (the spacecraft) is

$$\hat{v}^*(\vec{x}) = \frac{e^{jb}}{\lambda z_2} \int_{R_2=\infty} \left(\int_{R_1} \sqrt{\frac{P_t}{P_1}}\, u_o^*(\vec{\rho})\, \underline{h}(\vec{\rho}', \vec{\rho})\, d\vec{\rho} \right) d\vec{\rho}' \qquad \vec{x} \in R_4, \tag{205}$$

where b is a constant phase delay, and z_2 is the path length from R_2 to R_4. From (203) and (204), we have

$$\hat{v}^*(\vec{x}) = \sqrt{\frac{2P_t}{c\epsilon_o}}\, \frac{e^{jb}}{\lambda z_2}\, \frac{\int_{R_2=\infty} \left(\int_{R_1} \underline{z}^*(\vec{\rho})\, \underline{h}(\vec{\rho}', \vec{\rho})\, d\vec{\rho} \right) d\vec{\rho}'}{\left(\int_{R_1} |\underline{z}(\vec{\rho})|^2 \, d\vec{\rho} \right)^{1/2}} \qquad \vec{x} \in R_4. \tag{206}$$

By interchanging the orders of integration, using point reciprocity, and the definition of $\underline{z}$, $\hat{v}^*(\vec{x})$ may be written in the form

$$\hat{v}^*(\vec{x}) = \sqrt{\frac{2P_t}{c\epsilon_o}}\, \frac{e^{jb}}{\lambda z_2} \left(\int_{R_1} |\underline{z}(\vec{\rho})|^2 \, d\vec{\rho} \right)^{1/2} \qquad \vec{x} \in R_4. \tag{207}$$

Hence P_4, the power received by the spacecraft, is

$$P_4 = \frac{c\epsilon_o}{2} \int_{R_4} |\hat{v}^*(\vec{x})|^2 \, d\vec{x}$$

$$= \frac{P_t A_4}{(\lambda z_2)^2} \int_{R_1} |\underline{z}(\vec{\rho})|^2 \, d\vec{\rho}, \tag{208}$$

where A_4 is the area of the aperture R_4.

Using the results of section 5.4, we may evaluate the mean and the fluctuation about the mean of P_1 and P_4 (the expectation is over the turbulence ensemble), and obtain

$$E(P_1) = \frac{P_B A_3 A_1}{(\lambda z_1)^2} \tag{209}$$

$$E(P_4) = \frac{P_t A_1 A_4}{(\lambda z_2)^2} \tag{210}$$

$$\frac{(\mathrm{VAR}\,(P_1))^{1/2}}{E(P_1)} = \frac{(\mathrm{VAR}\,(P_4))^{1/2}}{E(P_4)} = \frac{(\mathrm{VAR}\,(|\underline{z}|^2))^{1/2}}{\sqrt{N_I}}, \tag{211}$$

where N_I is the number of intensity coherence areas in the aperture R_1. From the given data we conclude that

$$E(P_1) = \frac{(0.01)(\pi \times 10^{-2})(\pi/4)}{(0.63 \times 10^{-6} \times 3.6 \times 10^{7})^2}$$

$$= 5.1 \times 10^{-7}\ \mathrm{W} \tag{212}$$

and

$$E(P_4) = \frac{(0.1)(\pi/4)^2}{(0.63 \times 10^{-6} \times 1.29 \times 10^{11})^2}$$

$$= 1.0 \times 10^{-11}\ \mathrm{W}. \tag{213}$$

To obtain the fluctuation about the mean we must evaluate N_I. Really the quantity we need is $\mathrm{VAR}\left(\int_{R_1} |\underline{z}(\vec{\rho})|^2\, d\vec{\rho}\right)$. Fried[34] has studied this expression, and we rely on his results. Fried has shown that for zenith paths, under the assumption that the variance of $\log |\underline{z}|$ is 0.5 (a typical value),

$$\mathrm{VAR}\left(\int_{R_1} |\underline{z}(\vec{\rho})|^2\, d\vec{\rho}\right) = \frac{\mathrm{VAR}\,(|\underline{z}|^2)}{N_I},$$

where $N_I = 4A_1/\pi D_o^2$, and $D_o = 2.86 \times 10^{-2}$ m. Thus we have

$$\frac{(\mathrm{VAR}\,(P_1))^{1/2}}{E(P_1)} = \frac{(\mathrm{VAR}\,(P_4))^{1/2}}{E(P_4)} = \frac{(\mathrm{VAR}\,(|\underline{z}|^2)^{1/2}}{\sqrt{N_I}} =$$

$$= \frac{(e^{4\,\mathrm{VAR}\,(\log|\underline{z}|)} - 1)^{1/2}}{\left(4A_1/\pi D_o^2\right)^{1/2}}$$

$$= 6.9 \times 10^{-2}. \tag{214}$$

Equations 212-214 completely describe the performance of the system using an ideal conjugation operation transmitter in the absence of noise. Note that not only is there a large average power received at R_4 (see comparison with a microwave link below), but

there is also relatively little fading, as indicated by (214).

We have seen (section 8.5) that there exists Taylor series approximations of the ideal conjugation transmitter whose performance, as measured by a gain reduction factor, is essentially the same as that of the ideal system. The number of elements used in such an array is not only a measure of the system complexity, but also determines the system performance in the presence of noise. For that reason, we shall calculate the minimum number of array elements needed by zero-order and first-order Taylor series arrays to achieve gain reduction factors of approximately one. Our results, based upon the work of Fried,[2] are as follows.

1. n_o, the minimum number of elements needed by a circular zero-order Taylor series array, 1 m in diameter, to achieve a gain reduction factor of approximately one, is r_o^{-2}.

2. n_1, the minimum number of elements needed by a circular first-order Taylor series array, 1 m in diameter, to achieve a gain reduction factor of approximately one, is $(3.4\, r_o)^{-2}$.

3. The parameter r_o is the coherence length of the turbulence from the structure function of the phase. If we take $r_o = 4$ mm as a typical value, we have

$$n_o = 6.25 \times 10^4 \tag{215}$$

$$n_1 = 5.38 \times 10^3. \tag{216}$$

The parameter r_o is roughly the largest aperture over which the far-field beamwidth of a plane wave transmitter is diffraction-, rather than turbulence-limited. Therefore $4A_1/\pi r_o^2$ is the average power gain achieved by using a Q-kernel system instead of a nonadaptive plane-wave transmitter, since it is the ratio of the average power received over R_4 from a Q-kernel system to the average power received over R_4 from a plane-wave transmitter of diameter r_o using the same input power. For a Q-kernel system with a 1-m aperture and typical r_o this gain is enormous; that is,

$$4A_1/\pi r_o^2 = 6.25 \times 10^4$$

which is ≈48 dB.

We conclude the analysis of the noise-free case by comparing our Q-kernel system with a microwave link. We shall compute the input power required by a microwave system to achieve the same average power level at the spacecraft. We assume the following situation:

1. The microwave transmitter is a diffraction-limited parabolic dish 64 m (210 ft) in diameter.

2. The operating frequency is 2.1 GHz.

3. The power input is P_t'.

4. The antenna at R_4 (the spacecraft) is a parabolic dish, 1 m in diameter.

Table 4. System performance in the absence of noise.

RESULTS FOR IDEAL CONJUGATION TRANSMITTER

P_1 = RECEIVED BEACON POWER OVER R_1

$$= \frac{P_B A_3}{(\lambda z_1)^2} \int_{R_1} |z(\vec{\rho})|^2 \, d\vec{\rho}; \qquad E(P_1) = 5.1 \times 10^{-7} \text{ W}$$

$$\frac{(\text{VAR}(P_1))^{1/2}}{E(P_1)} = 6.9 \times 10^{-2}$$

P_4 = POWER RECEIVED OVER R_4

$$= \frac{P_t A_4}{(\lambda z_2)^2} \int_{R_1} |z(\vec{\rho})|^2 \, d\vec{\rho}; \qquad E(P_4) = 1.0 \times 10^{-11} \text{ W}$$

$$\frac{(\text{VAR}(P_4))^{1/2}}{E(P_4)} = 6.9 \times 10^{-2}$$

RESULTS FOR TAYLOR SERIES ARRAYS

n_o = minimum number of elements required by zero-order array to achieve $g \approx 1$ on a 1-m diameter circular aperture = 6.25×10^4

n_1 = minimum number of elements required by first-order array to achieve $g \approx 1$ on a 1-m diameter circular aperture = 5.38×10^3

It can be seen that the power received at the spacecraft from such a system, for which we have assumed that the atmosphere is completely transparent at 2.1 GHz, is

$$P'_4 = \frac{P'_t A_4 A'_1}{(\lambda' z_2)^2}, \tag{217}$$

where A'_1 is the area of the transmitting aperture, and λ' is the wavelength corresponding to a frequency of 2.1 GHz. For P'_4 to equal $E(P_4)$ from Eq. 213, P'_t must be

$$P'_t = \frac{P_t A_1}{A'_1} \left(\frac{\lambda'}{\lambda}\right)^2$$

$$= 1.03 \times 10^6 \text{ W}. \tag{218}$$

Equation 218 illustrates the tremendous antenna gains obtainable at optical wavelengths with physically small antennas. It is important to remember that we needed a Q-kernel system in order to achieve diffraction-limited performance (on the average) from antennas larger than r_o in diameter. Indeed if we used a nonadaptive optical system of the same power as the Q-kernel system, we would need only 16.5 W input to the microwave system to achieve the same average received power at the spacecraft.

This concludes our treatment of the noise-free case. The results are summarized in Table 4. Our next task is to evaluate system performance in the presence of noise.

9.2 SYSTEM PERFORMANCE IN THE PRESENCE OF NOISE

We begin our study of the noise-present case by evaluating the spectral density, $\frac{2N_o + \hbar\omega_c/\eta}{2}$, of the white Gaussian noise model of section 8.3. From measurements of the spectral radiance of the zenith sky by Bolle and Leupolt, as reported by Möller,[35] we conclude that at $\lambda = 0.6\mu$, we have $N_o \approx 10^{-26}$ W/Hz. (This is a daytime value of N_o, nighttime values of N_o are much smaller.) Assuming a photodetector with a quantum efficiency of 0.4, we have $\hbar\omega_c/\eta = 7.8 \times 10^{-19}$ W/Hz at $\lambda = 0.6\mu$. Thus the quantum shot noise is the dominant noise in the system.

Since a Taylor series array is likely to be used in a system that is actually built, we shall restrict ourselves here to considering only Taylor series arrays of zero and first order, as described in section 8.5. We assume that the integration time τ is 1 μs (corresponding to a 1-MHz bandwidth), and that in both cases the minimum number of elements required to achieve a gain reduction factor of approximately one in the absence of noise is used. Thus the average noise power collected by the Taylor series array is

$$\frac{n_o(2N_o + \hbar\omega_c/\eta)}{2\tau} = 2.44 \times 10^{-8} \text{ W} \tag{219}$$

for the zero-order array, and

$$\frac{n_1(2N_o + \hbar\omega_c/\eta)}{2\tau} = 2.04 \times 10^{-9} \text{ W} \tag{220}$$

for the first-order array. From (212) we conclude that the average signal-to-noise ratio at R_1 is approximately 13 dB for the zero-order array and 23 dB for the first-order array. In either case we expect that the weak-noise results of section 8.4 will apply. Furthermore, since the fluctuation of the received beacon energy about its mean is small, we may modify the results of section 8.43 as follows.

1. The average beacon power received over R_1, over the turbulence and the noise ensembles (By this we mean the average power received over R_1 in the spatial mode corresponding to the received beacon waveform in the absence of noise. From section 5.4 we know that the average power received at the spacecraft is proportional to this quantity.) is

$$E(P_1) + \frac{2N_o + \hbar\omega_c/\eta}{2\tau},$$

where $E(P_1)$ is the average beacon power received in the absence of noise. Since $E(P_1) \gg \frac{2N_o + \hbar\omega_c/\eta}{2\tau}$, this average power is about the same whether or not the noise is present.

2. The average power transmitted by a system that sends $\sqrt{P_t/E(P_1)}$ times the conjugate of the Taylor series approximation of the noisy received beacon field is

$$P_t\left(1 + \frac{n_o(2N_o+\hbar\omega_c/\eta)}{E(P_1)\,2\tau}\right)$$

for the zero-order system, and

$$P_t\left(1 + \frac{n_1(2N_o+\hbar\omega_c/\eta)}{E(P_1)\,2\tau}\right)$$

for the first-order system. In either case, since the noise is weak [compare (219) and (220) with (212)], the average transmitted power is approximately P_t, and the fluctuation about the mean is about the same as the noise-free result (214).

3. The fraction of the average transmitted power that is in the received beacon component of the field at R_1, that is, the gain reduction factor, is

$$\frac{1 + \dfrac{2N_o + \hbar\omega_c/\eta}{E(P_1)\,2\tau}}{1 + \dfrac{n_o(2N_o+\hbar\omega_c/\eta)}{E(P_1)\,2\tau}}$$

for the zero-order system, and

$$\frac{1 + \dfrac{2N_o + \hbar\omega_c/\eta}{E(P_1)\,2\tau}}{1 + \dfrac{n_1(2N_o+\hbar\omega_c/\eta)}{E(P_1)\,2\tau}}$$

for the first-order system. In both cases the fractions are close to one because of the weakness of the noise power compared with $E(P_1)$.

The main conclusion to be drawn from these results is that the noise power is weak enough that the system under consideration has virtually the same performance characteristics whether or not the noise is present.

9.3 CONCLUSIONS

We have demonstrated that a Q-kernel system, even one using an approximate transmitter realization in the presence of noise, performs quite well in terms of the power delivered to a spacecraft 80 million miles away. Although these results are true, they are only true when some stringent aiming and alignment requirements are met. We shall take explicit note of these requirements, and comment upon some other important aspects of the system.

9.31 Alignment Restrictions

There are 4 alignment restrictions that were assumed, either explicitly or implicitly in sections 9.1 and 9.2. These requirements have to do with aiming all of the antennas in the system (the beacon, transmitter at R_1, and spacecraft antennas) within a far-field beamwidth of their respective targets. Specifically, they are as follows.

1. The direction of propagation of the plane wave transmitted from R_3 (the synchronous satellite) to the ground must be aligned within $\sim 0.4\,\lambda/d$ rad of the perpendicular connecting R_3 and R_1, where $\lambda = 0.6\mu$ and $d = 20$ cm.

2. The aiming error a must be less than $0.4\,\lambda/D$ rad, where $\lambda = 0.6\mu$ and $D = 1$ meter. It may be possible, by using a corrective phase tilt at R_1, to tolerate an aiming error significantly greater than $0.4\,\lambda/D$. Whether or not this is possible depends on the size of the isoplanatic angle, but if such a system is feasible, the phase tilt at R_1 must be adjusted within $0.4\,\lambda/D$ of the desired tilt.

3. The Taylor series transmitter at R_1 must produce a waveform that over any one array element is aligned within $0.4\,\lambda/d_n$ rad of the estimate of the approximate incident-field amplitude, where $\lambda = 0.6\mu$ and d_n is the diameter of the n^{th}-order array element.

4. The antenna on the spacecraft, R_4, must be aligned within $0.4\,\lambda/\tilde{d}$ rad of the R_1-R_4 direction, where $\lambda = 0.6\mu$, and $\tilde{d}$ is the diameter of a diffraction-limited lens whose far-field beamwidth is the same as that of R_4.

Restriction 2 is the most severe, and it is indeed so because

$$0.4\,\lambda/D = 0.37\mu\ R = 0.076 \text{ seconds of arc.}$$

Alignment to this accuracy will require extremely delicate adjustments and virtually complete mechanical and electrical stability. On the other hand, if any of conditions 1-4 cannot be met, the performance of the system will not approach the values calculated in section 9.2. For instance, let us assume that conditions 1, 3, and 4 are satisfied, but that $a \approx \lambda/D$. The resulting average power received at R_4 will be $\sim 10^{-3}$ times the result given in section 9.2.

9.32 Point-Ahead Problem

There is an issue that we have ignored completely that may be critical to the operation of a deep-space Q-kernel system. That issue is the point-ahead problem. In general, the spacecraft that we wish to communicate with will have a nonzero relative

velocity with respect to the Earth transmitter, and this motion will necessitate our pointing the beam ahead of the spacecraft. For systems in which the beacon is on the spacecraft, the motion of the spacecraft relative to the Earth can cause the beacon to probe a different path through the atmosphere than the one we transmit through from the ground to the spacecraft. This could invalidate our Q-kernel performance results. If the isoplanatic angle of the turbulence is less than the point-ahead angle, then the correction at R_1 is just a deterministic tilt of the wavefront, and our performance results hold as given earlier. (The isoplanatic angle may be regarded as the maximum angular displacement between two infinite plane waves incident on the top of the atmosphere for which the effect of propagation to R_1 is the same for each plane wave.) Since the point-ahead angle for this system is $2v/c$, where v is the transverse speed of the spacecraft relative to the Earth and c is the speed of light, the isoplanatic angle will set an upper limit to the transverse speed (relative to the Earth) of a spacecraft for which a Q-kernel system will work as well as we have indicated. In numbers, the maximum allowable relative speed is 333 miles per hour times the isoplanatic angle in μrad. If the isoplanatic angle is greater than 20μ R or so, this maximum speed requirement will not be severe. Unfortunately, little theoretical or experimental evidence is available concerning the isoplanatic angle.

Let us not paint too gloomy a picture of this problem. Suppose that the beacon is not on the spacecraft, but is on a separate (synchronous) satellite. Then, regardless of the size of the isoplanatic angle, if the aiming error angle between the apparent position of the synchronous satellite and the predicted position of the spacecraft (after point-ahead correction) meets the alignment restriction set in section 9.31, then all of the performance results that we have derived are valid for this system. The isoplanatic angle does play a role in the system just described; it determines how long (in time) a particular synchronous satellite may be used as a beacon for the Earth-to-spacecraft path, before the beacon probes a "different" atmospheric path from the desired path.

Our final comments concern the sensitivity of our results to the zenith angle of the R_1-R_3 line (with point-ahead questions ignored). The work in sections 9.1 and 9.2 was predicated on this zenith angle being zero. Fried's work[34] indicates that as the zenith angle increases, for a fixed aperture on the ground, the fluctuation factor

$$\frac{(\mathrm{VAR}\,(P_4))^{1/2}}{E(P_4)}$$

increases in proportion to the square root of the secant of the zenith angle. If the zenith angle is very large the Q-kernel system of section 9.1 will exhibit severe signal fading at R_4. Although this fading may be decreased by increasing the size of R_1, if R_1 is made too large the path length assumption of section 3.3 will be violated by a beacon at synchronous altitude, thereby completely invalidating the results of section 9.1.

On the whole we conclude that, subject to the problems outlined above, the two-way system that we have discussed here will achieve excellent power transfer to the spacecraft with little fading.

X. SUGGESTIONS FOR FURTHER WORK

Perhaps the most important conclusion that we can draw is that more work needs to be done. Our study of adaptive spatially modulated transmitters was undertaken to find ways of improving optical communication through atmospheric turbulence. In this matter we have succeeded. Our results show that there are adaptive systems whose performance greatly exceeds the best nonadaptive system for communication through turbulence. With the exception of some of the basic properties of the turbulence that we have used, this conclusion is based wholly upon theoretical considerations. It is time that some experimental work be done.

Three areas in which work is needed are the following.

1. Channel Measurement

The instantaneous reciprocity of the atmosphere should be verified experimentally. The temporal statistics of the quantity

$$\iint_{R_2} \underset{\rightarrow}{\underset{\leftarrow}{K}}_{R_1}(\vec{\rho}', \vec{r}';t)\, d\vec{\rho}' d\vec{r}',$$

which is the energy received over an aperture R_1 when a plane wave is transmitted from R_2, and which determines the performance of a Q-kernel system operating between R_1 and R_2 using a plane-wave beacon, should be measured for various sizes of the R_1 and R_2 apertures. The isoplanatic angle of the turbulence, which is an important parameter to know when designing a deep-space Q-kernel system, should be measured.

2. Transmitter Implementation

An effort should be made to implement a conjugation transmitter, or some approximation of it such as the Taylor series array discussed in section 8.5.

3. System Implementation

An experimental Q-kernel system should be implemented and its performance characteristics compared with theoretical results.

This program is by no means exhaustive, but it is indicative of the work that needs to be done. On the other hand, there are other avenues of research, related to the material that we have presented, to be explored. The reciprocity of the atmosphere provides a powerful tool for measuring the atmospheric state. Further research is needed on adaptive systems (other than the kind that we have considered) that use this information to improve optical communication through the atmosphere. Another research area is the application of reciprocity, as we have defined it, to the study of other slowly fading channels.

APPENDIX A

Apodization for Reciprocal Channels

A.1 Conjugation Operation Transmitter

We shall prove that Eq. 12 does represent the "turned around" and renormalized field at R_1, in a two-way communication system. First, we show that for any field $u_o(\vec{\rho})$ received at R_1 from R_2, $u_o^*(\vec{\rho})$ represents a reversal in the direction of propagation of the waveform. We may represent $u_o(\vec{\rho})$ in R_1 as

$$u_o(\vec{\rho}) = |u_o(\vec{\rho})| \exp -j(\vec{k}(\vec{\rho}) \cdot (\vec{\rho}+z\vec{i}_z)+\phi), \tag{A.1}$$

where $\vec{k}(\vec{\rho})$ is the wave vector, $|\vec{k}(\vec{\rho})| = k$ is the wave number, and ϕ is the absolute phase of the waveform at the origin of R_1. The direction of propagation of a differential segment of phasefront centered on the point $\vec{\rho}_o$ is parallel to the vector $\vec{k}(\vec{\rho}_o)$. This may be verified as follows. We may regard the differential segment of phasefront as being a piece of plane wave; that is, there exists a $\delta > 0$ such that

$$u_o(\vec{\rho}) \approx |u_o(\vec{\rho}_o)| \exp -j(\vec{k}(\vec{\rho}_o) \cdot (\vec{\rho}+z\vec{i}_z)+\phi) \qquad \forall\, |\vec{\rho}-\vec{\rho}_o| < \delta. \tag{A.2}$$

(The smoothness of the inhomogeneities of the channel medium allows us to assume that all fields are continuous within the boundaries of R_1.) The direction of propagation of this plane-wave segment is parallel to $\vec{k}(\vec{\rho}_o)$. Hence if we conjugate Eq. A.1 we have

$$u_o^*(\vec{\rho}) = |u_o(\vec{\rho})| \exp -j(-\vec{k}(\vec{\rho}) \cdot (\vec{\rho}+z\vec{i}_z)-\phi) \tag{A.3}$$

and we see that locally (at $\vec{\rho}_o$) the waveform is propagating in the $-\vec{k}(\vec{\rho}_o)$ direction. Note that conjugating $u_o(\vec{\rho})$ does not change the shape of the surfaces of constant phase, although the ϕ_o surface of $u_o(\vec{\rho})$ becomes the $-\phi_o$ surface of $u_o^*(\vec{\rho})$ for any constant ϕ_o, and also conjugation does not change the amplitude of the wave. Thus conjugation does reverse the direction of propagation of an incident waveform.

To complete the verification of Eq. 12, we must show that the normalization and time-delay terms are correct. We have from Eq. 11 that

$$u_o(\vec{\rho}) = \int_{R_2} v(\vec{\rho}')\, \underline{h}(\vec{\rho}, \vec{\rho}')\, d\vec{\rho}' \tag{A.4}$$

so the energy in $u_o(\vec{\rho})$ is

$$\int_{R_1} |u_o(\vec{\rho})|^2\, d\vec{\rho} = \int_{R_1} d\vec{\rho} \iint_{R_2} v^*(\vec{\rho}')\, \underline{h}^*(\vec{\rho}, \vec{\rho}')\, \underline{h}(\vec{\rho}, \vec{r}')\, v(\vec{r}')\, d\vec{\rho}' d\vec{r}'. \tag{A.5}$$

Therefore the renormalized (to energy E_t) reversed direction-of-propagation waveform is

$$\tilde{u}^*(\vec{\rho}) = \left(\frac{E_t}{\iint_{R_2} v^*(\vec{\rho}') \underset{\leftrightarrow}{K}(\vec{\rho}', \vec{r}') v(\vec{r}') \, d\vec{\rho}' d\vec{r}'} \right)^{1/2} u_o^*(\vec{\rho}), \tag{A.6}$$

where we have used Eq. 7 for $\underset{\leftrightarrow}{K}(\vec{\rho}', \vec{r}')$.

Now we must account for the delay term in Eq. 12. The absolute phase, ϕ, of $u_o(\vec{\rho})$ represents a time delay in propagation from R_2 to R_1 (under the assumption that the beacon signal had zero absolute phase). Thus by conjugating $u_o(\vec{\rho})$, we have obtained a signal with a negative phase, corresponding to a signal beginning before $u_o(\vec{\rho})$ arrives at R_1. In order that the transmitter be realizable, we must add a delay term to the absolute phase of $\tilde{u}^*(\vec{\rho})$ in (A.6); the resulting expression when this delay is added is Eq. 12.

A.2 Heterodyne Receivers

We shall explain the difference between what we mean by heterodyning with $v(\vec{\rho}')$ and what we mean by measuring the $v(\vec{\rho}')$ component of a received field $\hat{v}^*(\vec{\rho}')$. We define the output of a receiver that heterodynes $\hat{v}^*(\vec{\rho}')$ with $v(\vec{\rho}')$ to be

$$\int_{R_2} \hat{v}^*(\vec{\rho}') \, v(\vec{\rho}') \, d\vec{\rho}'. \tag{A.7}$$

Since $v(\vec{\rho}')$ has unit energy, the energy in the receiver output is

$$\left| \int_{R_2} \hat{v}^*(\vec{\rho}') \, v(\vec{\rho}') \, d\vec{\rho}' \right|^2. \tag{A.8}$$

When we measure the $v(\vec{\rho}')$ component of the field $\hat{v}^*(\vec{\rho}')$ we are determining the coefficient of the $v(\vec{\rho}')$ term in an expansion of $\hat{v}^*(\vec{\rho}')$, using some complete orthonormal set of functions of which $v(\vec{\rho}')$ is one. Hence the $v(\vec{\rho}')$ component of $\hat{v}^*(\vec{\rho}')$ is

$$\left(\int_{R_2} \hat{v}^*(\vec{\rho}') \, v^*(\vec{\rho}') \, d\vec{\rho}' \right) v(\vec{\rho}') \tag{A.9}$$

which corresponds to heterodyning $\hat{v}^*(\vec{\rho}')$ with $v^*(\vec{\rho}')$. The energy in this component is

$$\left| \int_{R_2} \hat{v}^*(\vec{\rho}') \, v^*(\vec{\rho}') \, d\vec{\rho}' \right|^2, \tag{A.10}$$

since $v(\vec{\rho}')$ has unit energy.

A. 3 Reciprocity Conditions

We shall prove the reciprocity conditions Eqs. 25 and 30. First, consider a point reciprocal spatially invariant channel. Let $v(\vec{\rho}')$ be the output field (at R_2) that results when $u(\vec{\rho})$ is the input field. Consider the expression

$$\int_{R_2} u(-\vec{\rho}')\, \underline{h}(\vec{\rho}, \vec{\rho}')\, d\vec{\rho}'. \tag{A. 11}$$

We shall assume that R_2 is made large enough that

$$u(-\vec{\rho}') \equiv 0 \qquad \forall\ \vec{\rho}' \notin R_2. \tag{A. 12}$$

This can always be done, since we have

$$u(\vec{\rho}) \equiv 0 \qquad \forall\ \vec{\rho} \notin R_1 \tag{A. 13}$$

and R_1 is a finite aperture. Making the change of variable $\vec{\xi} = -\vec{\rho}'$ in (A. 11), and using (A. 12) and (A. 13) we have

$$\int_{R_2} u(-\vec{\rho}')\, \underline{h}(\vec{\rho}, \vec{\rho}')\, d\vec{\rho}' = \int_{\vec{\xi} \in R_1} u(\vec{\xi})\, \underline{h}(\vec{\rho}, -\vec{\xi})\, d\vec{\xi}. \tag{A. 14}$$

Now we may use the spatial invariance of the impulse responses and point reciprocity (see Eq. 23) to show that

$$\begin{aligned} \int_{\vec{\xi} \in R_1} u(\vec{\xi})\, \underline{h}(\vec{\rho}, -\vec{\xi})\, d\vec{\xi} &= \int_{\vec{\xi} \in R_1} u(\vec{\xi})\, F(-\vec{\xi}-\vec{\rho})\, d\vec{\xi} \\ &= \int_{\vec{\xi} \in R_1} u(\vec{\xi})\, \underline{h}(-\vec{\rho}, \vec{\xi})\, d\vec{\xi} \\ &= v(-\vec{\rho}) \end{aligned} \tag{A. 15}$$

which proves Eq. 25. Similarly, Eq. 28 may be proved by using $u(\zeta-\vec{\rho}')$ in (A. 11), and proceeding through the same argument.

Next consider a point reciprocal spatially invariant channel that is also isotropic. To prove Eq. 30, we proceed as follows. Again, let $v(\vec{\rho}')$ be the output field at R_2 when $u(\vec{\rho})$ is the input. We have to assume that R_2 is made large enough that

$$u(\vec{\rho}') \equiv 0 \qquad \forall\ \vec{\rho}' \notin R_2. \tag{A. 16}$$

Then we have

$$\int_{R_2} u(\vec{\xi})\, \underset{\rightarrow}{h}(\vec{\rho}, \vec{\xi})\, d\vec{\xi} = \int_{\vec{\xi} \in R_1} u(\vec{\xi})\, F(|\vec{\xi}-\vec{\rho}|)\, d\vec{\xi}$$

$$= \int_{\vec{\xi} \in R_1} u(\vec{\xi})\, \underset{\rightarrow}{h}(\vec{\rho}, \vec{\xi})\, d\xi$$

$$= v(\vec{\rho}) \qquad \text{(A.17)}$$

which proves Eq. 30.

Note that in both of these proofs we have relied on the fact that all of the spatial variables ($\vec{\rho}$, $\vec{\rho}'$, and $\vec{\xi}$) are two-dimensional vectors, which may be defined with respect to the origin of either aperture, R_1 or R_2. Although we have always tried to keep all unprimed vectors in the R_1 plane and all primed vectors in the R_2 plane, it was not possible here.

A.4 $Q = \underset{\leftarrow}{K}$ Identities

There are two statements to prove. First, we must show that if a channel is point reciprocal, then $\Phi_i^*(\vec{r})$ is an eigenfunction of $\underset{\rightarrow}{K}(\vec{\rho}, \vec{r})$ with eigenvalue λ_i. Second, that $Q = \underset{\leftarrow}{K}$ is also a sufficient condition for this result.

Suppose $\underset{\rightarrow}{h}(\vec{\rho}', \vec{\rho}) = \underset{\leftarrow}{h}(\vec{\rho}, \vec{\rho}')$. Consider

$$\int_{R_1} \underset{\rightarrow}{K}(\vec{\rho}, \vec{r})\, \Phi_i^*(\vec{r})\, d\vec{r} = \int_{R_1} \left(\int_{R_2} \underset{\rightarrow}{h}^*(\vec{\rho}', \vec{\rho})\, \underset{\rightarrow}{h}(\vec{\rho}', \vec{r})\, d\vec{\rho}' \right) \Phi_i^*(\vec{r})\, d\vec{r}. \qquad \text{(A.18)}$$

Interchanging the orders of integration, and using the fact that ϕ_i is an eigenfunction of Q we have

$$\int_{R_1} \underset{\rightarrow}{K}(\vec{\rho}, \vec{r})\, \Phi_i^*(\vec{r})\, d\vec{r} = \int_{R_2} \underset{\rightarrow}{h}^*(\vec{\rho}', \vec{\rho})\, \sqrt{\lambda_i}\, \phi_i^*(\vec{\rho}')\, d\vec{\rho}'. \qquad \text{(A.19)}$$

Now we may use point reciprocity and the fact that ϕ_i is an eigenfunction of $\underset{\leftarrow}{K}$ to show

$$\int_{R_1} \underset{\rightarrow}{K}(\vec{\rho}, \vec{r})\, \Phi_i^*(\vec{r})\, d\vec{r} = \lambda_i \Phi_i^*(\vec{\rho}). \qquad \text{(A.20)}$$

It remains for us to show that $Q = \underset{\leftarrow}{K}$ is sufficient to prove (A.20). Consider $\{\Phi_i^*\}$. We shall assume that this is a complete orthonormal set. Let us examine the integral

$$\int_{R_1} \underset{\rightarrow}{K}(\vec{\rho}, \vec{r})\, \Phi_i^*(\vec{r})\, d\vec{r}. \qquad \text{(A.21)}$$

Since this integral is a function on R_1 with finite energy, we may expand it in terms of the $\{\Phi_i^*\}$.

$$\int_{R_1} \underset{\rightarrow}{K}(\vec{\rho}, \vec{r})\ \Phi_i^*(\vec{r})\ d\vec{r} = \sum_{j=1}^{\infty} a_{ij}\Phi_j^*(\vec{\rho}), \tag{A.22}$$

where

$$a_{ij} = \iint_{R_1} \Phi_j(\vec{\rho})\ \underset{\rightarrow}{K}(\vec{\rho}, \vec{r})\ \Phi_i^*(\vec{r})\ d\vec{\rho}d\vec{r}. \tag{A.23}$$

We must show that

$$a_{ij} = \lambda_i \delta_{ij}.$$

To do this, we substitute the definition of $\underset{\rightarrow}{K}$ in (A.23), interchange the orders of integration, and obtain

$$a_{ij} = \int_{R_2} \left(\int_{R_1} \Phi_i^*(\vec{r})\ \underset{\rightarrow}{h}(\vec{\rho}', \vec{r})\ d\vec{r} \right) \left(\int_{R_1} \Phi_j(\vec{\rho})\ \underset{\rightarrow}{h}^*(\vec{\rho}', \vec{\rho})\ d\vec{\rho} \right) d\vec{\rho}'$$

$$= \int_{R_2} \sqrt{\lambda_i}\ \phi_i^*(\vec{\rho}')\sqrt{\lambda_j}\ \phi_j(\vec{\rho}')\ d\vec{\rho}'$$

$$= \lambda_i \delta_{ij}, \tag{A.24}$$

where we have used the properties of $\{\Phi_i^*\}$ that follow from $Q = \underset{\leftarrow}{K}$ and the orthonormality of the $\{\phi_i\}$.

APPENDIX B

Apodization through Atmospheric Turbulence

We shall show that the parameter a, defined in section 5.2 as

$$a = \frac{1}{\sqrt{A_2}} \left(\int_{R_1=\infty} \left| \int_{R_2} \underline{\underline{h}}(\vec{\rho}', \vec{\rho})\, d\vec{\rho}' \right|^2 d\vec{\rho} \right)^{1/2}, \tag{B.1}$$

is small, typically from 3 to 5. The argument presented here is not intended as a rigorous proof, since the point reciprocity of the atmosphere (proved in section 6.1) enables us to write immediately

$$a = \frac{1}{\sqrt{A_2}} \left(\int_{R_1=\infty} \left| \int_{R_2} \underline{\underline{h}}(\vec{\rho}, \vec{\rho}')\, d\vec{\rho}' \right|^2 d\vec{\rho} \right)^{1/2}$$

$$= \frac{1}{\sqrt{A_2}} \left(\iint_{R_2} \underline{\underline{K}}_{\infty}(\vec{\rho}', \vec{r}')\, d\vec{\rho}' d\vec{r}' \right)^{1/2} = 1, \tag{B.2}$$

where the last equality follows from the lemma of section 5.21.

In the argument presented here we shall use a physical interpretation of (B.1) that does not rely on the reciprocity of the atmosphere. We have

$$a^2 = \int_{R_1=\infty} \left| \int_{R_2} \frac{1}{\sqrt{A_2}}\, \underline{\underline{h}}(\vec{\rho}', \vec{\rho})\, d\vec{\rho}' \right|^2 d\vec{\rho}. \tag{B.3}$$

The impulse response $\underline{\underline{h}}(\vec{\rho}', \vec{\rho})$ may be regarded as the field at $\vec{\rho}'$ resulting from a point source at $\vec{\rho}$. Thus we may regard

$$\int_{R_2} \frac{1}{\sqrt{A_2}}\, \underline{\underline{h}}(\vec{\rho}', \vec{\rho})\, d\vec{\rho}'$$

as the output of a heterodyne receiver that heterodynes the field received at R_2 from a point source at $\vec{\rho}$ with a unit-energy normally incident plane wave. The quantity

$$\left| \int_{R_2} \frac{1}{\sqrt{A_2}}\, \underline{\underline{h}}(\vec{\rho}', \vec{\rho})\, d\vec{\rho}' \right|^2$$

is then the energy in the output of this heterodyne receiver, and therefore, from (B.3), a^2 may be interpreted as the sum of the heterodyne receiver output energies resulting from point sources in R_1.

Consider, for the moment, the nonturbulent case. The impulse response $\underset{\rightarrow}{h}$ is then[25]

$$\underset{\rightarrow}{h}(\vec{\rho}', \vec{\rho}) = \frac{-\exp -jk(|\vec{\rho}'-\vec{\rho}|^2+z^2)^{1/2} \cos\theta}{j\lambda(|\vec{\rho}'-\vec{\rho}|^2+z^2)^{1/2}}, \tag{B.4}$$

where z is the path length from R_1 to R_2, and θ is the angle between the z axis and the vector from $\vec{\rho}$ to $\vec{\rho}'$. Let us now apply a well-known result about heterodyning. The energy output of a heterodyne receiver using a normally incident plane wave of radius a for a local oscillator essentially results only from those plane-wave components of the received field that are less than $\lambda/2a$ rad away from normal incidence.[36]

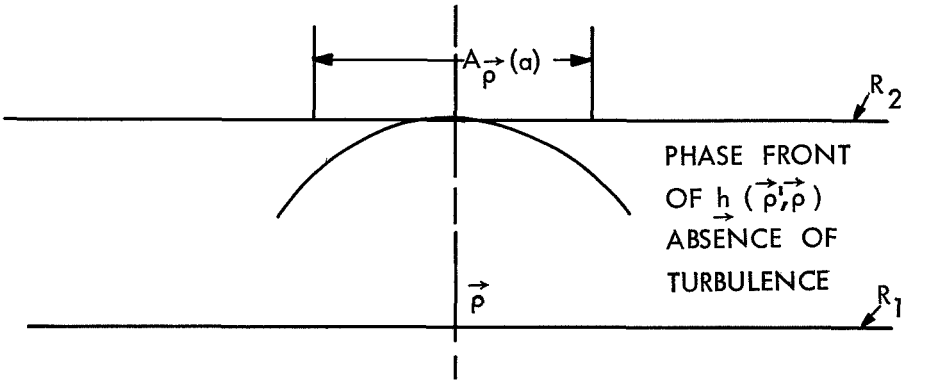

Fig. B-1. Phase-front curvature.

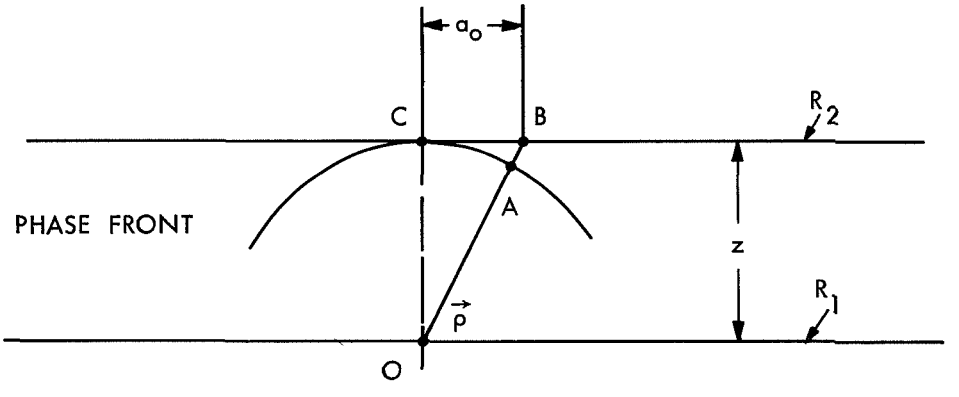

Note 1: $AB = \lambda/2$

Note 2: $\measuredangle COB \approx \measuredangle ACB$ (since $a_o << Z$)

$$\therefore \frac{a_o}{Z} = \frac{\lambda}{2a_o}$$

Fig. B-2. Calculation of a_o.

Referring to Fig. B-1, we see that for any $\vec{\rho} \in R_1$ the vector normal to the phase front received at R_2 is only close to normal incidence on R_2 in a small circular region of R_2 centered on the perpendicular projection of $\vec{\rho}$ onto R_2. Let $A_{\vec{\rho}}(a)$ denote the circular region of radius a centered on the projection of $\vec{\rho}$ onto R_2. Let a_o be the largest value of a for which the incident field is within $\lambda/2a$ rad of normal incidence on $A_{\vec{\rho}}(a)$. From Fig. B-2, we see that a_o satisfies the condition

$$\frac{\lambda}{2a_o} = \frac{a_o}{z}. \tag{B.5}$$

For such a_o, within the region $A_{\vec{\rho}}(a_o)$, we have

$$\left| \exp -jk(|\vec{\rho}'-\vec{\rho}|^2+z^2)^{1/2} \right| \approx 1, \qquad \cos\theta \approx 1.$$

Therefore from (B.4) and our statement about heterodyning we have

$$\left| \int_{R_2} \frac{1}{\sqrt{A_2}} \underline{\underline{h}}(\vec{\rho}', \vec{\rho})\, d\vec{\rho}' \right|^2 \approx \frac{\left(\pi a_o^2\right)^2}{(\lambda z)^2 A_2}. \tag{B.6}$$

If $\tilde{A}$ is the smallest circular region in the R_1 plane such that for all $\vec{\rho}$ not in $\tilde{A}$

$$\left| \int_{R_2} \frac{1}{\sqrt{A_2}} \underline{\underline{h}}(\vec{\rho}', \vec{\rho})\, d\vec{\rho}' \right|^2 \approx 0,$$

then we have

$$a^2 \approx \int_{\tilde{A}} \left| \int_{R_2} \frac{1}{\sqrt{A_2}} \underline{\underline{h}}(\vec{\rho}', \vec{\rho})\, d\vec{\rho}' \right|^2 d\vec{\rho}. \tag{B.7}$$

Applying (B.6) to (B.7) to show that

$$a^2 \approx \frac{\left(\pi a_o^2\right)^2 \tilde{A}}{(\lambda z)^2 A_2} \tag{B.8}$$

and substituting for a_o from (B.5), we have

$$a \approx \frac{\pi}{2} \left(\frac{\tilde{A}}{A_2} \right)^{1/2}. \tag{B.9}$$

From our discussion of heterodyning leading to (B.5) we may conclude that $\tilde{A}$ is

approximately the perpendicular projection of A_2 onto the R_1 plane; therefore, we have $\alpha \approx \pi/2$.

This result applies to the nonturbulent atmosphere, in which case we know that $\alpha = 1$. What we have demonstrated is a method of obtaining α, within an order of magnitude, in the absence of turbulence. We now assume that the same method will enable us to estimate α within an order of magnitude for the turbulent channel.

In the presence of turbulence $\underset{\rightarrow}{h}(\vec{\rho}', \vec{\rho})$ will have a basically spherical wavefront with perturbations caused by the turbulence. The local variations in the angle of arrival are the only perturbations that can affect our argument. Since these perturbations are typically only a few tens of microradians,[37] there will still be some circular region $A_{\underset{\rho}{\rightarrow}}(a_o)$ such that

$$\left| \int_{R_2} \frac{1}{\sqrt{A_2}} \underset{\rightarrow}{h}(\vec{\rho}', \vec{\rho})\, d\vec{\rho}' - \int_{A_{\underset{\rho}{\rightarrow}}(a_o)} \frac{1}{\sqrt{A_2}} \underset{\rightarrow}{h}(\vec{\rho}', \vec{\rho})\, d\vec{\rho}' \right|^2 \approx 0,$$

and the size of a_o will still be determined primarily by the basic curvature of the $\underset{\rightarrow}{h}$ phase front. Hence, within an order of magnitude, we conclude that α should be about the same in the presence of turbulence as in the absence of turbulence, which is the desired result.

APPENDIX C

Spatial Bandwidth and System Performance

We shall calculate the mean and the variance of

$$\left| \int_{R_1} \tilde{u}(\vec{\rho})\, u_o^*(\vec{\rho})\, d\vec{\rho} \right|^2,$$

where

$$\tilde{u}(\vec{\rho}) = \left(\frac{E_t}{\sum_{i=1}^{N} |a_i|^2 + \frac{N(2N_o+\hbar\omega_c/\eta)}{2\tau}} \right)^{1/2} \sum_{i=1}^{N} \hat{a}_{i_{ML}} u_i(\vec{\rho}) \tag{C.1}$$

$$\hat{a}_{i_{ML}} = \frac{1}{\tau} \int_0^\tau \left(\int_{R_1} u(\vec{\rho}, t)\, u_i^*(\vec{\rho})\, d\vec{\rho} \right) dt$$

$$a_i = \int_{R_1} u_o(\vec{\rho})\, u_i^*(\vec{\rho})\, d\vec{\rho}$$

$$u(\vec{\rho}, t) = u_o(\vec{\rho}) + n(\vec{\rho}, t)$$

and $n(\vec{\rho}, t)$ is the white Gaussian noise described in section 8.3. It is clear from the properties of $n(\vec{\rho}, t)$ that $\{\hat{a}_{i_{ML}}\}$ is a set of statistically independent complex Gaussian random variables, with means a_i and variances $\frac{2N_o + \hbar\omega_c/\eta}{2\tau}$. Furthermore, the real and imaginary parts of $\hat{a}_{i_{ML}}$ are statistically independent with equal variances for all i, $1 \leq i \leq N$. Therefore we have

$$\int_{R_1} \tilde{u}(\vec{\rho})\, u_o^*(\vec{\rho})\, d\vec{\rho} = \left(\frac{E_t}{\sum_{i=1}^{N} |a_i|^2 + \frac{N(2N_o+\hbar\omega_c/\eta)}{2\tau}} \right)^{1/2} \sum_{i=1}^{N} \left(|a_i|^2 + n_i a_i^* \right), \tag{C.2}$$

where $\{n_i : 1 \leq i \leq N\}$ is a set of statistically independent zero-mean Gaussian random variables, whose real and imaginary parts are statistically independent and identically distributed, and whose variances are $\frac{2N_o + \hbar\omega_c/\eta}{2\tau}$. From the properties of Gaussian random variables, we conclude that $\int_{R_1} \tilde{u}(\vec{\rho})\, u_o^*(\vec{\rho})\, d\vec{\rho}$ is a Gaussian random variable with mean

$$\left(\frac{E_t}{\sum_{i=1}^{N} |a_i|^2 + \frac{N(2N_o+\hbar\omega_c/\eta)}{2\tau}} \right)^{1/2} \sum_{i=1}^{N} |a_i|^2$$

and variance

$$\frac{E_t \sum_{i=1}^{N} |a_i|^2 \left(\frac{2N_o + \hbar\omega_c/\eta}{2\tau} \right)}{\sum_{i=1}^{N} |a_i|^2 + \frac{N(2N_o+\hbar\omega_c/\eta)}{2\tau}}.$$

Also, the real and imaginary parts of $\int_{R_1} \tilde{u}(\vec{\rho})\, u_o^*(\vec{\rho})\, d\vec{\rho}$ are independent with equal variances.

We wish to evaluate the mean and variance of $\left| \int_{R_1} \tilde{u}(\vec{\rho})\, u_o^*(\vec{\rho})\, d\vec{\rho} \right|^2$. We have immediately

$$E\left(\left| \int_{R_2} \tilde{u}(\vec{\rho})\, u_o^*(\vec{\rho})\, d\vec{\rho} \right|^2 \right) = \mathrm{VAR}\left(\int_{R_1} \tilde{u}(\vec{\rho})\, u_o^*(\vec{\rho})\, d\vec{\rho} \right) + \left| E\left(\int_{R_1} \tilde{u}(\vec{\rho})\, u_o^*(\vec{\rho})\, d\vec{\rho} \right) \right|^2$$

$$= \frac{E_t \sum_{i=1}^{N} |a_i|^2 \left(\sum_{i=1}^{N} |a_i|^2 + \frac{2N_o + \hbar\omega_c/\eta}{2\tau} \right)}{\sum_{i=1}^{N} |a_i|^2 + \frac{N(2N_o+\hbar\omega_c/\eta)}{2\tau}}. \qquad \text{(C.3)}$$

To obtain the variance of $\left| \int_{R_1} \tilde{u}(\vec{\rho})\, u_o^*(\vec{\rho})\, d\vec{\rho} \right|^2$, we evaluate the variance of $|n|^2$, where n is a complex Gaussian random variable whose real and imaginary parts are statistically independent and have equal variances. We have

$$\begin{aligned}
\mathrm{VAR}\,(|n|^2) &= E((|n|^2 - E(|n|^2))^2) \\
&= E(|\tilde{n}|^4 + (2\,\mathrm{Re}\,(E(n)\tilde{n}^*))^2) + E^2(|\tilde{n}|^2) \\
&\quad - 2E(|\tilde{n}|^2)\, E(|\tilde{n}|^2 + 2\,\mathrm{Re}\,(E(n)\tilde{n}^*)) \\
&= 3\,(\mathrm{VAR}^2(\mathrm{Re}\,(\tilde{n})) + \mathrm{VAR}^2(\mathrm{Im}\,(\tilde{n}))) \\
&\quad + 2\,\mathrm{VAR}\,(\mathrm{Re}\,(\tilde{n}))\,\mathrm{VAR}\,(\mathrm{Im}\,(\tilde{n})) \\
&\quad - (\mathrm{VAR}\,(\mathrm{Re}\,(\tilde{n})) + \mathrm{VAR}\,(\mathrm{Im}\,(\tilde{n})))^2 \\
&\quad + 2|E(n)|^2\,\mathrm{VAR}\,(\tilde{n}) \\
&= (\mathrm{VAR}\,(\tilde{n}) + 2|E(n)|^2)\,\mathrm{VAR}\,(\tilde{n}),
\end{aligned}$$

where $\tilde{n} = n - E(n)$, and we have used the moment-factoring property of real Gaussian variables. Thus for the case at hand we obtain

$$\mathrm{VAR}\left(\left|\int_{R_1} \tilde{u}(\vec{\rho})\, u_o^*(\vec{\rho})\, d\vec{\rho}\right|^2\right)$$

$$= 2\left(\frac{E_t\left(\sum_{i=1}^{N} |a_i|^2\right)^2}{\sum_{i=1}^{N} |a_i|^2 + \frac{N(2N_o+\hbar\omega_c/\eta)}{2\tau}}\right)^2 \left(\frac{2N_o + \hbar\omega_c/\eta}{2\tau \sum_{i=1}^{N} |a_i|^2}\right)\left(1 + \frac{2N_o + \hbar\omega_c/\eta}{4\tau \sum_{i=1}^{N} |a_i|^2}\right). \qquad \text{(C.4)}$$

Acknowledgment

It is with great pleasure that I express my gratitude to Professor Robert S. Kennedy, who supervised the research reported here. The guidance that he provided throughout my graduate studies has been invaluable. Professor Peter Elias and Professor Estil V. Hoversten, who served as thesis readers, also deserve mention. Their helpful comments and criticisms have greatly improved the final document.

I also wish to thank the National Science Foundation and the Fannie and John Hertz Foundation for the support that they gave me during the period of my research.

References

1. R. S. Kennedy and E. V. Hoversten, "On the Atmosphere as an Optical Communication Channel," IEEE Trans. on Information Theory, Vol. IT-14, No. 5, pp. 716-725, September 1968.

2. D. L. Fried, "Statistics of a Geometric Representation of Wavefront Distortion," J. Opt. Soc. Am., Vol. 55, No. 11, pp. 1427-1435, November 1965.

3. S. J. Halme, "Efficient Optical Communication in a Turbulent Atmosphere," Ph. D. Thesis, Department of Electrical Engineering, Massachusetts Institute of Technology, Cambridge, Mass., February 1970.

4. R. L. Greenspan, "Error Bounds for Digital Communication over Spatially Modulated Channels," Technical Report 470, Research Laboratory of Electronics, M. I. T., Cambridge, Mass., May 30, 1969.

5. J. L. Holsinger, "Digital Communication over Fixed Time-Continuous Channels with Memory – With Special Applications to Telephone Channels," Technical Report 430, Research Laboratory of Electronics, M. I. T., Cambridge, Mass., October 20, 1964.

6. R. G. Gallager, Information Theory and Reliable Communication (John Wiley and Sons, Inc., New York, 1968).

7. D. Slepian, "Analytic Solution of Two Apodization Problems," J. Opt. Soc. Am., Vol. 55, pp. 1110-1115, 1965.

8. D. Slepian, "Prolate Spheroidal Wave Functions, Fourier Analysis, and Uncertainty IV: Extensions to Many Dimensions; Generalized Prolate Spheroidal Functions," Bell System Tech. J., Vol. 43, pp. 3009-3057, 1964.

9. G. V. Borgiotti, "Maximum Power Transfer between Two Planar Antennas in the Fresnel Zone," IEEE Trans. on Antennas and Propagation, Vol. AP-14, pp. 158-163, March 1966.

10. R. Barakat, "Solution of the Luneberg Apodization Problems," J. Opt. Soc. Am., Vol. 52, pp. 264-275, 1962.

11. D. Slepian and H. O. Pollak, "Prolate Spheroidal Wave Functions, Fourier Analysis and Uncertainty I.," Bell System Tech. J., Vol. 40, pp. 43-64, 1961.

12. H. J. Landau and H. O. Pollak, "Prolate Spheroidal Wavefunctions, Fourier Analysis and Uncertainty III.," Bell System Tech. J., Vol. 41, pp. 1295-1336, 1962.

13. H. L. Van Trees, Detection, Estimation, and Modulation Theory, Vol. 1 (John Wiley and Sons, Inc., New York, 1968).

14. W. B. Davenport and W. L. Root, An Introduction to the Theory of Random Signals and Noise (McGraw-Hill Book Co., New York, 1958).

15. P. Beckmann, "Signal Degeneration in Laser Beams Propagated through a Turbulent Atmosphere," Radio Science, J. of Research NBS/USNC-URSI, Vol. 69D, No. 4, pp. 629-640, April 1965.

16. V. I. Tatarski, Wave Propagation in a Turbulent Medium (McGraw-Hill Book Co., New York, 1961).

17. R. E. Hufnagel and N. Stanley, "Modulation Transfer Function Associated with Image Transmission through Turbulent Media," J. Opt. Soc. Am., Vol. 54, No. 1, pp. 52-61, January 1964.

18. D. L. Fried and J. D. Cloud, "Propagation of an Infinite Plane Wave in a Randomly Inhomogeneous Medium," J. Opt. Soc. Am., Vol. 56, No. 12, pp. 1667-1676, December 1966.

19. R. W. Lee and J. C. Harp, "Weak Scattering in Random Media, with Applications to Remote Probing," Proc. IEEE, Vol. 57, No. 4, pp. 375-406, April 1969.

20. Proc. MIT/RLE-NASA/ERC Workshop on Optical Space Communication, held at Williams College, Williamstown, Mass., August 4, 1968, NASA Report SP-217.

21. A. A. M. Saleh, "An Investigation of Laser Wave Depolarization Due to Atmospheric Transmission," IEEE J. Quantum Electronics, Vol. QE-3, pp. 540-543, November 1967.

22. E. V. Hoversten, "The Atmosphere as an Optical Communication Channel," IEEE International Convention Record, Vol. 15, Pt. 2, pp. 137-145, March 1967.

23. W. D. Montgomery, "Basic Duality in the Algebraic Formulation of Electromagnetic Diffraction," J. Opt. Soc. Am., Vol. 59, No. 7, pp. 804-811, July 1969.

24. J. R. Shewell and E. Wolf, "Inverse Diffraction and a New Reciprocity Theorem," J. Opt. Soc. Am., Vol. 58, No. 12, pp. 1596-1603, December 1968.

25. J. W. Goodman, Introduction to Fourier Optics (McGraw-Hill Book Co., New York, 1968).

26. P. M. Morse and H. Feshbach, Methods of Theoretical Physics, Part I (McGraw-Hill Book Co., New York, 1953).

27. J. P. Moreland and S. A. Collins, "Optical Heterodyne Detection of a Randomly Distorted Signal Beam," J. Opt. Soc. Am., Vol. 59, No. 1, pp. 10-13, January 1969.

28. E. A. Quincy, "Maximum Energy Signals for Random Time-Varying Channels," IEEE Trans. on Information Theory, Vol. IT-15, No. 2, pp. 325-326, March 1969.

29. D. L. Fried, "Optical Heterodyne Detection of an Atmospherically Distorted Signal Wave Front," Proc. IEEE, Vol. 55, No. 1, pp. 57-67, January 1967.

30. L. Mandel, "Intensity Fluctuations of Partially Polarized Light," Proc. Phys. Soc. (London), Vol. 81, pp. 1104-1114, 1963.

31. C. W. Helstrom, "Detectability of Coherent Optical Signals in a Heterodyne Receiver," J. Opt. Soc. Am., Vol. 57, No. 3, pp. 353-361, March 1967.

32. O. E. DeLange, "Optical Heterodyne Detection," IEEE Spectrum, Vol. 5, No. 10, pp. 77-85, October 1968.

33. B. M. Oliver, "Thermal and Quantum Noise," Proc. IEEE, Vol. 53, No. 5, pp. 436-454, May 1965.

34. D. L. Fried, "Aperture Averaging of Scintillation," J. Opt. Soc. Am., Vol. 57, No. 2, pp. 169-175, February 1967.

35. F. Möller, "Optics of the Lower Atmosphere," Appl. Opt., Vol. 3, No. 2, pp. 157-166, February 1964.

36. M. Ross, Laser Receivers (John Wiley and Sons, Inc., New York, 1966).

37. J. H. Shapiro, "A Plane Wave Model for a Turbulence Corrupted Laser Beam," S. M. Thesis, Department of Electrical Engineering, Massachusetts Institute of Technology, September 1968.

JOINT SERVICES ELECTRONICS PROGRAM
REPORTS DISTRIBUTION LIST

Department of Defense

Asst Director/Research (Rm 3C128)
Office of the Secretary of Defense
Pentagon
Washington, D.C. 20301

Technical Library
DDR&E
Room 3C-122, The Pentagon
Washington, D.C. 20301

Director For Materials Sciences
Advanced Research Projects Agency
Room 3D179, Pentagon
Washington, D.C. 20301

Chief, R&D Division (340)
Defense Communications Agency
Washington, D.C. 20305

Defense Documentation Center
Attn: DDC-TCA
Cameron Station
Alexandria, Virginia 22314

Dr Alvin D. Schnitzler
Institute For Defense Analyses
Science and Technology Division
400 Army-Navy Drive
Arlington, Virginia 22202

Central Intelligence Agency
Attn: CRS/ADD/PUBLICATIONS
Washington, D.C. 20505

M. A. Rothenberg (STEPD-SC(S))
Scientific Director
Deseret Test Center
Bldg 100, Soldiers' Circle
Fort Douglas, Utah 84113

Department of the Air Force

Hq USAF (AFRDDD)
The Pentagon
Washington, D.C. 20330

Hq USAF (AFRDDG)
The Pentagon
Washington, D.C. 20330

Hq USAF (AFRDSD)
The Pentagon
Washington, D.C. 20330
Attn: LTC C. M. Waespy

Colonel E. P. Gaines, Jr.
ACDA/FO
1901 Pennsylvania Avenue N. W.
Washington, D.C. 20451

LTC H. W. Jackson (SREE)
Chief, Electronics Division
Directorate of Engineering Sciences
Air Force Office of Scientific Research
Arlington, Virginia 22209

Mr I. R. Mirman
Hq AFSC (SGGP)
Andrews Air Force Base
Washington, D.C. 20331

Rome Air Development Center
Attn: Documents Library (EMTLD)
Griffiss Air Force Base, New York 13440

Mr H. E. Webb, Jr (EMBIS)
Rome Air Development Center
Griffiss Air Force Base, New York 13440

Dr L. M. Hollingsworth
AFCRL (CRN)
L. G. Hanscom Field
Bedford, Massachusetts 01730

Hq ESD (ESTI)
L. G. Hanscom Field
Bedford, Massachusetts 01730

Professor R. E. Fontana, Head
Dept of Electrical Engineering
Air Force Institute of Technology
Wright-Patterson Air Force Base,
Ohio 45433

AFAL (AVT) Dr H. V. Noble, Chief
Electronics Technology Division
Air Force Avionics Laboratory
Wright-Patterson Air Force Base,
Ohio 45433

Director
Air Force Avionics Laboratory
Wright-Patterson Air Force Base,
Ohio 45433

AFAL (AVTA/R. D. Larson)
Wright-Patterson Air Force Base,
Ohio 45433

Director of Faculty Research
Department of the Air Force
U.S. Air Force Academy
Colorado 80840

Academy Library (DFSLB)
USAF Academy, Colorado 80840

Director of Aerospace Mechanics Sciences
Frank J. Seiler Research Laboratory (OAR)
USAF Academy, Colorado 80840

Major Richard J. Gowen
Tenure Associate Professor
Dept of Electrical Engineering
USAF Academy, Colorado 80840

Director, USAF PROJECT RAND
Via: Air Force Liaison Office
The RAND Corporation
Attn: Library D
1700 Main Street
Santa Monica, California 90406

Hq SAMSO (SMTAE/Lt Belate)
Air Force Unit Post Office
Los Angeles, California 90045

AUL3T-9663
Maxwell Air Force Base, Alabama 36112

AFETR Technical Library
(ETV, MU-135)
Patrick Air Force Base, Florida 32925

ADTC (ADBPS-12)
Eglin Air Force Base, Florida 32542

Mr B. R. Locke
Technical Adviser, Requirements
USAF Security Service
Kelly Air Force Base, Texas 78241

Hq AMD (AMR)
Brooks Air Force Base, Texas 78235

USAFSAM (SMKOR)
Brooks Air Force Base, Texas 78235

Commanding General
Attn: STEWS-RE-L, Technical Library
White Sands Missile Range,
New Mexico 88002

Hq AEDC (AETS)
Arnold Air Force Station, Tennessee 37389

European Office of Aerospace Research
Technical Information Office
Box 14, FPO New York 09510

Electromagnetic Compatibility Analysis
Center (ECAC) Attn: ACOAT
North Severn
Annapolis, Maryland 21402

VELA Seismological Center
300 North Washington Street
Alexandria, Virginia 22314

Capt C. E. Baum
AFWL (WLRE)
Kirtland Air Force Base, New Mexico 87117

Department of the Army

Director
Physical & Engineering Sciences Division
3045 Columbia Pike
Arlington, Virginia 22204

Commanding General
U.S. Army Security Agency
Attn: IARD-T
Arlington Hall Station
Arlington, Virginia 22212

Commanding General
U.S. Army Materiel Command
Attn: AMCRD-TP
Washington, D.C. 20315

Director
Advanced Materiel Concepts Agency
Washington, D.C. 20315

Commanding General
USACDC Institute of Land Combat
Attn: Technical Library, Rm 636
2461 Eisenhower Avenue
Alexandria, Virginia 22314

Commanding Officer
Harry Diamond Laboratories
Attn: Dr Berthold Altman (AMXDO-TI)
Connecticut Avenue and
Van Ness Street N. W.
Washington, D.C. 20438

Commanding Officer (AMXRO-BAT)
U.S. Army Ballistic Research Laboratory
Aberdeen Proving Ground
Aberdeen, Maryland 21005

Technical Director
U.S. Army Limited War Laboratory
Aberdeen Proving Ground
Aberdeen, Maryland 21005

U.S. Army Munitions Command
Attn: Science & Technology Information Branch, Bldg 59
Picatinny Arsenal, SMUPA-RT-S
Dover, New Jersey 07801

U.S. Army Mobility Equipment Research and Development Center
Attn: Technical Documents Center, Bldg 315
Fort Belvoir, Virginia 22060

Commanding Officer
U.S. Army Engineer Topographic Laboratories
Attn: STINFO Center
Fort Belvoir, Virginia 22060

Dr Herman Robl
Deputy Chief Scientist
U.S. Army Research Office (Durham)
Box CM, Duke Station
Durham, North Carolina 27706

Richard O. Ulsh (CRDARD-IP)
U.S. Army Research Office (Durham)
Box CM, Duke Station
Durham, North Carolina 27706

Technical Director (SMUFA-A2000-107-1)
Frankford Arsenal
Philadelphia, Pennsylvania 19137

Redstone Scientific Information Center
Attn: Chief, Document Section
U.S. Army Missile Command
Redstone Arsenal, Alabama 35809

Commanding General
U.S. Army Missile Command
Attn: AMSMI-RR
Redstone Arsenal, Alabama 35809

Commanding General
U.S. Army Strategic Communications Command
Attn: SCC-CG-SAE
Fort Huachuca, Arizona 85613

Commanding Officer
Army Materials and Mechanics Research Center
Attn: Dr H. Priest
Watertown Arsenal
Watertown, Massachusetts 02172

Commandant
U.S. Army Air Defense School
Attn: Missile Science Division, C&S Dept
P. O. Box 9390
Fort Bliss, Texas 79916

Commandant
U.S. Army Command and General Staff College
Attn: Acquisitions, Lib Div
Fort Leavenworth, Kansas 66027

Mr Norman J. Field, AMSEL-RD-S
Chief, Science and Technology Division
Research and Development Directorate
U.S. Army Electronics Command
Fort Monmouth, New Jersey 07703

Mr Robert O. Parker, AMSEL-RD-S
Executive Secretary, TAC/JSEP
U.S. Army Electronics Command
Fort Monmouth, New Jersey 07703

Commanding General
U.S. Army Electronics Command
Fort Monmouth, New Jersey 07703
Attn: AMSEL-SC
DL
GG-DD
XL-D
XL-DT
BL-FM-P
CT-D
CT-R
CT-S
CT-L (Dr W.S. McAfee)
CT-O
CT-I
CT-A
NL-D (Dr H. Bennett)
NL-A
NL-C
NL-P
NL-P-2
NL-R
NL-S
KL-D
KL-I
KL-E
KL-S
KL-SM
KL-T
VL-D
VL-F
WL-D

Director (NV-D)
Night Vision Laboratory, USAECOM
Fort Belvoir, Virginia 22060

Commanding Officer
Atmospheric Sciences Laboratory
U.S. Army Electronics Command
White Sands Missile Range,
New Mexico 88002

Commanding Officer (AMSEL-BL-WS-R)
Atmospheric Sciences Laboratory
U.S. Army Electronics Command
White Sands Missile Range,
New Mexico 88002

Chief
Missile Electronic Warfare Tech
Area (AMSEL-WL-M)
U.S. Army Electronics Command
White Sands Missile Range,
New Mexico 88002

Product Manager NAVCON
Attn: AMCPM-NS-TM, Bldg 439
(H. H. Bahr)
Fort Monmouth, New Jersey 07703

Department of the Navy

Director, Electronic Programs
Attn: Code 427
Department of the Navy
Washington, D.C. 20360

Commander
Naval Security Group Command
Naval Security Group Headquarters
Attn: Technical Library (G43)
3801 Nebraska Avenue, N. W.
Washington, D.C. 20390

Director
Naval Research Laboratory
Washington, D.C. 20390
Attn: Code 2027
Dr W. C. Hall, Code 7000
Mr A. Brodzinsky, Supt,
Electronics Div

Code 8050
Maury Center Library
Naval Research Laboratory
Washington, D.C. 20390

Dr G. M. R. Winkler
Director, Time Service Division
U.S. Naval Observatory
Washington, D.C. 20390

Naval Air Systems Command
AIR 03
Washington, D.C. 20360

Naval Ship Systems Command
Ship 031
Washington, D.C. 20360

Naval Ship Systems Command
Ship 035
Washington, D.C. 20360

U.S. Naval Weapons Laboratory
Dahlgren, Virginia 22448

Naval Electronic Systems Command
ELEX 03, Rm 2534 Main Navy Bldg
Department of the Navy
Washington, D.C. 20360

Commander
U.S. Naval Ordnance Laboratory
Attn: Librarian
White Oak, Maryland 20910

Director
Office of Naval Research
Boston Branch
495 Summer Street
Boston, Massachusetts 02210

Commander (ADL)
Naval Air Development Center
Attn: NADC Library
Johnsville, Warminster,
Pennsylvania 18974

Commander (Code 753)
Naval Weapons Center
Attn: Technical Library
China Lake, California 93555

Commanding Officer
Naval Weapons Center
Corona Laboratories
Attn: Library
Corona, California 91720

Commanding Officer (56322)
Naval Missile Center
Point Mugu, California 93041

W. A. Eberspacher, Associate Head
Systems Integration Division, Code 5340A
U.S. Naval Missile Center
Point Mugu, California 93041

Commander
Naval Electronics Laboratory Center
Attn: Library
San Diego, California 92152

Deputy Director and Chief Scientist
Office of Naval Research Branch Office
1030 East Green Street
Pasadena, California 91101

Library (Code 2124)
Technical Report Section
Naval Postgraduate School
Monterey, California 93940

Glen A. Myers (Code 52 Mv)
Assoc Professor of Electrical Engineering
Naval Postgraduate School
Monterey, California 93940

Commanding Officer (Code 2064)
Navy Underwater Sound Laboratory
Fort Trumbull
New London, Connecticut 06320

Commanding Officer
Naval Avionics Facility
Indianapolis, Indiana 46241

Director
Naval Research Laboratory
Attn: Library, Code 2039 (ONRL)
Washington, D.C. 20390

Commanding Officer
Naval Training Device Center
Orlando, Florida 32813

Other Government Agencies

Dr H. Harrison, Code RRE
Chief, Electrophysics Branch
National Aeronautics and
Space Administration
Washington, D.C. 20546

NASA Lewis Research Center
Attn: Library
21000 Brookpark Road
Cleveland, Ohio 44135

Los Alamos Scientific Laboratory
Attn: Reports Library
P. O. Box 1663
Los Alamos, New Mexico 87544

Mr M. Zane Thornton, Chief
Network Engineering, Communications
and Operations Branch
Lister Hill National Center for
Biomedical Communications
8600 Rockville Pike
Bethesda, Maryland 20014

U.S. Post Office Department
Library - Room 6012
12th & Pennsylvania Ave. N. W.
Washington, D.C. 20260

Non-Government Agencies

Director
Research Laboratory of Electronics
Massachusetts Institute of Technology
Cambridge, Massachusetts 02139

Mr Jerome Fox, Research Coordinator
Polytechnic Institute of Brooklyn
333 Jay Street
Brooklyn, New York 11201

Director
Columbia Radiation Laboratory
Columbia University
538 West 120th Street
New York, New York 10027

Director
Coordinated Science Laboratory
University of Illinois
Urbana, Illinois 61801

Director
Stanford Electronics Laboratory
Stanford University
Stanford, California 94305

Director
Microwave Laboratory
Stanford University
Stanford, California 94305

Director
Electronics Research Laboratory
University of California
Berkeley, California 94720

Director
Electronics Sciences Laboratory
University of Southern California
Los Angeles, California 90007

Director
Electronics Research Center
The University of Texas at Austin
Engineering-Science Bldg 110
Austin, Texas 78712

Division of Engineering and
Applied Physics
210 Pierce Hall
Harvard University
Cambridge, Massachusetts 02138

Dr G. J. Murphy
The Technological Institute
Northwestern University
Evanston, Illinois 60201

Dr John C. Hancock, Head
School of Electrical Engineering
Purdue University
Lafayette, Indiana 47907

Dept of Electrical Engineering
Texas Technological University
Lubbock, Texas 79409

Aerospace Corporation
P. O. Box 95085
Attn: Library Acquisitions Group
Los Angeles, California 90045

Airborne Instruments Laboratory
Deerpark, New York 11729

The University of Arizona
Department of Electrical Engineering
Tucson, Arizona 85721

Chairman, Electrical Engineering
Arizona State University
Tempe, Arizona 85281

Engineering and Mathematical
Sciences Library
University of California at Los Angeles
405 Hilgred Avenue
Los Angeles, California 90024

Sciences-Engineering Library
University of California
Santa Barbara, California 93106

Professor Nicholas George
California Institute of Technology
Pasadena, California 91109

Aeronautics Library
Graduate Aeronautical Laboratories
California Institute of Technology
1201 E. California Boulevard
Pasadena, California 91109

Hunt Library
Carnegie-Mellon University
Schenley Park
Pittsburgh, Pennsylvania 15213

Dr A. G. Jordan
Head of Dept of Electrical Engineering
Carnegie-Mellon University
Pittsburg, Pennsylvania 15213

Case Institute of Technology
Engineering Division
University Circle
Cleveland, Ohio 44106

Hollander Associates
Attn: Librarian
P. O. Box 2276
Fullerton, California 92633

Dr Sheldon J. Welles
Electronic Properties Information Center
Mail Station E-175
Hughes Aircraft Company
Culver City, California 90230

Illinois Institute of Technology
Department of Electrical Engineering
Chicago, Illinois 60616

Government Documents Department
University of Iowa Libraries
Iowa City, Iowa 52240

The Johns Hopkins University
Applied Physics Laboratory
Attn: Document Librarian
8621 Georgia Avenue
Silver Spring, Maryland 20910

Lehigh University
Department of Electrical Engineering
Bethlehem, Pennsylvania 18015

Mr E. K. Peterson
Lenkurt Electric Co. Inc.
1105 County Road
San Carlos, California 94070

MIT Lincoln Laboratory
Attn: Library A-082
P. O. Box 73
Lexington, Massachusetts 02173

Miss R. Joyce Harman
Project MAC, Room 810
545 Main Street
Cambridge, Massachusetts 02139

Professor R. H. Rediker
Electrical Engineering, Professor
Massachusetts Institute of Technology
Building 13-3050
Cambridge, Massachusetts 02139

Professor Joseph E. Rowe
Chairman, Dept of Electrical Engineering
The University of Michigan
Ann Arbor, Michigan 48104

Dr John R. Ragazzini, Dean
School of Engineering and Science
New York University
University Heights
Bronx, New York 10453

Professor James A. Cadzow
Department of Electrical Engineering
State University of New York at Buffalo
Buffalo, New York 14214

Department of Electrical Engineering
Clippinger Laboratory
Ohio University
Athens, Ohio 45701

Raytheon Company
Research Division Library
28 Seyon Street
Waltham, Massachusetts 02154

Rice University
Department of Electrical Engineering
Houston, Texas 77001

Dr Leo Young, Program Manager
Stanford Research Institute
Menlo Park, California 94025

Sylvania Electronic Systems
Applied Research Laboratory
Attn: Documents Librarian
40 Sylvan Road
Waltham, Massachusetts 02154

Dr W. R. LePage, Chairman
Department of Electrical Engineering
Syracuse University
Syracuse, New York 13210

Dr F. R. Charvat
Union Carbide Corporation
Materials Systems Division
Crystal Products Department
8888 Balboa Avenue
P. O. Box 23017
San Diego, California 92123

Utah State University
Department of Electrical Engineering
Logan, Utah 84321

Research Laboratories for the
Engineering Sciences
School of Engineering and Applied Science
University of Virginia
Charlottesville, Virginia 22903

Department of Engineering and
Applied Science
Yale University
New Haven, Connecticut 06520

UNCLASSIFIED

Security Classification

DOCUMENT CONTROL DATA - R & D

(Security classification of title, body of abstract and indexing annotation must be entered when the overall report is classified)

1. ORIGINATING ACTIVITY *(Corporate author)* Research Laboratory of Electronics Massachusetts Institute of Technology Cambridge, Massachusetts 02139	2a. REPORT SECURITY CLASSIFICATION Unclassified 2b. GROUP None

3. REPORT TITLE

Optimal Spatial Modulation for Reciprocal Channels

4. DESCRIPTIVE NOTES *(Type of report and inclusive dates)*

Technical Report

5. AUTHOR(S) *(First name, middle initial, last name)*

Jeffrey H. Shapiro

6. REPORT DATE	7a. TOTAL NO. OF PAGES	7b. NO. OF REFS
April 30, 1970	136	37

8a. CONTRACT OR GRANT NO.	9a. ORIGINATOR'S REPORT NUMBER(S)
DA 28-043-AMC-02536(E) b. PROJECT NO. 20061102B31F c. NASA Grant NGL 22-009-013 d.	Technical Report 476 9b. OTHER REPORT NO(S) *(Any other numbers that may be assigned this report)* None

10. DISTRIBUTION STATEMENT

This document has been approved for public release and sale; its distribution is unlimited.

11. SUPPLEMENTARY NOTES	12. SPONSORING MILITARY ACTIVITY
	Joint Services Electronics Program Through U. S. Army Electronics Command

13. ABSTRACT

The purpose of this research is to find ways of improving optical communication through atmospheric turbulence by using spatial modulation. The performance of a class of adaptive spatially modulated communication systems, in which the antenna pattern at the transmitter is modified in accordance with the knowledge of the channel state obtained from a beacon signal transmitted from the receiving terminal to the transmitter, is examined.

For time-invariant channels satisfying a certain reciprocity condition, there exists an adaptive system that achieves the maximum energy transfer possible from transmitter to receiver. This result is applied to the turbulent atmospheric channel by regarding the atmosphere as undergoing a succession of fixed states, and proving that instantaneously the atmosphere is reciprocal. The performance of adaptive spatially modulated systems for the turbulent channel is derived for both point-to-point and deep-space applications. In the deep-space case we find that the turbulence does not increase the average far-field beamwidth attainable with a given diameter aperture, but fluctuations about this average beamwidth do occur as the state of the atmosphere changes.

The effects of noise and approximate transmitter implementations on the performance of the adaptive systems under discussion are considered. A hypothetical deep-space system is specified and its performance is evaluated.

14. KEY WORDS	LINK A		LINK B		LINK C	
	ROLE	WT	ROLE	WT	ROLE	WT
Adaptive Communication						
Apodization						
Atmospheric Turbulence						
Optical Communication						
Reciprocity						
Spatial Modulation						